U.PORTO

FEP FACULDADE DE ECONOMIA UNIVERSIDADE DO PORTO

Multivariate Forecasting of Renewable Energy Generation

José Pedro dos Santos Leite Ferreira

Master's Thesis in Modeling, Data Analysis
and Decision Support Systems

Supervisor: Doutor Ricardo Jorge Gomes de Sousa Bento Bessa
Co-supervisor: Professor Doutor João Manuel Portela da Gama

Faculdade de Economia

Universidade do Porto

2021

Acknowledgements

As I conclude yet another chapter of my personal and academic life, I could not miss out on the opportunity to thank those who, in some way or another, have contributed to make this thesis possible.

To my parents and relatives, without whom none of this would be possible, I want to thank for the endless support and patience throughout the past two years.

To my friends, I want to thank for the comfort and the laughs, both of which were fundamental to endure the difficult times we have gone through in the past year and a half.

To my colleagues at DouroECI, I want to thank for the patience and the encouragement to pursue different areas of knowledge.

To Carla Gonçalves from INESC TEC, I want to thank for the continuous support and guidance throughout the past five months.

To Professor João Gama, I want to thank for the inspiration and the invaluable teachings provided throughout the past two years.

To Ricardo Bessa, I want to thank for the countless meetings and the knowledgeable observations, both of which were fundamental to the completion of this thesis.

Last but not least, I want to thank the University of Porto, in the person of its professors and employees, for the diligent work and enthusiasm, values which have had a profound impact on me and which I hope embody in my future endeavours.

Abstract

As the capacity to generate renewable energy increases worldwide, private companies and public utilities operating in the energy sector must be capable of dealing with the high variability and seasonality of these energy sources. As such, renewable power forecasting is likely to play a key role in the global movement for carbon neutrality. In fact, as of today, forecasts of a few hours to multiple days-ahead are already widely used by energy market participants. The present work reports new results in using autoregression-based models to forecast renewable power generation. Besides the standard Autoregressive (AR) model, different approaches within the autoregressive framework are pursued, namely: the use of weather forecasts as exogenous predictors, the use of geographically distributed data (spatiotemporal models), the use of additive models with splines to model the non-linear relation between the weather forecasts and the power generated, and the use of different objective functions within the Least Absolute Shrinkage and Selection Operator (LASSO) regularization framework. The implemented models were used to forecast wind power generation up to 24 hours-ahead in 10 Wind Power Plants (WPP) in Australia. The models were compared with performance metrics and statistical tests. The use of exogenous variables proved to have a positive impact on the forecasts, particularly in forecasts of more than a few hours-ahead. The use of geographically used data provided marginal improvements over the univariate models. The use of additive models led to significant improvements in the longer-term horizons. Overall, even though not all results proved to be statistically significant, it is possible to conclude that additive vector autoregressive models can match up to machine learning based models and even improve on their results for forecasting horizons of up to 12 hours-ahead.

Keywords: wind power forecasting, autoregressive models, spatiotemporal models, additive models.

Resumo

Há medida que a capacidade de produção de energia renovável instalada no Mundo cresce, as empresas privadas e os serviços de utilidade pública que operam no setor da energia têm de ser capazes de lidar com a alta variabilidade e sazonalidade destas fontes de energia. Sendo assim, é expectável que a previsão de energia renovável desempenhe um papel fundamental no movimento global pela neutralidade carbónica. De facto, hoje-em-dia, previsões de algumas horas até vários dias à frente são já amplamente utilizadas pelos operadores do mercado da energia. O presente trabalho apresenta novos resultados utilizando modelos baseados em autoregressão para fazer previsões da potência gerada por fontes de energia renovável. Para além do modelo autoregressivo (AR), diferentes abordagens neste âmbito são exploradas, nomeadamente: a utilização de previsões meteorológicas na previsão (variáveis exógenas), a utilização de dados geograficamente distribuídos (modelos espaço-temporais), a utilização de modelos aditivos com *splines* para modelar a relação não linear entre as previsões meteorológicas e a potência gerada, e a utilização de diferentes funções objetivo aplicadas à regularização LASSO (*Least Absolute Shrinkage and Selection Operator*). Os modelos implementados foram utilizados para fazer previsões de potência eólica até 24 horas à frente em 10 parques eólicos na Austrália. Os modelos foram comparados com métricas e testes estatísticos. A utilização de variáveis exógenas provou ter um impacto positivo nas previsões, em particular em horizontes superiores a duas horas à frente. A utilização de dados geograficamente distribuídos proporcionou benefícios marginais sobre os modelos univariados. A utilização de modelos aditivos proporcionou benefícios significativos nos horizontes mais longos. De maneira geral, embora nem todos os resultados seja estatisticamente significantes, é possível concluir que modelos vetoriais autorregressivos aditivos conseguem rivalizar com modelos baseados em aprendizagem automática e, inclusive, melhorar os resultados destes em horizontes de até 12 horas à frente.

Palavras-chave: previsão de energia renovável, modelos autoregressivos, modelos espaço-temporais, modelos aditivos.

List of Abbreviations

AAR-X Additive Autoregressive Model with Exogenous Variables

AR Autoregressive Model

AR-X Autoregressive Model with Exogenous Variables

AVAR-X Additive Vector Autoregressive Model with Exogenous Variables

GW Gigawatt

LASSO Least Absolute Shrinkage and Selection Operator

VAR Vector Autoregressive Model

VAR-X Vector Autoregressive Model with Exogenous Variables

WPP Wind Power Plant

XGB Gradient Boosting Trees Model

Contents

List of Figures

List of Tables

Chapter 1

Introduction

1.1 Motivation

Renewable energy production has seen a remarkable increase over the past decade. Prompted by the growing concern over global warming, which took unprecedented proportions in the 2010s, the wind industry saw the total installed capacity quadruple since 2009, reaching 744 GW in 2020.

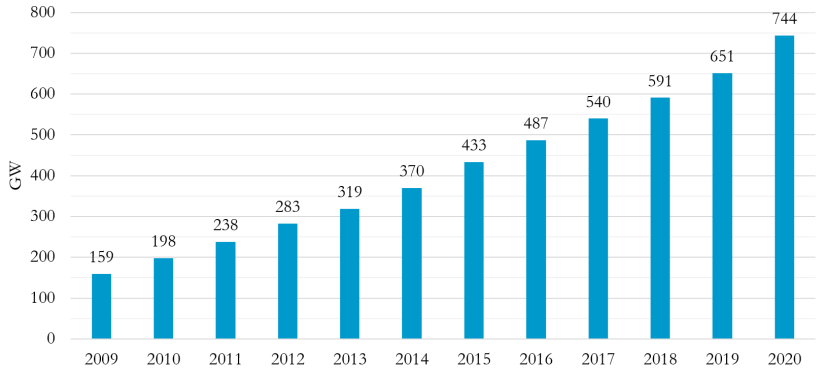

Figure 1.1: Wind power global capacity, 2009-2020 [Adapted from GWEC (2021)]

One of the most relevant trends in the market has been the increase of the offshore wind power segment, from 1.8 GW installed in 2009 (around 1.1%) to 35.1 GW in 2019 (around 4.7%). The 2010s have also seen China establish itself as the biggest market for wind energy production, representing more than one in every three GW installed worldwide.

The total wind power capacity installed globally is expected to keep growing for the foreseeable future. According to the Global Wind Report 2021 from the Global Wind Energy Council (GWEC, 2021), despite the impact of the COVID-19 pandemic, the wind energy market is expected to grow 4% a year for the next five years, bringing the total installed capacity just over 1200 GW in 2025.

Two fundamental factors when planning for a greener, highly renewable energy sector are the seasonality and short-term variability of these resources. Seasonality refers to the recurrence

of predictable patterns or fluctuations in a time series. In renewable power forecasting, seasonality arises from the underlying relation between the weather (and other natural phenomena) and renewable power generation. For instance, in Europe, wind power generation is generally stronger in winter than in summer months, while solar power generation is lower in winter and non-existent during night-time throughout the year. Short-term variability refers to the stochastic nature of the weather and of renewable power generation, which limits the ability to make predictions and hinders the operation and management of power grids (Tastu, Pinson, Trombe, & Madsen, 2014). The negative effects of seasonality and short-term variability in renewable energy production may be mitigated with adequate storage capacity, diversified energy sources, and accurate forecasting. Forecasting allows for a cost-efficient balancing of load and generation in intra-day and day ahead scheduling, reducing fuel costs, improving system reliability, and increasing productivity (Leisch & Cochran, 2016).

1.2 Renewable power generation forecasting

As discussed in Section 1.1, renewable power generation is variable and intermittent even in timescales of a few minutes. In this context, accurate forecasting of variables such as generated power and consumption is extremely relevant for decision-makers, whether they are market participants, looking to buy or sell energy, or power system operators. The former use forecasts to manage risks and optimize their investments, while the latter are concerned with maintaining a steady energy supply under all possible market and weather conditions (Sweeney, Bessa, Browell, & Pinson, 2019).

Renewable energy forecasts are usually divided into 3 groups, depending on the forecasting horizon: intraday forecasts, day-ahead forecasts, and long-term forecasts. A brief description of the applications of each timescale is presented in Table 1.1.

Table 1.1: Time-horizon classification for wind forecasting [Adapted from Wang et al. (2011)]

Timescale	Applications
Intraday	Real-time grid operations Regulation procedures
Day-ahead	Economic load dispatch planning Load management decisions Operational security measures
Long-term (multiple days ahead)	Maintenance planning Operations management Optimal operating cost

Renewable power forecasting usually makes use of variables such as past power generation measurements and weather forecasts. A new trend in renewable power forecasting concerns the use of power generation data from multiple sites (geographically distributed data). In the case of

wind power forecasting, the geographical dispersion of wind farms allows for the understanding of the propagation of meteorological systems and power forecast errors. Spatiotemporal models, as they are designated, take advantage of the correlations in power generation data collected in neighbouring sites, warranting significant gains in forecast accuracy (Tastu et al., 2014).

Renewable power forecasting models can be classified according to the underlying methodology observed. In this case, one should distinguish between physical and statistical models. The first are concerned with modelling the governing equations taking place in the atmosphere and the latter focus on modelling the statistical relationship between meteorological forecasts and the power generated (Sweeney et al., 2019). Statistical models usually rely on time series analysis (classical statistics) or machine learning techniques. Both physical and statistical models are discussed thoroughly in Section 2.1.

1.3 Aim and objectives

Examples of statistical models using time series analysis include autoregression-based models. Autoregressive models make use of past observations of the target variables to make predictions. The standard Autoregressive (AR) model is used to make forecasts of one target variable using past observations of itself. The Autoregressive model with exogenous (AR-X) is used to make forecasts of one target variable using past observations of itself and linear combinations of other relevant exogenous variables (e.g., weather forecasts for the forecasting hour). In the context of autoregression, endogenous variables are variables that are assumed to be correlated and, thus, are potentially effective at forecasting each other, while exogenous variables are independent variables that are assumed to affect the system. In wind power generation forecasting, wind speed and direction at different levels above the ground are often considered to have a positive impact on the forecast.

Attempting to capture the correlations in geographically distributed data described in Section 1.2., the Vector Autoregressive (VAR) model is used to make forecasts of the target variable at n geographically distributed sites using the past observations of the same variable in all n sites (spatiotemporal model). Like the AR-X model, the Vector Autoregressive model with exogenous variables (VAR-X) model uses both the past observations at the n geographically distributed sites and relevant exogenous variable collected in one or more relevant sites (typically the same sites as the endogenous variables). In wind power forecasting, recent works show that models that use linear combinations of geographically distributed sites are competitive in forecasting timescales of up to 6 hours-ahead (Cavalcante et al., 2017).

While the AR-X and VAR-X models make use of linear combinations of the exogenous variables in the prediction, in reality, the relation between the weather forecasts and the renewable power generated is not linear. In wind power forecasting, this problem originates from the transfer functions of wind turbines, in which there is frequently no power generation below a minimum speed of 3 m/s and no increase in power generation for speeds above 15 m/s (Monteiro et al., 2009). Furthermore, while the relation between wind speed and power generation is well understood and modelled, the available forecasts are rarely the ones needed to proceed with this calculation.

To describe the non-linear relation between the weather forecasts and power generation in a time series analysis setting, one option is to adapt traditional linear AR-X and VAR-X models into additive models with splines. Additive models, such as the Additive AR-X (AAR-X) and Additive VAR-X (AVAR-X) models, are obtained from the sum of the explanatory variables' individual effects. These models are quite good at modelling non-linearities in the data, while maintaining some of the positive aspects of the linear approaches.

The present work will make use of the autoregressive models mentioned above to produce intraday and day-ahead forecasts of wind power generation, benchmarking the results against standard approaches, such as Persistence and machine learning-based models (gradient boosting trees). An illustration of the problem is presented in Figure 1.2.

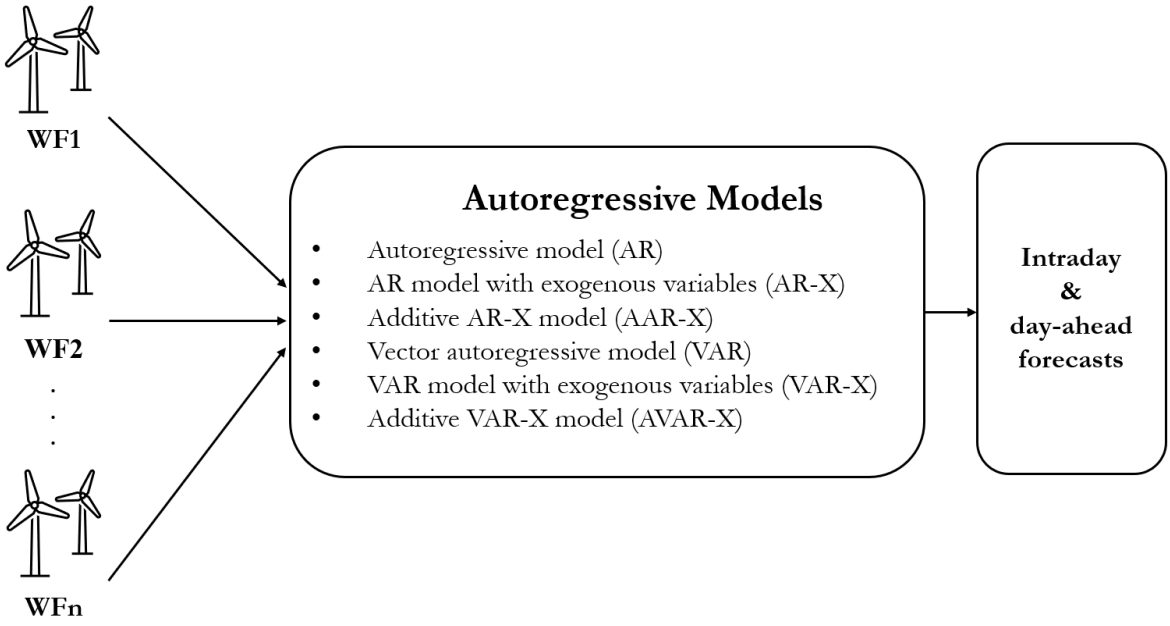

Figure 1.2: Problem illustration [Adapted from Cavalcante et al. (2017)]

The aim of the present work is to answer a set of research questions regarding the implementation of the different autoregressive models, namely:

- Does the inclusion of exogenous variables improve the quality of the forecast for all timescales?
  - AR model vs. AR-X model
  - VAR model vs. VAR-X model
- Does the inclusion of data from other Wind Power Plants (WPP) improve the quality of the forecast for all timescales?
  - AR model vs. VAR model
  - AR-X model vs. VAR-X model

  - AAR-X model vs. AVAR-X model

- Are models that use weather forecasts in additive settings better at forecasting wind power generation than models which use linear combinations of these variables?
  - AR-X model vs. AAR-X model
  - VAR-X model vs. AVAR-X model
- How do the autoregressive-based models implemented compare with other commonly used methods, such as Persistence and gradient boosting trees at forecasting energy production?

1.4 Structure of the Report

The present thesis is structured into five major chapters. A brief description of each chapter is provided below.

In Chapter 1, Introduction, the subject of renewable energy forecasting is introduced, as well as the most used forecasting timescales. The aim of the present work is presented, as well as the research questions it intends to address.

In Chapter 2, State-of-the-art in Renewable Power Generation Forecasting, the two main approaches to renewable power generation forecasting are discussed – physical models and statistical models. Models such as Persistence and gradient boosting trees are introduced.

In Chapter 3, Time Series Models for Renewable Power Generation Forecasting, the subject of autoregression is introduced, as well as the models that are to be implemented in Chapter 4. The subject of LASSO regression is introduced.

In Chapter 4, Forecasting Results and Discussion, the data used to assess the models is thoroughly analysed and discussed. The performance metrics and statistical testes used to compare the forecasting results are introduced, as well as the subject of Bayesian Optimization. The results of the intraday and day-ahead forecasts are presented. The in-depth discussion of the results is performed.

In Chapter 5, 'Conclusions and Future Work', the main conclusions of the present work are presented, as well as possible future works on this subject.

Chapter 2

State-of-the-Art in Renewable Power Forecasting

Forecasting is the art of making informed estimates about the future behaviour of a given process or trend using historical and present data. Focussing on the evolution of a given variable, y, in time, forecasting is based on the premise that the modelled behaviour will continue in the future. In renewable power forecasting, y is the generated power by a given turbine or WPP(Bessa, 2008).

As discussed in Chapter 1, physical models and statistical models, or a combination of both, are the main approaches to renewable power forecasting. This section of the report is centred around these two methods.

2.1 Physical Models

Physical models rely on Numerical Weather Prediction (NWP) to forecast renewable power generation. NWP is concerned with accurately representing the interactions between wind, pressure, density, and temperature, which take place in the Earth's atmosphere. For a given point in time and space, this means solving the Navier-Stokes and mass continuity equations, as well as the first law of thermodynamics and the ideal gas law. To obtain a solution, these equations must be solved numerically using temporal and spatial discretization (Bauer et al., 2015).

The idea of using the governing laws of physics to forecast the weather was first introduced by Abbe (1901) and Bjerknes, Volken, and Brönnimann (1904) in the first decades of the twentieth century. Revolutionary at the time, the idea was only fully realized with the appearance of the first computers. The full set of governing equations was first solved in the 1970s, after two decades of attempts at using computers for weather prediction. Since then, the sharp increase in computing power has made it possible to consider larger numbers of grid-points, meaning models can cover wider areas and present, at worst, the same levels of accuracy. Today, NWP can provide predictions at kilometre scale multiple times per day and at tens of kilometres monthly (Bauer et al., 2015).

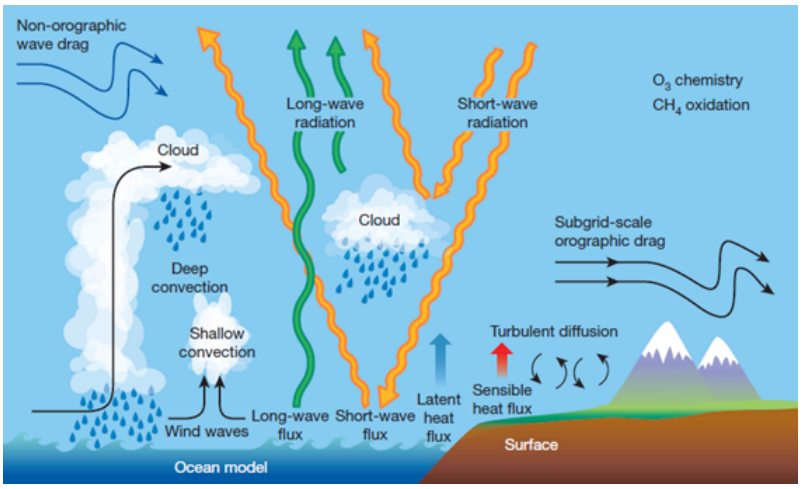

Figure 2.1: Physical processes of importance to weather prediction (Bauer et al., 2015)

Even though the physical process is well understood and modelled, since the output and input variables are often not the same, determining power generation from weather forecasts is not always straightforward. One way to circumvent this issue is to construct a statistical model of the relation between the outcome of the NWP and the power generated, in what is commonly known as an hybrid model (Sweeney et al., 2019).

2.2 Statistical Models

Statistical models aim at bridging the gap between weather forecasts and renewable power observations. In NWP postprocessing, statistical models are used to generate power production forecasts of a few hours to days ahead (hybrid models). In forecast horizons of less than two hours, statistical models are used to predict the next values of power production time series. Furthermore, given their high computational costs, physical models are practically unusable in timescales of minutes, making statistical models the best suited for very short-term forecasting(Sweeney et al., 2019).

Most statistical forecasting models follow either a time series analysis or a machine learning approach. It is also relevant to make a distinction between linear and non-linear models. As the name suggests, non-linear models are those in which the fitting function, f, is a non-linear function. Non-linear models may also be obtained by adding several functions in a piecewise manner (e.g., splines). In general, non-linear models are more flexible, but also more prone to overfitting than linear ones.

2.2.1 Persistence

The simplest very short-term statistical model is Persistence, in which the forecast is equal to the most recent observation. Persistence is commonly used as a benchmark in very-short term forecasting (Sweeney et al., 2019).

2.2.2 Time series models

Time-series models make use of classical statistics methods, such as regression, to model the evolution of a target variable, *y*, in time. If only the past measurements of *y* are used, the model is said to be a univariate model. However, if past measurements from other variables are used, the model is often described as a multivariate one.

Univariate regression models take the form

$$\hat{y}_t = f(y_{t-1}, ..., y_{t-n}) + e_t \tag{2.1}$$

where f is a generic function, $y_{t-1}, \ldots, y_{t-n}$ are the past values of the target variable *y* and e_t are variations that cannot be explained by the regression model (white noise) (Monteiro et al., 2009).

One example of a time series regression model is the Autoregressive (AR) model. Discussed thoroughly in Section 3.1.1., an AR(*p*) model takes the form of a linear combination of the *p* past observations of the target variable. If one or more external (exogenous) variables are thought to affect the system, these may be included in the model in an AR model with exogenous variables (AR-X), model discussed thoroughly in Section 3.1.2.

Forecasting with geographically distributed data

As discussed in Section 1.2., models that take in geographically distributed data in the forecast are able take advantage of the correlations in power generation data collected in neighbouring sites. As such, spatiotemporal models make use of past values of the target variable at multiple geographically distributed sites (multivariate regression).

Spatiotemporal models take the form

$$\hat{y}_t = f(y_{t-1}, \ldots, y_{t-n}, \chi_{t-1}, \chi_{t-2}, \ldots, \chi_{t-n}) + e_t \tag{2.2}$$

where $\chi_{t-1}, \chi_{t-2}, \ldots, \chi_{t-n}$ are the past values of variables χ.

Ghofrani and Alolayan (2018) presents a review of studies applying time series analysis techniques to renewable power forecasting. These include the use the Vector Autoregressive (VAR) model, method which is thoroughly discussed in Section 3.2.1.

2.2.3 Machine learning models

A machine learning approach makes use of computing systems such as Artificial Neural Networks (ANN) and Support Vector Machines (SVM) to model complex relations between the input variables and the target variable. Machine learning uses past observations of one or more variables to acquire knowledge on a given process (inductive learning). The tasks conducted by machine learning take either the form of supervised learning, unsupervised learning or reinforcement learning tasks. In supervised learning tasks, which include classification and regression problems, labelled data is used to train the model, which is then used to make predictions on unlabelled data. The main goal of unsupervised learning tasks is to explore and describe a given dataset. These include clustering and association problems (Gama, Carvalho, Faceli, Lorena, & Oliveira, 2012).

Tree-based models and gradient boosting

Tree-based models work by recursively partitioning the predictor space into a number of simpler non-overlapping regions. Widely used for both classification (decision trees) and regression (regression trees) problems, tree models are acyclic graphs where each node is either a leaf node or a decision node. Corresponding to the final subsets of a tree model, leaf nodes usually take the value of the mode (classification) or the mean (regression) of the response values of the training observations in that subset of the predictor space. The prediction for a given observation in a regression setting is, then, the mean of the response values of the training observations that have fallen on the same leaf node. Decision nodes are intermediate nodes where, based on a conditional test, the splitting is performed (Gama et al., 2012).

While simple and easily interpretable, standard tree-based methods are usually not as accurate as other machine learning algorithms. As a consequence, a number of approaches aiming to enhance the capabilities of these models have been developed. Two of such approaches are bagging and gradient boosting.

One of the problems with standard tree-based methods is the propensity to overfitting the training dataset, resulting in models with high variance. Designed to reduce the variance of statistical learning methods, the Bootstrap Aggregation (Bagging) procedure consists in extracting many training sets from the population, building separate models for each subset, and averaging the predictions. In Bagging, the training sets are generated independently by taking repeated samples from the original training dataset (bootstrap) (James, Witten, Hastie, & Tibshirani, 2000)).

Another approach to improve standard tree-based methods is boosting. While bagging generates independent training datasets from the original dataset, the boosting procedure consists in training trees sequentially, using the residuals from the trees that preceded it. This approach aims to slowly improve the model in areas of the predictor space where it performs poorly (James et al., 2000).

Algorithm 1 Boosting for Regressions Trees (James et al., 2000).

1. Set $\hat{f}(x) = 0$ and $r_i = y_i$ for all i in the training set.
2. For $b = 1, 2, ..., B$, repeat:
   (a) Fit a tree $\hat{f}^b$ with d splits ($d + 1$ terminal nodes) to the training data (X,r).
   (b) Update $\hat{f}$ by adding in a shrunken version of the new tree:

$$\hat{f}(x) \leftarrow \hat{f}(x) + \lambda \hat{f}^b(x). \tag{2.3}$$

   where λ is the shrinkage parameter.
   (c) Update the residuals,

$$r_i \leftarrow r_i - \lambda \hat{f}^b(x_i) \tag{2.4}$$

3. Output the boosted model,

$$\hat{f}(x) = \sum_{b=1}^{B} \lambda \hat{f}^b(x). \tag{2.5}$$

The term gradient boosting refers to the numerical optimization problem of a boosting procedure, where the objective is to minimize the loss function of the model by successively adding trees. In gradient boosting, this optimization is performed using gradient descent, an optimization algorithm for finding a local minimum of a differentiable function (Mujtaba, 2020).

An up-to-date literature review on renewable power forecasting using machine learning approaches can be found at Lai, Chang, Chen, and Pai (2020). Commonly applied methods include SVM-based approaches and ANN-based approaches, models which will not be discussed in the present work. Bessa, Trindade, and Miranda (2015) combines VAR and gradient boosting to explore Photovoltaic (PV) observations from a smart grid.

Chapter 3

Time Series Models for Renewable Power Forecasting

This chapter introduces the time series regression frameworks that will be implemented and compared in Chapter 4.

The first section concerns the use of autoregression-based models in a univariate setting. The second section introduces the subject of vector autoregression, i.e., autoregression-based models in a multivariate setting. In the third section, the subject of LASSO regularization is discussed, as well as its use in vector autoregressive models.

3.1 Autoregressive Processes

Autoregressive processes are trends that can be explained by their own preceding values. AR models usually take the form of a linear combination of the *p* lagged values, where *p* refers to the order of the process.

This section introduces the different AR models to be implemented.

3.1.1 Autoregressive (AR) model

The standard AR model predicts each WPP power measurement time series separately by using a linear combination of the most recent observations.

The future trajectory of an AR model of order *p*, AR(*p*), is given by

$$y_{i,t} = \mu + \sum_{l=1}^{p} \beta^{(l)} \cdot y_{i,t-l} + \epsilon_t \tag{3.1}$$

where $\{y_{i,t}\}_{t=1}^{T}$ is the time series containing the power measurements at WPP$_i$, μ is a constant or intercept term, $\beta^{(l)}$ is the model coefficient associated with lag l of the wind power time series and ϵ_t is an error term with zero mean and constant variance σ_ϵ^2 (Cavalcante et al., 2017).

3.1.2 Autoregressive Model with Exogenous Variables (AR-X)

An AR process may be affected by other variables which are determined outside the system (exogenous). AR models that use exogenous variables are commonly designated AR-X models.

An AR-X model of order p with s exogenous variables takes the form

$$y_{i,t} = \mu + \sum_{l=1}^{p} \beta^{(l)} \cdot y_{i,t-l} + \sum_{k=1}^{s} \alpha^{(k)} \cdot x_{k,t} + \epsilon_t \tag{3.2}$$

where $\{y_{i,t}\}_{t=1}^{T}$ is the time series containing the power measurements at WPP$_i$, $\{x_{k,t}\}_{t=1}^{T}$ is the time series corresponding to the k^{th} exogenous variable, μ is a constant or intercept term, $\beta^{(l)}$ is the model coefficient associated with lag l of the wind power time series, $\alpha^{(k)}$ is the coefficient associated with the k^{th} exogenous variable and ϵ_t is an error term with zero mean and constant variance σ_ϵ^2.

3.1.3 Additive Autoregressive Model with Exogenous Variables (AAR-X)

Designed to overcome the lack of flexibility of linear models, additive models are obtained from the sum of the partial responses of each predictor variable.

Additive models are used in renewable power forecasting to model the non-linear relation between the weather forecasts and renewable power generation. In an AAR-X, the relation between the target variable and its lagged values is modelled in the same manner as the standard AR and AR-X models, while the relation between the exogenous variables and the target variable is modelled using smooth functions. This is performed in an additive way, so that each function is smoothed in a restricted part of the training data.

To fit the training data, additive models make use of smooth functions such as splines. Splines are polynomial functions defined in a piecewise manner. In an additive model, each spline is used to model a particular section of the observed data. The degree of a spline is given by the maximum degree of the corresponding polynomial function. For instance, a linear spline has degree one, whereas a cubic spline has degree three.

The points where the separate regression splines connect are called knots. The fact that the number and location of the knots may not be known a priori means that smoothing regression splines can become very computationally demanding without an efficient strategy (Wand, 2000).

Instead of specifying the number of knots, it is possible to refer to the number of degrees of freedom of a spline. An additive model with *df* degrees of freedom will have $k = df - degree - 1$ (if there is an intercept) knots.

An additive AR-X model with d degrees of freedom, p lags and s exogenous variables takes the form

$$y_{i,t} = \mu + \sum_{l=1}^{p} \beta^{(l)} \cdot y_{i,t-l} + \sum_{k=1}^{s} \sum_{j=1}^{d} f_j(x_{k,t}) + \epsilon_t \tag{3.3}$$

where $\{y_{i,t}\}_{t=1}^{T}$ is the time series containing the power measurements at WPP_i, $\{x_{k,t}\}_{t=1}^{T}$ is the time series corresponding to thek^{th} exogenous variable, μ is a constant or intercept term, $\beta^{(l)}$ is

the model coefficient associated with lag l of the wind power time series, f_j are smooth functions and ϵ_t is an error term with zero mean and constant variance σ_ϵ^2.

The present work will make use of two different types of splines: natural cubic splines and B splines of the third degree (cubic B splines). The main difference between the two is that, whereas the natural cubic splines model extrapolates beyond the knots, in the B splines model, the second derivative of each polynomial is set to zero at the knots, which constitutes a necessary boundary condition. This difference tends to make natural cubic splines less flexible than B splines but also less susceptible to oscillations at the knots.

3.2 Vector Autoregressive (VAR) Processes

This section introduces the models capable of capturing the correlations in power generation data collected in geographically distributed sites (spatiotemporal models).

3.2.1 Vector Autoregressive (VAR) Model

Introduced by Sims (1980), VAR models are widely used in economics and finance. They make use of past (lagged) observations to describe the dynamic behaviour of multiple time series, being an extension of the AR model to multivariate time series. In a VAR model, each variable is explained both by its own lagged values and current and past values of the remaining variables included in the model. A VAR model is, therefore, capable of capturing the linear interdependencies between the various time series (Cavalcante et al., 2017).

A VAR model consists of a multi-equation system where all the variables are treated as endogenous, meaning that it is presumed to exist correlation between them. A p_{th} order VAR model takes the form

$$Y_t = \eta + \sum_{l=1}^{p} B^{(l)} \cdot Y_{t-l} + e_t \tag{3.4}$$

where $\{Y_t\}_{t=1}^{T}$ is a n-dimensional time series containing the power measurements at the n WPPs, $\eta = [\eta_1, ..., \eta_n]$ is a vector of constant terms, $B^{(l)}$ is the coefficient matrix associated with lag l of the wind power time series and e_t is a vector of error terms with zero mean and constant variance σ_e^2 (Cavalcante et al., 2017).

If Y_t is assumed to follow a centred process ($\eta = 0$), a $\text{VAR}_{n(p)}$ model can be written in matrix form as

$$Y = BZ + E \tag{3.5}$$

where $Y = [y_1, ..., y_T]$, $B = [B^{(1)}, ..., B^{(p)}]$, $Z = [z_1, ..., z_T]$, $z_t = [Y_{t-1}^\top, \ldots, Y_{t-l}^\top]$, and $E = [e_1, ..., e_T]$.

3.2.2 Vector Autoregressive Model with Exogenous Variables (VAR-X)

VAR models that use exogenous variables are designated VAR-X models. Although deterministic variables can be used, exogenous variables are often defined in probabilistic terms.

Variables related to stochastic processes, such as the weather, are often used in VAR-X models (Lütkepohl, 2005). A VAR-X model of order p with s exogenous variables takes the form

$$Y_t = \eta + \sum_{l=1}^{p} B^{(l)} \cdot Y_{t-l} + \sum_{k=1}^{s} \alpha^{(k)} \cdot x_{k,t} + e_t \tag{3.6}$$

where $\{Y_t\}_{t=1}^{T}$ is a n-dimensional time series containing the average power measurements at the n WPPs, $\{x_{t,k}\}_{t=1}^{T}$ is the time series corresponding to the k^{th} exogenous variable, $\eta = [\eta_1, ..., \eta_n]$ is a vector of constant terms, $B^{(l)}$ is the coefficient matrix associated with lag l of the wind power time series, $\alpha^{(k)}$ is the coefficient vector associated with the k^{th} exogenous variable and e_t is a vector of error terms with zero mean and constant variance σ_e^2.

3.2.3 Additive Vector Autoregressive Model with Exogenous Variables (AVAR-X)

Identically to AAR-X models, AVAR-X models are implemented to model non-linear relations between the target variables and the exogenous variables.

An AVAR-X model with d degrees of freedom, p lags and s exogenous variables takes the form

$$Y_t = \eta + \sum_{l=1}^{p} B^{(l)} \cdot Y_{t-l} + \sum_{k=1}^{s} \sum_{j=1}^{d} f_j(x_{k,t}) + e_t \tag{3.7}$$

where $\{Y_t\}_{t=1}^{T}$ is a n-dimensional time series containing the power measurements at the n WPPs, $\{x_{k,t}\}_{t=1}^{T}$ is the time series corresponding to the k^{th} exogenous variable, $\eta = [\eta_1, ..., \eta_n]$ is a vector of constant terms, $B^{(l)}$ is the coefficient matrix associated with lag l of the wind power time series, f_j are smooth functions and e_t is a vector of error terms with zero mean and constant variance σ_e^2.

3.3 Least Absolute Shrinkage and Selection Operator (LASSO)

Introduced by Tibshirani (1996), LASSO is a regularization method used in statistics to prevent overfitting the model to the data. It is also useful to assure computational viability in models with many variables. LASSO works by adding a L_1 penalty to the value of the coefficients, meaning that some coefficients may become equal to zero. The result is a simpler sparse model where only the coefficients with the strongest contributions are considered.

The combination of LASSO and VAR was introduced in Hsu, Hung, and Chang (2008) to overcome the difficulty of VAR in handling high-dimensional data, which results from the coefficients matrix growing quadratically with the number of time series being considered in the model (Cavalcante et al., 2017).

LASSO can generate different sets of sparse models, depending on the loss function used. The standard LASSO-VAR (sLV) loss function is given by

$$\frac{1}{2}\|Y - BZ\|_2^2 + \lambda\|B\|_1 \tag{3.8}$$

where $\lambda > 0$ is a scalar regularization parameter controlling the amount of shrinkage. Hence the LASSO-VAR coefficients can be estimated by computing

$$\hat{B} = argmin_B \left(\frac{1}{2} \|Y - BZ\|_2^2 + \lambda \|B\|_1 \right) \tag{3.9}$$

Another approach consists in grouping the coefficients by their time lags, meaning that, for a given time, either all or none of the lags are considered. The lag-group LASSO-VAR (lLV) loss function is given by

$$\frac{1}{2} \|Y - BZ\|_2^2 + \lambda \sum_{l=1}^{p} \|B^{(l)}\|_2 \tag{3.10}$$

where $B^{(l)}$ is a matrix that contains the lag l coefficients.

While this approach can be useful for lag selection, it is sometimes inefficient, since it may include or exclude an entire lag even if only a small number of coefficients is significant.

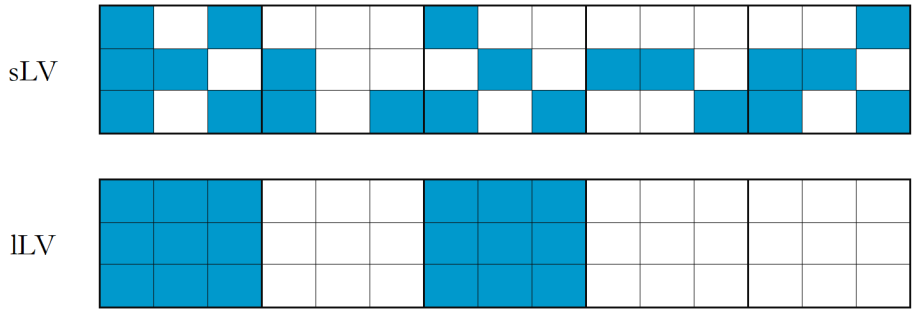

Figure 3.1: Example of sLV and lLV structures [Adapted from Cavalcante et al. (2017)].

LASSO-VAR models have been successfully used in renewable power forecasting. Cavalcante et al. (2017) uses VAR with several variants of LASSO for very-short term wind power forecasting, concluding that the sparse model outperformed Persistence, the AR model, and the standard VAR model. Other examples of the use of VAR in renewable energy forecasting are presented in Bessa et al. (2015) and Messner and Pinson (2019).

LASSO-VAR model fitting with ADMM

Introduced by Boyd, Parikh, Chu, Peleato, and Eckstein (2010), the Alternating Direction Method of Multipliers (ADMM) is a recent algorithm used to solve complex optimization problems. Developed as a combination of the dual ascent method and the method of multipliers, ADMM enables parallel estimation for data divided by records or features. In ADMM form, the objective function is split into two distinct objective functions. This is done by replicating variable B in variable H and adding an equality restriction.

Hence, the objective function in (3.8) is given by

$$minimize \quad \frac{1}{2}\|Y - BZ\|_2^2 + \lambda\|H\|_1 \tag{3.11}$$

$$subject\ to \quad B - H = 0$$

And the solution for (3.9) by

$$argmin_B \left(\frac{1}{2}\|Y - BZ\|_2^2 + \lambda\|H\|_1\right) \tag{3.12}$$

$$subject\ to \quad H = B$$

The solution to the ADMM problem can then be obtained by performing alternating minimization of the augmented Lagrangian of (3.12) over B and H (Cavalcante et al., 2017).

Chapter 4

Forecasting Results and Discussion

4.1 Data and Tools

The present work makes use of data provided at the *Global Energy Forecasting Competition* (GEFCom) 2014. GEFCom is one of the leading competitions for probabilistic energy forecasting, with over 200 participants from more than 40 countries taking part in the 2014 edition. The competition was divided into four tracks: electric load, electricity price, wind power, and solar power forecasting.

The goal of the wind power forecasting track of GEFCom was to predict the wind power generation 24 hours-ahead in 10 zones, corresponding to 10 Wind Power Plants (WPPs) in Australia.

The explanatory variables available are past power measurements in all 10 WPPs, normalized by the respective nominal capacity of each WPP, which takes values between zero and one, and input weather forecasts, given as the zonal and meridional wind components, u and v, at two heights, 10 and 100 m. Although these components were not altered in any way before being used in the models, if necessary, they can be used to deduce wind and direction forecasts. Provided for the location of each WPP, these forecasts were issued every day at midnight, meaning that the observations registered at 01:00 refer to a forecast made one hour before, the observations registered at 02:00 refer to a forecast made two hours before, and so on. In total, five variables were provided for each WPP location.

The dataset used in the present work corresponds to Task 15 of the wind power track of GEFCom 2014 and comprises hourly observations of the five aforementioned variables (power generated, u at 10 m, v at 10 m, u at 100 m, and v at 100 m) for each of the 10 WPPs (50 variables in total) between 01/01/2012 and 01/12/2013 (16800 observations).

The present work makes use of a previously developed VAR model written in R programming language.

4.2 Exploratory Data Analysis

Corresponding to the normalized past power measurements in 10 WPPs (ZONE1, ZONE2, and so on), the target variables take values between zero and one. The mean value of all observations at the 10 WPPs is 0.3615, whereas the highest mean was recorded in ZONE10 and the lowest mean in ZONE9.

Table 4.1: Mean value of power generated at each WPP.

ZONE1	ZONE2	ZONE3	ZONE4	ZONE5	ZONE6	ZONE7	ZONE8	ZONE9	ZONE10
0.304	0.319	0.41	0.356	0.43	0.436	0.304	0.303	0.297	0.456

Figure 4.1 presents the boxplots for the power measurement time series at all WPPs.

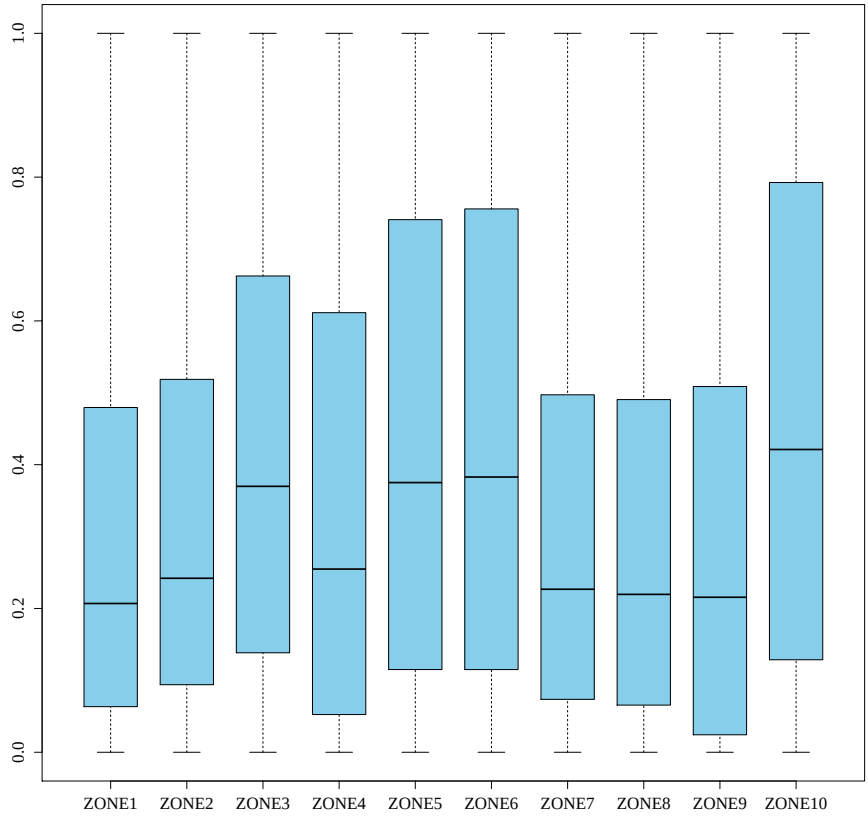

Figure 4.1: Distribution of power generation values in all WPPs.

4.2.1 Autocorrelation

Autocorrelation can be seen as the capacity of a variable to predict itself. In a time series, autocorrelation measures the degree of correlation between a lagged value of the variable and its present value.

Introduced by Geurts, Box, and Jenkins (1977), the autocorrelation coefficient is a widely used indicator of autocorrelation. In autoregression-based models, the autocorrelation coefficient can be used to identify the appropriate number of lags to consider in a model, i.e., the order of the model. The autocorrelation coefficient takes values between +1 and -1, where the first represents a perfect positive correlation and the latter a perfect negative correlation.

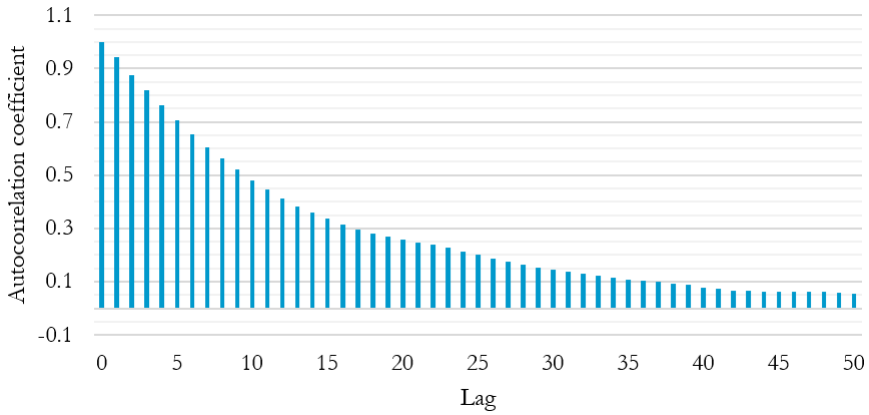

Figure 4.2: Lag autocorrelation for ZONE1.

Figure 4.2 presents the mean autocorrelation coefficients for the first 50 lags of ZONE1 (complete results in Appendix A.1) and Table 4.2 displays the mean autocorrelation coefficients for the first 20 lags of all WPPs.

It is possible to conclude that, on average, the power measurement at any given time displays a positive correlation with the first 20 lags. For all WPPs, the first lags display a very high autocorrelation with the present values (>0.9), whereas the twentieth lags have coefficients, in general, around 0.25.

The WPPs with the worst mean correlation for the first 20 lags are ZONE10 (0.391), ZONE6 (0.464) and ZONE5 (0.474).

On the opposite side, the WPPs with the best mean correlation for the first 20 lags are ZONE7 (0.530), ZONE2 (0.524) and ZONE3 (0.519).

Although these results were ultimately not used, due to the use of Bayesian Optimization to optimize the number of lags, it is reasonable to say that, since they display significantly high levels of correlation with the respective present values, all 20 first lags for each time series could be used in an autoregressive model.

Table 4.2: Autocorrelation Coefficients for all WPPs (20 lags)

Lag	ZONE1	ZONE2	ZONE3	ZONE4	ZONE5	ZONE6	ZONE7	ZONE8	ZONE9	ZONE10
1	0.9423	0.9488	0.9496	0.9337	0.9457	0.9439	0.9433	0.9266	0.9283	0.9361
2	0.8764	0.8770	0.8820	0.8515	0.8672	0.8652	0.8772	0.8476	0.8447	0.8369
3	0.8179	0.8103	0.8200	0.7839	0.7910	0.7882	0.8170	0.7816	0.7752	0.7426
4	0.7616	0.7494	0.7614	0.7235	0.7170	0.7137	0.7624	0.7238	0.7150	0.6555
5	0.7063	0.6937	0.7083	0.6685	0.6453	0.6424	0.7127	0.6741	0.6623	0.5753
6	0.6538	0.6425	0.6603	0.6219	0.5809	0.5766	0.6653	0.6272	0.6128	0.5046
7	0.6058	0.5972	0.6160	0.5786	0.5228	0.5173	0.6220	0.5850	0.5680	0.4414
8	0.5611	0.5572	0.5752	0.5406	0.4723	0.4642	0.5820	0.5457	0.5265	0.3836
9	0.5195	0.5209	0.5358	0.5071	0.4294	0.4183	0.5433	0.5087	0.4884	0.3322
10	0.4802	0.4870	0.4974	0.4788	0.3931	0.3803	0.5055	0.4715	0.4525	0.2884
11	0.4448	0.4546	0.4627	0.4539	0.3632	0.3509	0.4700	0.4378	0.4187	0.2518
12	0.4118	0.4246	0.4310	0.4302	0.3403	0.3275	0.4367	0.4089	0.3908	0.2232
13	0.3830	0.3995	0.4010	0.4055	0.3216	0.3087	0.4074	0.3812	0.3644	0.2043
14	0.3586	0.3775	0.3719	0.3816	0.3077	0.2955	0.3807	0.3558	0.3421	0.1936
15	0.3352	0.3589	0.3440	0.3611	0.2990	0.2879	0.3564	0.3316	0.3233	0.1878
16	0.3142	0.3432	0.3184	0.3426	0.2943	0.2823	0.3361	0.3105	0.3053	0.1889
17	0.2965	0.3288	0.2945	0.3266	0.2933	0.2794	0.3190	0.2915	0.2895	0.1970
18	0.2815	0.3145	0.2710	0.3111	0.2947	0.2786	0.3037	0.2778	0.2754	0.2103
19	0.2680	0.3008	0.2491	0.2997	0.2990	0.2801	0.2893	0.2647	0.2652	0.2283
20	0.2574	0.2891	0.2308	0.2934	0.3038	0.2837	0.2777	0.2542	0.2583	0.2463

4.2.2 Cross-correlation

Cross-correlation refers to the quality of variables to predict each other. Variables that are strongly correlated are usually good at predicting each other, whereas poorly correlated variables are not.

Between Endogenous Variables

The cross-correlation coefficient measures the degree of correlation between different time series. Like the autocorrelation coefficient, it takes values between +1 and -1, where the positive values indicate a positive correlation and the negative values a negative one.

The mean cross-correlation coefficients for the first 10 lags of all WPPs were computed. Table 4.3 displays the results obtained for ZONE1 (complete results in Appendix A.2). The results show that, in general, the power measurement in ZONE1 is positively correlated with the first 10 lags of the remaining WPPs. With all coefficients of the first 10 lags above 0.4, ZONE3 seems to be the WPP better suited to forecast ZONE1. These results could also indicate a proximity between the location of these two WPPs.

Table 4.3: Cross-correlation Coefficients for ZONE1

Lag	ZONE2	ZONE3	ZONE4	ZONE5	ZONE6	ZONE7	ZONE8	ZONE9	ZONE10
0	0.3343	0.6322	0.395	0.611	0.6497	0.6601	0.31	0.2818	0.3384
1	0.327	0.649	0.3807	0.5963	0.6222	0.6268	0.3021	0.2734	0.344
2	0.3171	0.6503	0.3597	0.5666	0.5771	0.5782	0.2897	0.2603	0.3433
3	0.3044	0.6386	0.3336	0.5297	0.5213	0.523	0.2751	0.2454	0.3346
4	0.2907	0.6179	0.3057	0.4911	0.4639	0.466	0.2603	0.2309	0.322
5	0.2738	0.5926	0.2778	0.453	0.407	0.4115	0.2439	0.2163	0.306
6	0.2559	0.5625	0.249	0.4159	0.3554	0.3599	0.228	0.2009	0.286
7	0.2351	0.53	0.2226	0.3785	0.3078	0.3104	0.2094	0.1833	0.2626
8	0.2136	0.4975	0.1974	0.3431	0.2647	0.2664	0.1878	0.1635	0.2369
9	0.1927	0.4639	0.1731	0.3096	0.2281	0.2287	0.1657	0.1436	0.2121
10	0.1727	0.4325	0.1503	0.2781	0.1975	0.1965	0.1449	0.1245	0.1891

The mean cross-correlation coefficients for each WPP were computed (Table 4.4).

The WPPs with the lowest correlation with the remaining WPPs for the first 10 lags are ZONE2 (0.316), ZONE1 (0.349) and ZONE10 (0.349). The WPPs with the highest correlation are ZONE9 (0.476), ZONE3 (0.466) and ZONE7 (0.463).

Table 4.4: Mean Cross-correlation Coefficients with the remaining WPP for each WPP.

Lag	ZONE1	ZONE2	ZONE3	ZONE4	ZONE5	ZONE6	ZONE7	ZONE8	ZONE9	ZONE10
0	0.4681	0.4516	0.4481	0.5781	0.5724	0.5758	0.5544	0.5201	0.5210	0.4681
1	0.4579	0.4304	0.4645	0.5647	0.5628	0.5689	0.5422	0.5094	0.5221	0.4579
2	0.4380	0.4045	0.4751	0.5410	0.5415	0.5489	0.5237	0.4929	0.5177	0.4380
3	0.4117	0.3759	0.4808	0.5135	0.5149	0.5233	0.5038	0.4751	0.5105	0.4117
4	0.3832	0.3459	0.4828	0.4832	0.4853	0.4949	0.4835	0.4571	0.4998	0.3832
5	0.3535	0.3164	0.4811	0.4505	0.4533	0.4636	0.4634	0.4393	0.4860	0.3535
6	0.3237	0.2870	0.4762	0.4182	0.4219	0.4319	0.4432	0.4212	0.4708	0.3237
7	0.2933	0.2575	0.4690	0.3878	0.3920	0.4018	0.4232	0.4027	0.4535	0.2933
8	0.2634	0.2291	0.4599	0.3591	0.3636	0.3732	0.4039	0.3856	0.4351	0.2634
9	0.2353	0.2025	0.4487	0.3335	0.3376	0.3470	0.3852	0.3690	0.4163	0.2353
10	0.2096	0.1775	0.4375	0.3104	0.3140	0.3233	0.3671	0.3530	0.3978	0.2096

Between Endogenous and Exogenous Variables

To study the relation between the weather forecasts and power generation, scatter plots were computed for all WPPs (results in Appendix A.2). Although the relation between these variables is known to be not linear, linear regression models were fitted to assess potential positive or negative linear correlations.

For the power generation at ZONE1, the results seem to display a mild positive correlation with the zonal wind component, *u*, at both 10m and 100m heights, and a mild negative correlation with the meridional wind component, *v*. The same applies to ZONES 2, 4, 5, 6 and 9. ZONES 7 and 8 seem to display a mild positive correlation with the zonal wind component at both heights and a very small to non-existent correlation with the meridional wind component.

ZONE3 displays positive correlations with both the zonal and meridional wind components at both heights and ZONE10 seems to display a very small to non-existent linear correlation with both variables.

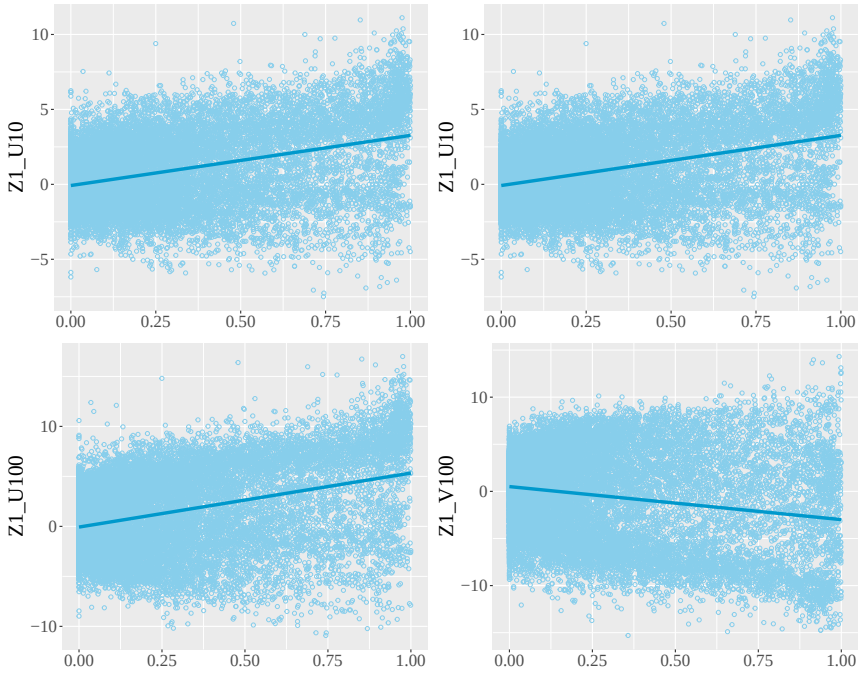

Figure 4.3: Correlation between power production and the weather forecasts, z and u, for ZONE1.

4.3 Model Performance Comparison and Metrics

This section introduces the performance metrics and statistical tests used to assess the quality of the models.

4.3.1 Performance Metrics

The two metrics most widely used to assess the quality of the models employed in renewable power forecasting are the Mean Absolute Error (MAE) and the Root Mean Squared Error (RMSE). Other tools for performance evaluation include histograms of the frequency distribution of the error, the correlation coefficient, R, the Mean Absolute Percentage Error (MAPE) and the coefficient of determination, R^2 (Wang et al., 2011). Given that they are industry standards, the RMSE and MAE metrics were computed.

Mean Absolute Error (MAE)

The MAE is given by

$$MAE = \frac{1}{n}\sum_{i=1}^{n}|\tilde{x}_i - x| \tag{4.1}$$

where n is the total number of samples, $\tilde{x}$ is the predicted value and x is the observed value.

Root Mean Squared Error (RMSE)

The RMSE is given by

$$RMSE = \sqrt{\frac{1}{n}\sum_{i=1}^{n}(\tilde{x}_i - x)^2} \tag{4.2}$$

4.3.2 Comparison Tests

Two statistical tests will be used to compare the performance of the models: the Friedman test, which compares the performance of multiple models, and the Diebold-Mariano test, which compares the performance of two models.

Friedman Test

The Friedman test is a statistical test used to compare the performance of multiple models. It compares the mean ranks for each group of forecasts and shows how the groups differ.

Under the null hypothesis, which states that all models are equivalent in terms of their predictive capability, the test statistics, F_F, follows a chi-squared distribution (Gama et al., 2012).

If the null hypothesis is rejected, it is possible to conclude that there is a significant difference in performance between the models. However, to assess which particular models are dissimilar, a post-test must be performed. In the post-test, two models are said to be statistically different if their mean ranks are greater or equal than the Critical Difference, CD, where

$$CD = q_\alpha\sqrt{\frac{A(A+1)}{6N}} \tag{4.3}$$

where N in the number of blocks of observations used in the ranking, A is the number of models being tested and q_α can be obtained from the Nemenyi statistics (Nemenyi, 1963).

Diebold-Mariano Test

Introduced by Diebold and Mariano (1995), the Diebold-Mariano test is a statistical test designed to determine whether the forecasts produced by two models are significantly different.

For $h \geq 0$, the Diebold-Mariano statistic is given by

$$DM = \frac{\bar{d}}{\sqrt{[\gamma_0 + 2\sum_{k=1}^{h-1}\gamma_k]/n}} \tag{4.4}$$

where $\bar{d}$ is the sample mean of the loss differential time series, $\{d_t\}_{t=1}^{T}$, and γ_k is the autocovariance at lag k.

According to the null hypothesis, which states that there is no significant difference between the two models, DM follows a standard normal distribution.

$$DM \sim N(0, 1) \tag{4.5}$$

If $|DM| > Z_{crit}$, the null hypothesis is rejected and, therefore, it is possible to conclude that there is a significant difference between the predictive capabilities of the two models.

4.4 Model Optimization

Like most statistical learning models, autoregression-based models like the ones described in Chapter 3 contain hyperparameters, i.e., parameters that are not directly estimated by the model and need to be set manually. Hence, hyperparameter optimization (tunning) is necessary to obtain the set of parameters that will lead to the best results.

The simplest approach would be to run the model iteratively, changing the parameters at each iteration, and choose the set of parameters that leads to the smallest error. This strategy is, however, very inefficient and time consuming.

Introduced by Mockus, Tiesis, and Zilinskas (1978), Bayesian Optimization is a more efficient way to tackle the issue of parameter optimization. It assumes that the function to be optimized was sampled from a Gaussian process, maintaining a posterior distribution as new observations are introduced. The process can be driven by the maximization of either the Expected Improvement (EI) or the Gaussian process Upper Confidence Bound (UCB) (Snoek, Larochelle, & Adams, 2012).

Algorithm 2 Pseudo-code for Bayesian Optimization (Frazier, 2018).

Place a Gaussian process prior on f.
Observe f at n_0 points according to an initial space-filling experimental design. Set $n = n_0$.
while $n \leq N$ **do**
    Update the posterior probability distribution on f using all available data.
    Let x_n be a maximizer of the acquisition function over x, where the acquisition function is computed using the current posterior distribution.
    Observe $y_n = f(x_n)$.
    Increment n.
end while
Return a solution: either the point evaluated with the largest $f(x)$, or the point with the largest posterior mean.

In the case of the AR models, Bayesian Optimization was used to optimize the following parameters:

- λ hyperparameter

- ρ hyperparameter
- number of lags used in the model
- degrees of freedom of the splines used in the additive models

In the Gradient Boosting algorithm, Bayesian Optimization was used to optimize:

- maximum tree depth
- minimum child weight, i.e., the minimum instance weight required for a leaf node to be kept in the model
- subsampling ratio of the training observations
- number of lags used in the model

The parameters introduced and results of the Bayesian Optimization are presented in Appendix A.3.

Even though the optimization space was significantly restricted for computational reasons, the results obtained indicate that the models without exogenous variables seem to benefit from the use of more lags, whereas the models using weather forecasts in additive settings seem to perform better by using just one to three lagged values. In these models, the optimal number of degrees of freedom seems to be around four.

4.5 Intraday and Day-Ahead Forecasting Results

This sections presents the results of the application of the AR models introduced in Chapter 3 to the GEFCom 2014 dataset described in Section 4.1.

The models were used to make forecasts of 1 to 24 hours-ahead of the wind power generated in 10 WPPs.

4.5.1 AR model

The AR model described in Section 3.1.1. was implemented. For each WPP (10 models), only the past power measurements recorded at that specific location are used. The mean RMSE and MAE obtained with the model for each timescale are displayed in Figure 4.4 and Table 4.5.

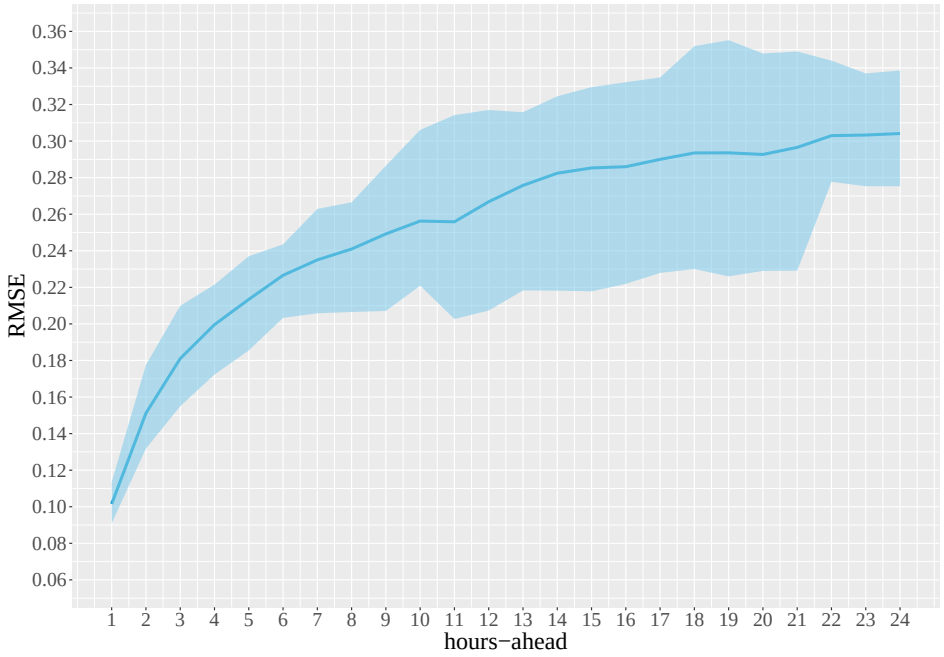

Figure 4.4: Mean RMSE for all WPPs and Max/Min values obtained with the AR model.

The AR model yielded mean RMSE values between 0.10, for the 1 hour-ahead forecast, and 0.30, for the 24 hours-ahead forecast. ZONE9 was the WPP with the best results in most timescales (between 11 hours-ahead and 21 hours-ahead), whereas ZONE10 was the worst in 11 timescales (between 2 hours-ahead and 12 hours-ahead). At this point, it is relevant to remember that ZONE10 was the WPP that displayed the lowest mean autocorrelation coefficient in Section 4.2.1, while ZONE9 displayed average results for the first 20 lags.

As expected, the AR model performs better when forecasting the first few hours-ahead. As the time interval between the lags used in the model and the forecast increases, the model starts to lose its predictive capability, yielding RMSE values above 0.25 for the 10 hours-ahead forecast onward.

Regarding the MAE, the AR model yielded mean results between 0.071, for the 1 hour-ahead forecast, and 0.26, for the 24 hours-ahead forecast.

Table 4.5: AR Model Results Summary

hours-ahead	RMSE					MAE				
	Mean Value	Maximum Value		Minimum Value		Mean Value	Maximum Value		Minimum Value	
		Value	WPP	Value	WPP		Value	WPP	Value	WPP
1	0.10154	0.1135	ZONE9	0.0909	ZONE5	0.07096	0.0758	ZONE4	0.0622	ZONE2
2	0.15118	0.1776	ZONE10	0.1318	ZONE2	0.11098	0.13	ZONE10	0.0969	ZONE2
3	0.18106	0.2099	ZONE10	0.155	ZONE2	0.13641	0.165	ZONE10	0.1127	ZONE2
4	0.19961	0.2215	ZONE10	0.1723	ZONE2	0.15466	0.1797	ZONE10	0.1283	ZONE2
5	0.21341	0.237	ZONE10	0.1855	ZONE7	0.16762	0.1908	ZONE10	0.1447	ZONE2
6	0.22658	0.2435	ZONE10	0.2033	ZONE2	0.17958	0.199	ZONE10	0.1554	ZONE2
7	0.23501	0.2629	ZONE10	0.2058	ZONE7	0.18656	0.2181	ZONE10	0.1611	ZONE2
8	0.24096	0.2665	ZONE10	0.2065	ZONE7	0.19319	0.2231	ZONE10	0.162	ZONE7
9	0.24922	0.2865	ZONE10	0.2071	ZONE7	0.2013	0.2396	ZONE10	0.1623	ZONE7
10	0.25625	0.3061	ZONE10	0.2209	ZONE7	0.20856	0.2614	ZONE10	0.1758	ZONE7
11	0.25585	0.3142	ZONE10	0.2027	ZONE9	0.20866	0.2678	ZONE10	0.1627	ZONE9
12	0.26682	0.317	ZONE10	0.2073	ZONE9	0.21868	0.2721	ZONE10	0.1689	ZONE9
13	0.27575	0.3158	ZONE4	0.2183	ZONE9	0.2268	0.261	ZONE10	0.1813	ZONE9
14	0.28242	0.3245	ZONE4	0.2182	ZONE9	0.2332	0.2704	ZONE5	0.1792	ZONE9
15	0.28531	0.3295	ZONE4	0.2178	ZONE9	0.23539	0.2747	ZONE5	0.1765	ZONE9
16	0.28598	0.3322	ZONE4	0.2219	ZONE9	0.23527	0.2771	ZONE4	0.1799	ZONE9
17	0.29	0.3348	ZONE4	0.2279	ZONE9	0.24092	0.2815	ZONE4	0.1847	ZONE9
18	0.29352	0.3519	ZONE4	0.23	ZONE9	0.24554	0.2964	ZONE4	0.1901	ZONE9
19	0.29357	0.3552	ZONE4	0.226	ZONE9	0.24628	0.298	ZONE4	0.1867	ZONE9
20	0.29269	0.3479	ZONE4	0.229	ZONE9	0.24638	0.2899	ZONE4	0.188	ZONE9
21	0.29654	0.349	ZONE4	0.2291	ZONE9	0.25213	0.2927	ZONE6	0.1906	ZONE9
22	0.30297	0.344	ZONE4	0.2777	ZONE7	0.25737	0.2944	ZONE5	0.231	ZONE9
23	0.3033	0.337	ZONE5	0.2753	ZONE7	0.25615	0.2955	ZONE5	0.2249	ZONE7
24	0.30413	0.3386	ZONE5	0.2753	ZONE2	0.25652	0.2982	ZONE5	0.2251	ZONE7

4.5.2 AR-X model

The AR-X model described in Section 3.1.2 was implemented. For each WPP (10 models), both past power measurements and weather forecasts, u and v, recorded at that specific location, are used. The mean RMSE and MAE obtained with the model for each timescale are displayed in Figure 4.5 and Table 4.6.

The AR-X model yielded mean RMSE values between 0.10, for the 1 hour-ahead forecast, and 0.27, for the 24 hours-ahead forecast. Once more, ZONE9 was the WPP with the best results in more timescales (between 11 hours-ahead and 21 hours-ahead), whereas ZONE10 was the worst in 14 timescales.

Besides displaying the lowest mean autocorrelation for the first 20 lags, ZONE10 also displayed a very small to non-existent linear correlation with the weather forecasts (Section 4.2.2) , which could explain the results for this WPP. On the other hand, ZONE9 displayed mild correlation with both variables, u and v.

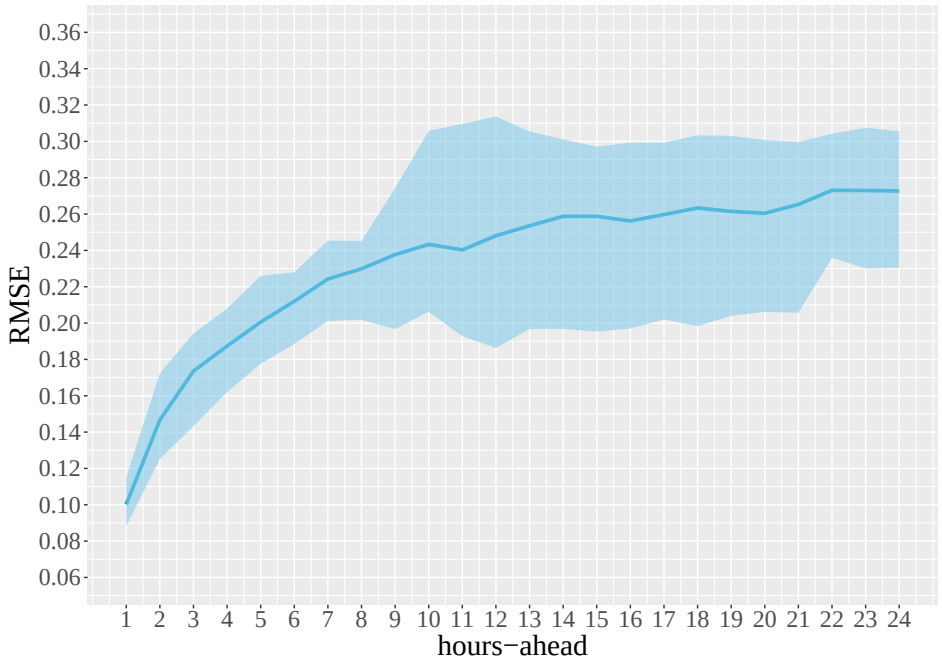

Figure 4.5: Mean RMSE for all WPP and Max/Min values obtained with the AR-X model.

Like the AR model, the AR-X model yields better results for the forecasts performed a few hours-ahead. For this timescale, the mean RMSE values obtained with AR-X model represent only a marginal improvement from the ones yielded by the AR model. This is likely due to the prevalence of the lags' coefficients for the few hours-ahead forecasts. However, as the forecasting timescale increases, the use of a linear combination of the weather forecasts seems to improve upon the AR model's results, yielding mean RMSE values below 0.28 for all timescales.

Regarding the MAE, the AR-X model yielded mean results between 0.070, for the 1 hour-ahead forecast, and 0.23, for the 24 hours-ahead forecast.

Table 4.6: AR-X Model Results Summary

hours-ahead	RMSE					MAE				
	Mean Value	Maximum Value		Minimum Value		Mean Value	Maximum Value		Minimum Value	
		Value	WPP	Value	WPP		Value	WPP	Value	WPP
1	0.10028	0.1153	ZONE9	0.0883	ZONE5	0.07004	0.0766	ZONE4	0.0609	ZONE2
2	0.14674	0.1724	ZONE10	0.1252	ZONE2	0.10684	0.1208	ZONE10	0.0912	ZONE2
3	0.17355	0.1942	ZONE10	0.1433	ZONE2	0.12887	0.1453	ZONE10	0.1054	ZONE2
4	0.18734	0.208	ZONE10	0.162	ZONE2	0.14183	0.161	ZONE10	0.1215	ZONE2
5	0.20055	0.226	ZONE10	0.1776	ZONE7	0.15435	0.1781	ZONE10	0.1344	ZONE2
6	0.212	0.228	ZONE3	0.1885	ZONE2	0.16452	0.1845	ZONE3	0.1432	ZONE2
7	0.22426	0.2454	ZONE10	0.2012	ZONE7	0.17551	0.1985	ZONE10	0.158	ZONE2
8	0.22988	0.2452	ZONE6	0.2018	ZONE7	0.18118	0.1963	ZONE10	0.1608	ZONE7
9	0.23768	0.2743	ZONE10	0.1967	ZONE7	0.18953	0.2218	ZONE10	0.1558	ZONE7
10	0.24331	0.3058	ZONE10	0.2062	ZONE7	0.1959	0.2526	ZONE10	0.1642	ZONE7
11	0.24028	0.3096	ZONE10	0.1928	ZONE9	0.19571	0.2593	ZONE10	0.1559	ZONE9
12	0.24807	0.3137	ZONE10	0.1863	ZONE9	0.20288	0.2646	ZONE10	0.1509	ZONE9
13	0.25355	0.3055	ZONE10	0.1967	ZONE9	0.20754	0.255	ZONE10	0.1617	ZONE9
14	0.25875	0.3011	ZONE10	0.1968	ZONE9	0.21259	0.2544	ZONE10	0.1604	ZONE9
15	0.25876	0.2971	ZONE10	0.1953	ZONE9	0.21116	0.2475	ZONE10	0.1575	ZONE9
16	0.25621	0.2993	ZONE5	0.197	ZONE9	0.20844	0.2457	ZONE5	0.1583	ZONE9
17	0.25972	0.2993	ZONE5	0.202	ZONE9	0.21056	0.2449	ZONE10	0.1613	ZONE9
18	0.26337	0.3033	ZONE4	0.1983	ZONE9	0.21543	0.2517	ZONE4	0.1599	ZONE9
19	0.26145	0.3031	ZONE4	0.204	ZONE9	0.2161	0.2523	ZONE4	0.1668	ZONE9
20	0.26044	0.3008	ZONE4	0.2061	ZONE9	0.21526	0.2495	ZONE4	0.1712	ZONE9
21	0.2653	0.2997	ZONE5	0.2057	ZONE9	0.21973	0.2539	ZONE10	0.1713	ZONE9
22	0.27305	0.3042	ZONE5	0.2359	ZONE2	0.22763	0.2593	ZONE5	0.1905	ZONE2
23	0.27296	0.3075	ZONE10	0.2301	ZONE2	0.2267	0.2646	ZONE10	0.1888	ZONE2
24	0.27269	0.3056	ZONE10	0.2304	ZONE2	0.22609	0.2598	ZONE10	0.1863	ZONE2

4.5.3 AAR-X model

The AAR-X model described in Section 3.1.3 was implemented. Both past power measurements and weather forecasts, u and v, recorded at each WPP (10 models), are used in the forecast. The model uses natural cubic splines to model the non-linear relation between the weather forecasts and the power generated at each WPP. The mean RMSE and MAE obtained with the AAR-X model for each timescale are displayed in Figure 4.6 and Table 4.7.

The results display a significant improvement in regards to the AR and AR-X models. Mean RMSE values between 0.095 and 0.20 were obtained with the AAR-X model.

The WPPs that yielded the best and worst results for more timescales were ZONE9 and ZONE10, respectively.

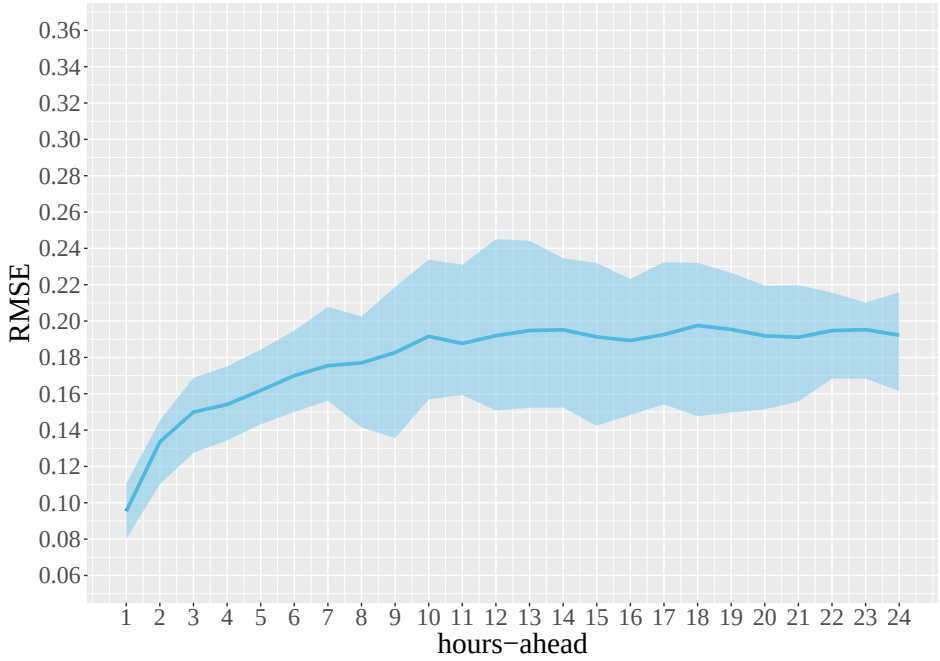

Figure 4.6: Mean RMSE for all WPPs and Max/Min values obtained with the AAR-X model.

As anticipated, the use of additive smooth functions in the forecast seems to better capture the relation between the weather forecasts and the power generated, yielding significantly lower mean RMSE values than the AR-X. This is particularly true for timescales larger than 2 to 3 hours-ahead.

Regarding the MAE, the AR-X model yielded mean results between 0.067, for the 1 hour-ahead forecast, and 0.15, for the 22 hours-ahead forecast.

Table 4.7: AAR-X Model Results Summary

hours-ahead	RMSE					MAE				
	Mean Value	Maximum Value		Minimum Value		Mean Value	Maximum Value		Minimum Value	
		Value	WPP	Value	WPP		Value	WPP	Value	WPP
1	0.09534	0.1104	ZONE9	0.0801	ZONE5	0.06733	0.0726	ZONE8	0.0606	ZONE5
2	0.13351	0.1453	ZONE10	0.1102	ZONE3	0.09587	0.1073	ZONE1	0.0838	ZONE3
3	0.14992	0.1688	ZONE9	0.1275	ZONE2	0.10916	0.1195	ZONE1	0.0935	ZONE2
4	0.15411	0.175	ZONE1	0.1343	ZONE2	0.11507	0.1353	ZONE1	0.1003	ZONE2
5	0.16181	0.1843	ZONE9	0.1432	ZONE5	0.12148	0.1428	ZONE1	0.1084	ZONE7
6	0.16996	0.1948	ZONE1	0.15	ZONE5	0.12813	0.151	ZONE1	0.1144	ZONE2
7	0.17545	0.2078	ZONE10	0.1562	ZONE7	0.13088	0.1581	ZONE10	0.115	ZONE7
8	0.17699	0.2025	ZONE10	0.1414	ZONE7	0.13247	0.1563	ZONE10	0.1038	ZONE7
9	0.18268	0.2188	ZONE10	0.1356	ZONE7	0.13784	0.1711	ZONE10	0.1032	ZONE7
10	0.1916	0.2338	ZONE10	0.1569	ZONE7	0.14838	0.186	ZONE10	0.1203	ZONE7
11	0.1877	0.231	ZONE10	0.1593	ZONE9	0.14741	0.1892	ZONE10	0.1224	ZONE2
12	0.19195	0.2451	ZONE10	0.1508	ZONE9	0.15108	0.198	ZONE10	0.1199	ZONE9
13	0.19478	0.2442	ZONE10	0.1523	ZONE9	0.15325	0.1963	ZONE10	0.1197	ZONE9
14	0.19517	0.2346	ZONE10	0.1524	ZONE9	0.15257	0.189	ZONE10	0.1208	ZONE9
15	0.19129	0.2319	ZONE10	0.1424	ZONE9	0.14969	0.1862	ZONE10	0.1099	ZONE9
16	0.18928	0.2231	ZONE10	0.1483	ZONE9	0.14773	0.1796	ZONE10	0.1139	ZONE9
17	0.19257	0.2324	ZONE10	0.1542	ZONE9	0.14837	0.1862	ZONE10	0.1135	ZONE9
18	0.19761	0.232	ZONE10	0.1476	ZONE9	0.15204	0.1857	ZONE10	0.1124	ZONE9
19	0.19538	0.2266	ZONE10	0.1497	ZONE9	0.15174	0.1858	ZONE10	0.1144	ZONE9
20	0.1919	0.2195	ZONE10	0.1514	ZONE9	0.15038	0.1801	ZONE10	0.1184	ZONE9
21	0.19109	0.2197	ZONE10	0.1557	ZONE9	0.14905	0.1801	ZONE10	0.1219	ZONE9
22	0.19475	0.2157	ZONE6	0.1683	ZONE3	0.15207	0.171	ZONE6	0.1326	ZONE2
23	0.19526	0.2102	ZONE6	0.1683	ZONE2	0.15035	0.1678	ZONE10	0.124	ZONE2
24	0.19224	0.2158	ZONE10	0.1615	ZONE2	0.14756	0.1691	ZONE10	0.1178	ZONE2

4.5.4 VAR model

The VAR model described in Section 3.2.1 was implemented. As discussed, the VAR model is capable of capturing the linear correlations between the power generated in all WPP locations. As such, a unique model, using the power generation time series in all WPPs, was implemented.

To assess whether the use of different LASSO-VAR frameworks significantly impacted the results, the two methods discussed in Section 3.3 were implemented in different versions of the model.

Standard LASSO-VAR (sLV)

The first method corresponds to sLV and uses the lagged values of the variables without grouping them in any way, meaning that each lagged value of any variable can be removed or added to the model by the use of LASSO regularization.

The mean RMSE and MAE obtained with the VAR model with sLV for each timescale are presented in Figure 4.7 and Table 4.8.

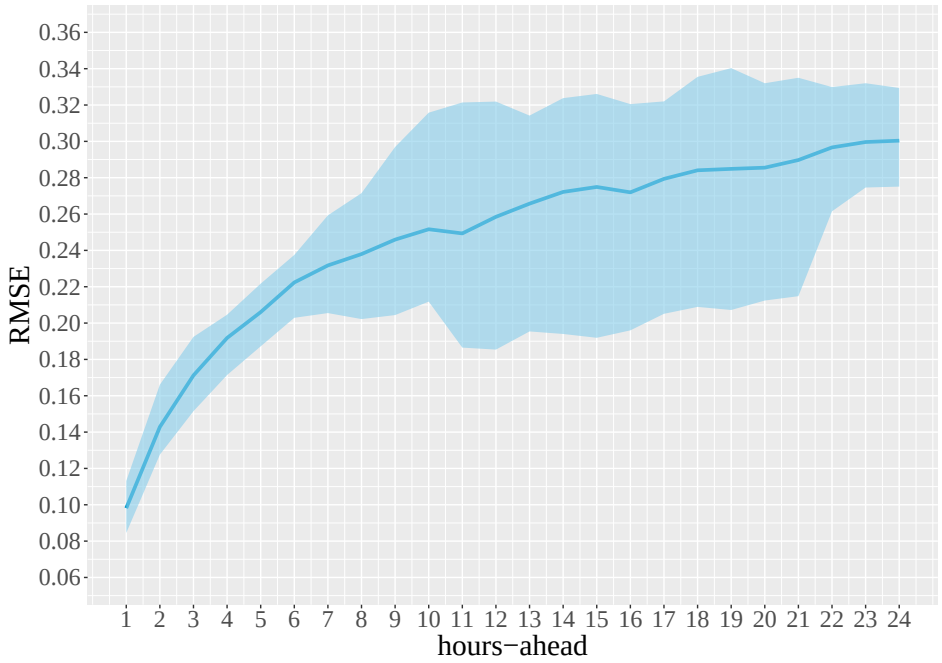

Figure 4.7: Mean RMSE for all WPPs and Max/Min values obtained with the VAR model.

The VAR model with sLV yielded mean RMSE values between 0.098, for the 1 hour-ahead forecast, and 0.30, for the 24 hours-ahead forecast. ZONE9 was the WPP with the best results in more timescales (between 11 hours-ahead and 22 hours-ahead), whereas ZONE10 was the worst in 10 timescales. One of the reasons behind the good results in ZONE9 is likely the high cross-correlation with the remaining WPPs' lagged values (Section 4.2.2).

On average, the VAR model seems to marginally improve the results obtained with the AR model, meaning that the use of geographically distributed data likely had a positive impact on the accuracy of the forecasts.

Like the previous models, the VAR model yields better results for the forecasts performed a few hours-ahead.

Regarding the MAE, the VAR model yielded mean results between 0.069, for the 1 hour-ahead forecast, and 0.25, for the 24 hours-ahead forecast.

Table 4.8: VAR Model Results Summary

hours-ahead	RMSE					MAE				
	Mean Value	Maximum Value		Minimum Value		Mean Value	Maximum Value		Minimum Value	
		Value	WPP	Value	WPP		Value	WPP	Value	WPP
1	0.09813	0.1131	ZONE9	0.0845	ZONE5	0.06914	0.0754	ZONE9	0.0632	ZONE5
2	0.14285	0.1661	ZONE10	0.1276	ZONE3	0.10566	0.1179	ZONE10	0.0958	ZONE2
3	0.17122	0.1924	ZONE10	0.1515	ZONE2	0.12943	0.1407	ZONE10	0.1132	ZONE2
4	0.19182	0.2046	ZONE8	0.1714	ZONE2	0.1475	0.1568	ZONE8	0.1316	ZONE2
5	0.20604	0.2217	ZONE6	0.1872	ZONE7	0.15971	0.1741	ZONE6	0.1453	ZONE2
6	0.22236	0.2375	ZONE6	0.2029	ZONE2	0.17317	0.1853	ZONE6	0.1561	ZONE2
7	0.23173	0.2593	ZONE10	0.2055	ZONE7	0.181	0.2082	ZONE10	0.16	ZONE2
8	0.23797	0.2715	ZONE10	0.2022	ZONE7	0.18703	0.2203	ZONE10	0.1577	ZONE7
9	0.24593	0.2969	ZONE10	0.2044	ZONE7	0.19482	0.2414	ZONE10	0.1609	ZONE7
10	0.25163	0.3158	ZONE10	0.2118	ZONE7	0.20002	0.2619	ZONE10	0.1663	ZONE7
11	0.24934	0.3214	ZONE10	0.1865	ZONE9	0.19998	0.2667	ZONE10	0.148	ZONE9
12	0.25847	0.3219	ZONE10	0.1854	ZONE9	0.20786	0.2681	ZONE10	0.1499	ZONE9
13	0.26572	0.3142	ZONE10	0.1954	ZONE9	0.2153	0.2607	ZONE10	0.1581	ZONE9
14	0.27217	0.3238	ZONE4	0.194	ZONE9	0.22177	0.2652	ZONE5	0.1548	ZONE9
15	0.27491	0.3261	ZONE4	0.1919	ZONE9	0.2224	0.2642	ZONE4	0.1528	ZONE9
16	0.27195	0.3205	ZONE4	0.196	ZONE9	0.21948	0.2617	ZONE4	0.1582	ZONE9
17	0.27936	0.322	ZONE4	0.2051	ZONE9	0.22792	0.2705	ZONE10	0.1635	ZONE9
18	0.28408	0.3355	ZONE4	0.2089	ZONE9	0.2345	0.2768	ZONE4	0.167	ZONE9
19	0.28486	0.3403	ZONE4	0.2072	ZONE9	0.23537	0.2775	ZONE4	0.1669	ZONE9
20	0.28553	0.332	ZONE4	0.2124	ZONE9	0.23598	0.2723	ZONE10	0.1707	ZONE9
21	0.28973	0.335	ZONE4	0.2148	ZONE9	0.2411	0.2804	ZONE10	0.1731	ZONE9
22	0.29667	0.3299	ZONE4	0.2615	ZONE9	0.24731	0.283	ZONE5	0.2106	ZONE9
23	0.29964	0.332	ZONE10	0.2746	ZONE7	0.24825	0.2868	ZONE10	0.2192	ZONE7
24	0.30039	0.3294	ZONE5	0.2751	ZONE7	0.24896	0.2822	ZONE5	0.2209	ZONE7

Lag-Group LASSO-VAR (lLV)

The second LASSO-VAR framework implemented corresponds to lLV, method which applies LASSO on the lagged values of the variables grouped by their time lags (first order lags, second order lags, and so on). The mean RMSE and MAE obtained with the VAR model with lLV for each timescale are presented in Figure 4.8 and Table 4.9.

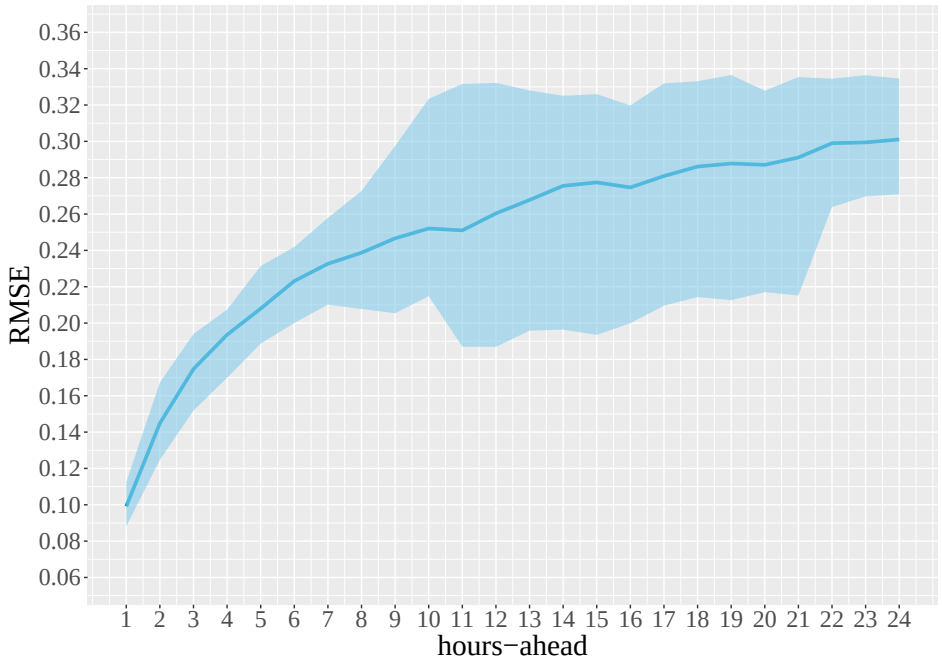

Figure 4.8: Mean RMSE for all WPPs and Max/Min values obtained with the VAR model with lag-group LASSO-VAR.

The VAR model with lLV yielded mean RMSE values between 0.099, for the 1 hour-ahead forecast, and 0.30, for the 24 hours-ahead forecast. Once again, ZONE9 was the WPP with the best results in more timescales (between 11 hours-ahead and 22 hours-ahead). ZONE10 was the worst in 13 timescales.

Regarding the MAE, the VAR model with lLV yielded mean results between 0.069, for the 1 hour-ahead forecast, and 0.25, for the 24 hours-ahead forecast.

Table 4.9: VAR Model with Lag Group LASSO Results Summary

hours-ahead	RMSE					MAE				
	Mean Value	Maximum Value		Minimum Value		Mean Value	Maximum Value		Minimum Value	
		Value	WPP	Value	WPP		Value	WPP	Value	WPP
1	0.09912	0.1124	ZONE9	0.0881	ZONE3	0.06887	0.0739	ZONE4	0.0613	ZONE2
2	0.14485	0.1673	ZONE10	0.1248	ZONE3	0.10626	0.1185	ZONE10	0.0949	ZONE2
3	0.17471	0.194	ZONE10	0.1518	ZONE2	0.13153	0.144	ZONE10	0.1133	ZONE2
4	0.19357	0.2074	ZONE6	0.1699	ZONE2	0.14789	0.16	ZONE6	0.1298	ZONE2
5	0.20796	0.2314	ZONE6	0.1887	ZONE2	0.16104	0.1808	ZONE6	0.1434	ZONE2
6	0.22315	0.2419	ZONE6	0.2	ZONE2	0.17422	0.1883	ZONE6	0.1545	ZONE2
7	0.23264	0.2579	ZONE10	0.2102	ZONE2	0.18248	0.206	ZONE10	0.162	ZONE2
8	0.23871	0.2727	ZONE10	0.2078	ZONE7	0.18829	0.2212	ZONE10	0.1646	ZONE7
9	0.24664	0.2975	ZONE10	0.2054	ZONE7	0.19741	0.2443	ZONE10	0.1643	ZONE7
10	0.25204	0.3234	ZONE10	0.2148	ZONE7	0.20131	0.2724	ZONE10	0.1692	ZONE1
11	0.25101	0.3316	ZONE10	0.187	ZONE9	0.20209	0.281	ZONE10	0.1502	ZONE9
12	0.26034	0.3322	ZONE10	0.1869	ZONE9	0.20994	0.2832	ZONE10	0.1503	ZONE9
13	0.26775	0.328	ZONE10	0.1958	ZONE9	0.21614	0.274	ZONE10	0.1574	ZONE9
14	0.27553	0.3251	ZONE10	0.1964	ZONE9	0.22244	0.2696	ZONE10	0.1566	ZONE9
15	0.27741	0.326	ZONE4	0.1935	ZONE9	0.223	0.2685	ZONE10	0.152	ZONE9
16	0.27464	0.3198	ZONE10	0.1999	ZONE9	0.22056	0.2623	ZONE10	0.1592	ZONE9
17	0.28091	0.3319	ZONE10	0.2096	ZONE9	0.22731	0.2796	ZONE10	0.1648	ZONE9
18	0.28614	0.3331	ZONE10	0.2143	ZONE9	0.23317	0.2828	ZONE10	0.1704	ZONE9
19	0.2878	0.3365	ZONE4	0.2126	ZONE9	0.23566	0.2814	ZONE10	0.1707	ZONE9
20	0.28709	0.3279	ZONE4	0.217	ZONE9	0.23563	0.2799	ZONE10	0.1728	ZONE9
21	0.29111	0.3354	ZONE4	0.2152	ZONE9	0.24052	0.2884	ZONE10	0.1719	ZONE9
22	0.299	0.3345	ZONE4	0.2639	ZONE9	0.24747	0.2878	ZONE10	0.2115	ZONE9
23	0.29942	0.3364	ZONE5	0.2697	ZONE7	0.24652	0.2881	ZONE10	0.2144	ZONE7
24	0.30107	0.3346	ZONE5	0.2709	ZONE7	0.24717	0.2821	ZONE5	0.2169	ZONE7

The VAR with lLV displays a similar behaviour to VAR with sLV in terms of the RMSE values.

4.5.5 VAR-X model

The VAR-X introduced in Section 3.2.2 was implemented. In the VAR-X model developed, all 50 variables provided at GEFCom 2014 are used, corresponding to the power generation time series and the weather forecasts for all WPPs.

As in the VAR model's case, both the sLV and lLV frameworks were tested.

Standard LASSO-VAR (sLV)

The mean RMSE and MAE obtained with the VAR-X model with sLV for each timescale are presented in Figure 4.9 and Table 4.10.

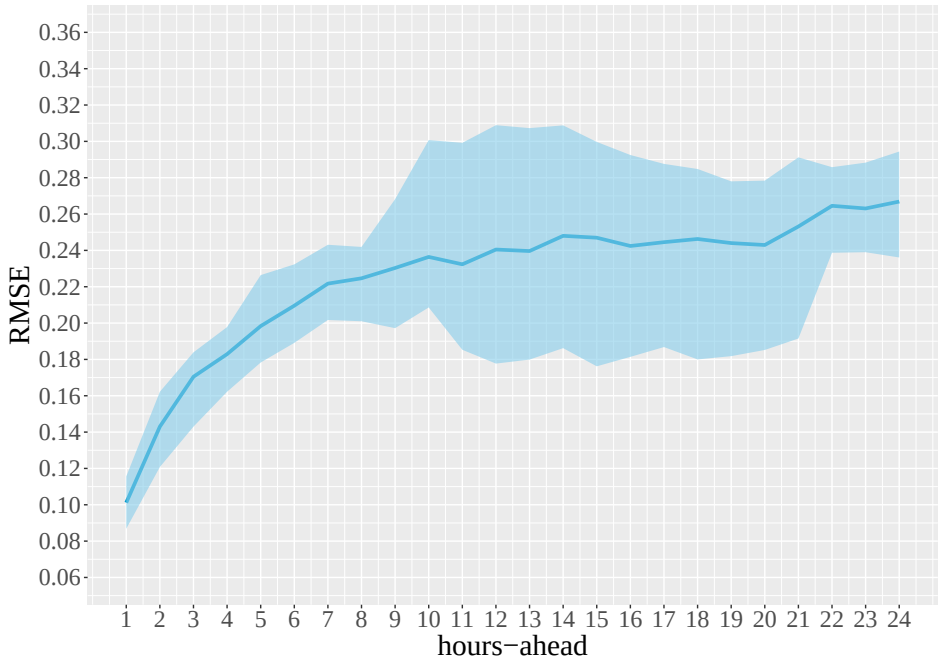

Figure 4.9: Mean RMSE for all WPPs and Max/Min values obtained with the VAR-X model.

The VAR-X model with sLV yielded mean RMSE values between 0.10, for the 1 hour-ahead forecast, and 0.27, for the 24 hours-ahead forecast. Once more, ZONE9 and ZONE10 were the WPPs with the best and worst results, respectively.

As in the AR-X and AR models' case, the VAR-X model significantly improves the accuracy of the forecasts obtained with the VAR model, particularly for timescales of more than a few hours-ahead.

Regarding the MAE, the VAR-X model with sLV yielded mean results between 0.071, for the 1 hour-ahead forecast, and 0.22, for the 24 hours-ahead forecast.

Table 4.10: VAR-X Model Results Summary

hours-ahead	RMSE					MAE				
	Mean Value	Maximum Value		Minimum Value		Mean Value	Maximum Value		Minimum Value	
		Value	WPP	Value	WPP		Value	WPP	Value	WPP
1	0.10117	0.1156	ZONE9	0.0868	ZONE3	0.07128	0.0759	ZONE4	0.0617	ZONE2
2	0.14303	0.1622	ZONE10	0.1208	ZONE3	0.10519	0.1167	ZONE10	0.0911	ZONE2
3	0.17046	0.1839	ZONE8	0.143	ZONE2	0.12664	0.1349	ZONE6	0.1059	ZONE2
4	0.18291	0.1978	ZONE8	0.1622	ZONE2	0.13773	0.1476	ZONE8	0.121	ZONE2
5	0.19834	0.2264	ZONE6	0.1783	ZONE2	0.15099	0.1688	ZONE6	0.1351	ZONE2
6	0.20958	0.2323	ZONE6	0.1891	ZONE2	0.16085	0.1725	ZONE6	0.1468	ZONE2
7	0.22172	0.2431	ZONE6	0.2017	ZONE2	0.1737	0.1916	ZONE10	0.1573	ZONE2
8	0.22464	0.2419	ZONE5	0.201	ZONE7	0.17511	0.1904	ZONE10	0.1585	ZONE7
9	0.23032	0.2682	ZONE10	0.1972	ZONE7	0.18069	0.216	ZONE10	0.1533	ZONE1
10	0.23641	0.3007	ZONE10	0.2086	ZONE1	0.18823	0.2473	ZONE10	0.1625	ZONE1
11	0.23234	0.2992	ZONE10	0.1853	ZONE9	0.18714	0.2474	ZONE10	0.1462	ZONE9
12	0.24047	0.3089	ZONE10	0.1777	ZONE9	0.19324	0.2509	ZONE10	0.1408	ZONE9
13	0.23964	0.3073	ZONE10	0.1799	ZONE9	0.19404	0.253	ZONE10	0.1442	ZONE9
14	0.24801	0.3088	ZONE10	0.1862	ZONE9	0.19947	0.2557	ZONE10	0.1476	ZONE9
15	0.24698	0.2997	ZONE10	0.1762	ZONE9	0.19889	0.2475	ZONE10	0.1397	ZONE9
16	0.24243	0.2925	ZONE10	0.1814	ZONE9	0.19292	0.2365	ZONE10	0.1393	ZONE9
17	0.24452	0.2876	ZONE10	0.1868	ZONE9	0.19343	0.2368	ZONE10	0.1449	ZONE9
18	0.24628	0.2848	ZONE10	0.18	ZONE9	0.19564	0.2374	ZONE10	0.1399	ZONE9
19	0.24403	0.278	ZONE10	0.1818	ZONE9	0.1964	0.2312	ZONE10	0.1413	ZONE9
20	0.24297	0.2784	ZONE10	0.1852	ZONE9	0.1957	0.2298	ZONE10	0.1485	ZONE9
21	0.25315	0.2912	ZONE10	0.1915	ZONE9	0.20574	0.24	ZONE10	0.1545	ZONE9
22	0.26454	0.2858	ZONE6	0.2387	ZONE2	0.217	0.241	ZONE5	0.1926	ZONE2
23	0.26307	0.2883	ZONE10	0.239	ZONE2	0.21449	0.239	ZONE10	0.1958	ZONE2
24	0.26687	0.2944	ZONE10	0.2361	ZONE2	0.21639	0.2448	ZONE10	0.1905	ZONE2

Lag-Group LASSO-VAR (lLV)

The mean RMSE and MAE obtained with the VAR-X model with lLV for each timescale are presented in Figure 4.10 and Table 4.11. In this case, not only the lagged values were grouped by their time lags, but also the weather forecasts were grouped by location, meaning that, for a given WPP, either all or none of the weather forecasts were considered.

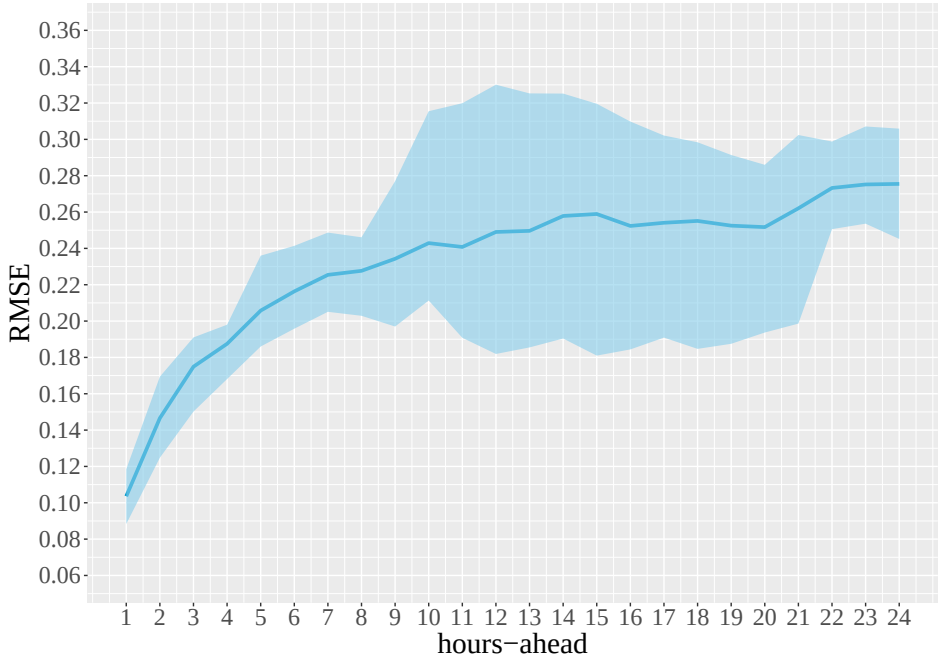

Figure 4.10: Mean RMSE for all WPPs and Max/Min values obtained with the VAR-X model with lag-group LASSO-VAR.

The VAR-X model with lLV yielded similar mean RMSE values than the VAR-X model with sLV. The minimum error was obtained for the 1 hour-ahead forecast (0.10) and the maximum value for the 24 hours-ahead forecast (0.28).

Regarding the MAE, the VAR-X model with lLV yielded mean results between 0.074, for the 1 hour-ahead forecast, and 0.22, for the 24 hours-ahead forecast.

As in the case of the VAR model, the grouping of the lags and weather forecasts does not seem to result in an improvement of the mean RMSE results obtained with the VAR-X model with sLV.

Table 4.11: VAR-X Model with Lag Group LASSO Results Summary

hours-ahead	RMSE					MAE				
	Mean Value	Maximum Value		Minimum Value		Mean Value	Maximum Value		Minimum Value	
		Value	WPP	Value	WPP		Value	WPP	Value	WPP
1	0.10358	0.1185	ZONE9	0.0883	ZONE3	0.07409	0.0795	ZONE4	0.0652	ZONE2
2	0.14659	0.1694	ZONE10	0.1248	ZONE3	0.10791	0.1209	ZONE10	0.0938	ZONE2
3	0.1749	0.191	ZONE6	0.1502	ZONE2	0.12944	0.1403	ZONE6	0.1091	ZONE2
4	0.1875	0.198	ZONE8	0.1681	ZONE2	0.13982	0.1478	ZONE6	0.1236	ZONE2
5	0.20576	0.236	ZONE6	0.186	ZONE2	0.15429	0.1737	ZONE6	0.1367	ZONE2
6	0.21634	0.2414	ZONE6	0.1958	ZONE2	0.16406	0.1763	ZONE6	0.1503	ZONE2
7	0.22544	0.2487	ZONE6	0.2051	ZONE7	0.17652	0.1933	ZONE6	0.1617	ZONE2
8	0.22765	0.2461	ZONE10	0.2029	ZONE7	0.17675	0.1939	ZONE10	0.1611	ZONE7
9	0.23428	0.277	ZONE10	0.197	ZONE7	0.1818	0.2203	ZONE10	0.1543	ZONE1
10	0.24291	0.3155	ZONE10	0.2113	ZONE1	0.19119	0.2547	ZONE10	0.1638	ZONE1
11	0.24079	0.3199	ZONE10	0.1908	ZONE9	0.19225	0.2601	ZONE10	0.149	ZONE9
12	0.24904	0.3301	ZONE10	0.1819	ZONE9	0.19784	0.2652	ZONE10	0.1426	ZONE9
13	0.24965	0.3253	ZONE10	0.1855	ZONE9	0.19932	0.261	ZONE10	0.1473	ZONE9
14	0.25784	0.3252	ZONE10	0.1904	ZONE9	0.20506	0.2653	ZONE10	0.1494	ZONE9
15	0.25893	0.3196	ZONE10	0.181	ZONE9	0.20518	0.2585	ZONE10	0.1427	ZONE9
16	0.25236	0.3098	ZONE10	0.1844	ZONE9	0.19809	0.2457	ZONE10	0.1407	ZONE9
17	0.2541	0.3021	ZONE10	0.1909	ZONE9	0.1982	0.2451	ZONE10	0.1471	ZONE9
18	0.25511	0.2984	ZONE10	0.1847	ZONE9	0.19966	0.2392	ZONE10	0.1418	ZONE9
19	0.25251	0.2914	ZONE10	0.1875	ZONE9	0.20099	0.2366	ZONE10	0.1465	ZONE9
20	0.25171	0.286	ZONE10	0.1937	ZONE9	0.19992	0.2336	ZONE10	0.1563	ZONE9
21	0.26206	0.3024	ZONE10	0.1986	ZONE9	0.20983	0.2435	ZONE10	0.1603	ZONE9
22	0.27325	0.2988	ZONE10	0.2506	ZONE2	0.22138	0.2488	ZONE10	0.1976	ZONE9
23	0.27519	0.3071	ZONE10	0.2536	ZONE7	0.22097	0.2531	ZONE10	0.1993	ZONE7
24	0.27549	0.3059	ZONE10	0.2452	ZONE2	0.21816	0.2461	ZONE10	0.1936	ZONE2

4.5.6 AVAR-X model

The AVAR-X model discussed in Section 3.2.3 was implemented. The model uses both the past power measurements and the weather forecasts, u and v, recorded at all locations. As in the VAR and VAR-X models' case, both the sLV and lLV frameworks were tested.

Given the good results obtained with the natural cubic splines model, a different set of smooth functions was also tested (cubic B splines).

Standard LASSO-VAR (sLV) and Natural Cubic Splines

The mean RMSE and MAE obtained with the AVAR-X model with sLV and natural cubic splines for each timescale are presented in Figure 4.11 and Table 4.12.

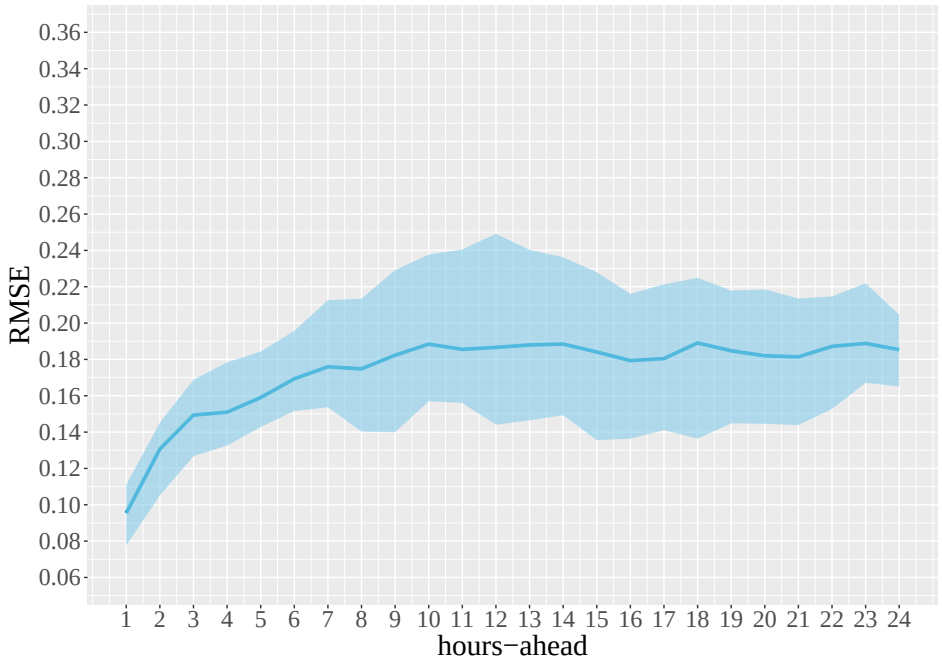

Figure 4.11: Mean RMSE for all WPPs and Max/Min values obtained with the AVAR-X model (Natural Cubic Splines).

The AVAR-X model with sLV and natural cubic splines yielded mean RMSE values between 0.095, for the 1 hour-ahead forecast, and 0.19, for the 18 hours-ahead forecast.

Regarding the MAE, the AVAR-X model with sLV and natural cubic splines yielded mean results between 0.067 and 0.15.

Table 4.12: AVAR-X Model with Natural Cubic Splines Results Summary

hours-ahead	RMSE					MAE				
	Mean Value	Maximum Value		Minimum Value		Mean Value	Maximum Value		Minimum Value	
		Value	WPP	Value	WPP		Value	WPP	Value	WPP
1	0.09542	0.111	ZONE9	0.0776	ZONE5	0.06684	0.0721	ZONE4	0.0595	ZONE5
2	0.13063	0.1452	ZONE10	0.1052	ZONE3	0.0951	0.1053	ZONE10	0.0807	ZONE3
3	0.14937	0.1688	ZONE9	0.1267	ZONE2	0.10802	0.1186	ZONE8	0.0912	ZONE2
4	0.15096	0.1784	ZONE9	0.1326	ZONE2	0.11206	0.1261	ZONE9	0.0961	ZONE2
5	0.15903	0.1843	ZONE9	0.1428	ZONE2	0.1183	0.1287	ZONE10	0.1013	ZONE2
6	0.16931	0.1957	ZONE9	0.1516	ZONE2	0.12679	0.141	ZONE10	0.108	ZONE2
7	0.17595	0.2126	ZONE10	0.1537	ZONE2	0.13168	0.1572	ZONE10	0.1111	ZONE2
8	0.17482	0.2134	ZONE10	0.1403	ZONE7	0.13026	0.161	ZONE10	0.1078	ZONE7
9	0.1823	0.2292	ZONE10	0.1399	ZONE7	0.1355	0.1696	ZONE10	0.102	ZONE1
10	0.18841	0.2377	ZONE10	0.157	ZONE7	0.1453	0.1899	ZONE10	0.1204	ZONE1
11	0.18553	0.2405	ZONE10	0.156	ZONE9	0.14486	0.1963	ZONE10	0.1188	ZONE1
12	0.18663	0.2492	ZONE10	0.1441	ZONE9	0.14633	0.2	ZONE10	0.1134	ZONE9
13	0.18795	0.2403	ZONE10	0.1465	ZONE9	0.14832	0.1946	ZONE10	0.1142	ZONE9
14	0.18844	0.2362	ZONE10	0.1493	ZONE9	0.14676	0.1926	ZONE10	0.1158	ZONE1
15	0.18408	0.228	ZONE10	0.1356	ZONE9	0.14308	0.1828	ZONE10	0.1063	ZONE9
16	0.17933	0.2161	ZONE6	0.1364	ZONE9	0.13898	0.1704	ZONE6	0.1049	ZONE9
17	0.18045	0.2213	ZONE10	0.1411	ZONE9	0.1387	0.1798	ZONE10	0.1024	ZONE9
18	0.18908	0.2249	ZONE8	0.1364	ZONE9	0.1428	0.175	ZONE6	0.1008	ZONE9
19	0.18475	0.2179	ZONE10	0.1448	ZONE9	0.14319	0.1787	ZONE10	0.1052	ZONE9
20	0.18199	0.2185	ZONE10	0.1446	ZONE9	0.14162	0.1773	ZONE10	0.1093	ZONE9
21	0.1814	0.2135	ZONE10	0.1439	ZONE9	0.14164	0.1747	ZONE10	0.111	ZONE1
22	0.18719	0.2147	ZONE10	0.1527	ZONE1	0.14645	0.1735	ZONE10	0.1127	ZONE1
23	0.18879	0.2219	ZONE10	0.1671	ZONE1	0.14631	0.1783	ZONE10	0.121	ZONE7
24	0.18538	0.2046	ZONE10	0.1651	ZONE7	0.1427	0.1631	ZONE10	0.1233	ZONE7

Standard LASSO-VAR (sLV) and B Splines

The mean RMSE and MAE obtained with the AVAR-X model with sLV and B splines for each timescale are presented in Figure 4.12 and Table 4.13.

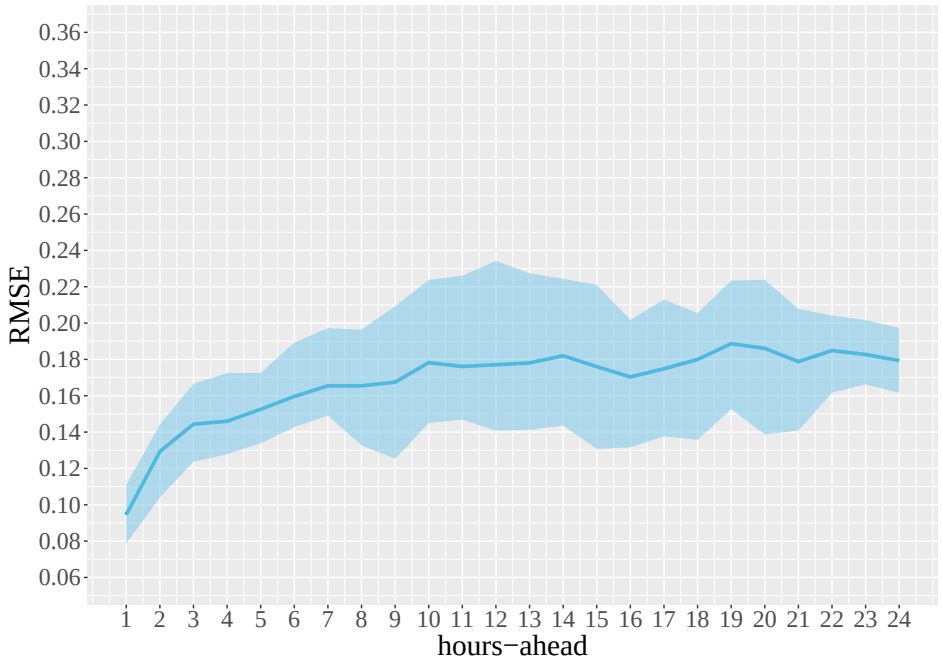

Figure 4.12: Mean RMSE for all WPPs and Max/Min values obtained with the AVAR-X model (B Splines).

The AVAR-X model with sLV and B splines yielded mean RMSE values between 0.095, for the 1 hour-ahead forecast, and 0.18, for the 19 hours-ahead forecast.

Regarding the MAE, the AVAR-X model with sLV and B splines yielded mean results between 0.067 and 0.14.

In general, the mean RMSE values obtained with the AVAR-X model with the B splines constitute an improvement on the natural cubic splines model, yielding mean RMSE values below 0.19 for most forecasting horizons greater than 10 hours.

Table 4.13: AVAR-X Model with B Splines Results Summary

hours-ahead	RMSE					MAE				
	Mean Value	Maximum Value		Minimum Value		Mean Value	Maximum Value		Minimum Value	
		Value	WPP	Value	WPP		Value	WPP	Value	WPP
1	0.09453	0.111	ZONE9	0.0787	ZONE5	0.06634	0.072	ZONE7	0.0592	ZONE2
2	0.12931	0.1441	ZONE8	0.104	ZONE3	0.09328	0.1025	ZONE10	0.0796	ZONE3
3	0.14436	0.1666	ZONE9	0.1237	ZONE2	0.10444	0.1157	ZONE9	0.0885	ZONE2
4	0.14597	0.1725	ZONE8	0.1278	ZONE2	0.10848	0.1262	ZONE8	0.0932	ZONE2
5	0.15257	0.1726	ZONE8	0.1339	ZONE2	0.11384	0.1271	ZONE8	0.0964	ZONE2
6	0.15961	0.1893	ZONE9	0.1427	ZONE2	0.11964	0.1321	ZONE9	0.1043	ZONE2
7	0.16548	0.1972	ZONE10	0.1491	ZONE7	0.1234	0.1476	ZONE10	0.1074	ZONE2
8	0.16546	0.1964	ZONE10	0.1327	ZONE7	0.12245	0.1474	ZONE10	0.0995	ZONE7
9	0.16747	0.2093	ZONE10	0.1252	ZONE7	0.12507	0.1578	ZONE10	0.0941	ZONE7
10	0.17824	0.2237	ZONE10	0.145	ZONE7	0.13523	0.175	ZONE10	0.1085	ZONE7
11	0.17612	0.2261	ZONE10	0.1469	ZONE3	0.13509	0.1809	ZONE10	0.1105	ZONE2
12	0.17707	0.2342	ZONE10	0.1408	ZONE9	0.13688	0.1836	ZONE10	0.1099	ZONE9
13	0.17806	0.2274	ZONE10	0.1413	ZONE9	0.13878	0.1798	ZONE10	0.1087	ZONE9
14	0.18203	0.2244	ZONE10	0.1436	ZONE9	0.14033	0.1785	ZONE10	0.1116	ZONE9
15	0.17603	0.221	ZONE10	0.1308	ZONE9	0.13604	0.172	ZONE10	0.1016	ZONE9
16	0.17036	0.2018	ZONE10	0.1316	ZONE9	0.13122	0.1564	ZONE10	0.1012	ZONE9
17	0.17486	0.2129	ZONE10	0.1377	ZONE9	0.13306	0.1681	ZONE10	0.0994	ZONE9
18	0.17997	0.2055	ZONE10	0.1357	ZONE9	0.13675	0.1619	ZONE6	0.1003	ZONE9
19	0.18867	0.2234	ZONE6	0.1526	ZONE7	0.13904	0.1664	ZONE10	0.1047	ZONE9
20	0.18609	0.2238	ZONE1	0.1387	ZONE9	0.13808	0.166	ZONE10	0.105	ZONE9
21	0.1788	0.2078	ZONE10	0.1408	ZONE9	0.1369	0.1651	ZONE10	0.1093	ZONE9
22	0.18487	0.2042	ZONE10	0.1617	ZONE3	0.14165	0.1606	ZONE10	0.1236	ZONE1
23	0.18269	0.2017	ZONE10	0.1663	ZONE3	0.14023	0.1593	ZONE5	0.1214	ZONE7
24	0.17934	0.1973	ZONE10	0.1616	ZONE2	0.13627	0.1542	ZONE6	0.1192	ZONE2

Lag-Group LASSO-VAR (lLV) and Natural Cubic Splines

As in the VAR-X model's case, in AVAR-X with lLV not only the lagged values were grouped by their time lags, but also the weather forecasts were grouped by location. The mean RMSE and MAE obtained with the AVAR-X model with lLV and natural cubic splines for each timescale are presented in Figure 4.13 and Table 4.14.

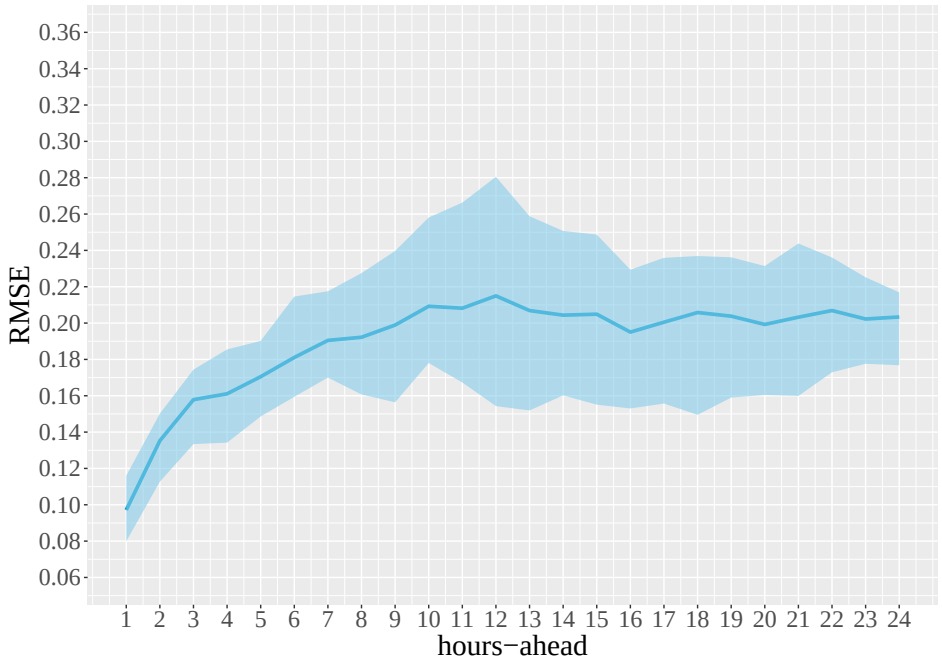

Figure 4.13: Mean RMSE for all WPPs and Max/Min values obtained with the AVAR-X model (Natural Cubic Splines) with lag-group LASSO-VAR.

The AVAR-X model with lLV and natural cubic splines yielded mean RMSE values between 0.097, for the 1 hour-ahead forecast, and 0.21, for the 10 hours-ahead forecast.

Regarding the MAE, the AVAR-X model with lLV and natural cubic splines yielded mean results between 0.070 and 0.17.

Table 4.14: AVAR-X Model with Natural Cubic Splines and Lag Group LASSO Results Summary

hours-ahead	RMSE					MAE				
	Mean Value	Maximum Value		Minimum Value		Mean Value	Maximum Value		Minimum Value	
		Value	WPP	Value	WPP		Value	WPP	Value	WPP
1	0.09713	0.116	ZONE9	0.0799	ZONE5	0.06973	0.076	ZONE9	0.0619	ZONE2
2	0.13525	0.1502	ZONE10	0.1127	ZONE3	0.09937	0.111	ZONE10	0.0861	ZONE3
3	0.15784	0.1744	ZONE9	0.1334	ZONE2	0.11477	0.1265	ZONE9	0.0981	ZONE2
4	0.16109	0.1855	ZONE9	0.1342	ZONE2	0.11941	0.1315	ZONE9	0.0986	ZONE2
5	0.1705	0.1902	ZONE9	0.1486	ZONE2	0.12639	0.1356	ZONE9	0.1075	ZONE2
6	0.18107	0.2146	ZONE9	0.1594	ZONE2	0.13539	0.1567	ZONE9	0.1152	ZONE2
7	0.19047	0.2175	ZONE10	0.17	ZONE2	0.14106	0.1669	ZONE10	0.1221	ZONE2
8	0.1922	0.2275	ZONE10	0.1607	ZONE7	0.14102	0.1723	ZONE10	0.1155	ZONE7
9	0.19891	0.2397	ZONE10	0.1564	ZONE7	0.14696	0.1787	ZONE10	0.1159	ZONE7
10	0.20925	0.2581	ZONE10	0.178	ZONE3	0.15768	0.1991	ZONE10	0.1315	ZONE2
11	0.20818	0.2663	ZONE10	0.1673	ZONE3	0.16023	0.2148	ZONE10	0.1254	ZONE3
12	0.21498	0.2805	ZONE10	0.1543	ZONE9	0.16547	0.2165	ZONE10	0.1215	ZONE9
13	0.20688	0.2588	ZONE10	0.1519	ZONE9	0.15861	0.2068	ZONE10	0.1188	ZONE9
14	0.20436	0.2507	ZONE4	0.1602	ZONE9	0.15534	0.1903	ZONE4	0.1243	ZONE9
15	0.20489	0.2487	ZONE4	0.1551	ZONE9	0.15566	0.1903	ZONE4	0.1203	ZONE9
16	0.19503	0.2294	ZONE4	0.153	ZONE9	0.15009	0.1754	ZONE4	0.1201	ZONE9
17	0.20049	0.2359	ZONE10	0.1557	ZONE9	0.15179	0.1861	ZONE10	0.1153	ZONE9
18	0.20581	0.2369	ZONE6	0.1495	ZONE9	0.15592	0.1879	ZONE6	0.1116	ZONE9
19	0.2038	0.2362	ZONE4	0.159	ZONE9	0.1554	0.1821	ZONE10	0.1169	ZONE9
20	0.19924	0.2314	ZONE4	0.1604	ZONE9	0.15386	0.1834	ZONE6	0.1219	ZONE9
21	0.20325	0.2438	ZONE10	0.1599	ZONE9	0.15764	0.1925	ZONE10	0.1254	ZONE9
22	0.2069	0.2361	ZONE10	0.1729	ZONE1	0.16012	0.1913	ZONE10	0.1283	ZONE1
23	0.20224	0.2252	ZONE10	0.1776	ZONE7	0.15611	0.1782	ZONE10	0.1337	ZONE7
24	0.20336	0.2169	ZONE10	0.1768	ZONE2	0.15593	0.1712	ZONE6	0.1333	ZONE2

Once more, the grouping of the lags and weather variables did not yield any significant improvement over the sLV model.

Lag-Group LASSO-VAR (lLV) and B Splines

The mean RMSE and MAE obtained with the AVAR-X model with lLV and B splines for each timescale are presented in Figure 4.14 and Table 4.15.

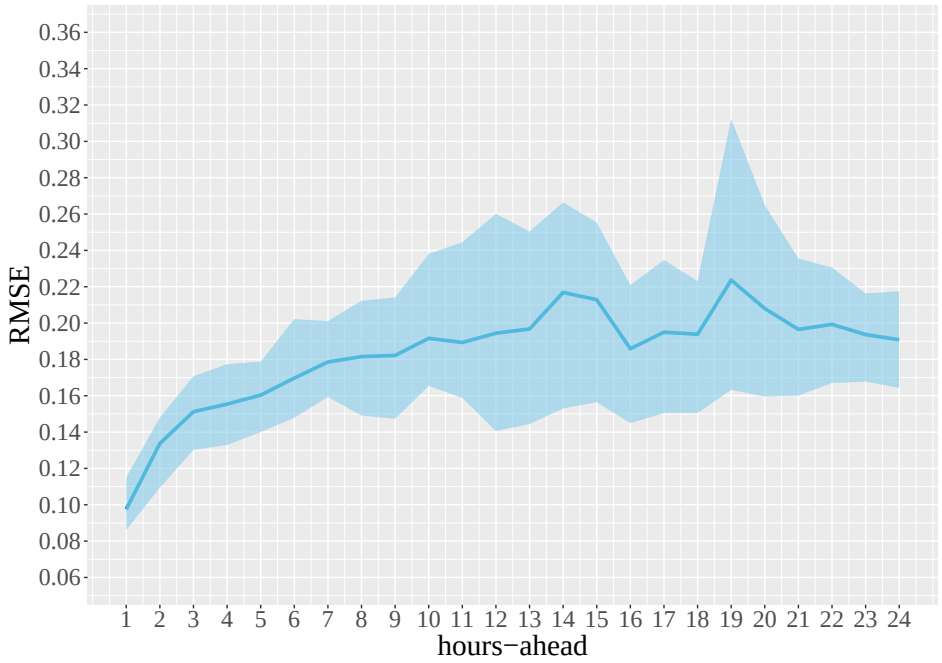

Figure 4.14: Mean RMSE for all WPPs and Max/Min values obtained with the AVAR-X model (B Splines) with lag-group LASSO-VAR.

The AVAR-X model with lLV and B splines yielded mean RMSE values between 0.098, for the 1 hour-ahead forecast, and 0.19, for the 24 hours-ahead forecast.

Regarding the MAE, the AVAR-X model with lLV and B splines yielded mean results between 0.070 and 0.15.

Table 4.15: AVAR-X Model with B Splines and Lag Group LASSO Results Summary

hours-ahead	RMSE					MAE				
	Mean Value	Maximum Value		Minimum Value		Mean Value	Maximum Value		Minimum Value	
		Value	WPP	Value	WPP		Value	WPP	Value	WPP
1	0.09754	0.1151	ZONE9	0.0861	ZONE3	0.06953	0.0753	ZONE9	0.0603	ZONE2
2	0.13375	0.148	ZONE8	0.1094	ZONE3	0.09715	0.1064	ZONE10	0.0835	ZONE3
3	0.15122	0.1707	ZONE9	0.1302	ZONE2	0.10937	0.1203	ZONE9	0.0928	ZONE2
4	0.1554	0.1774	ZONE8	0.1329	ZONE2	0.11376	0.1275	ZONE8	0.0954	ZONE2
5	0.16035	0.1788	ZONE8	0.14	ZONE2	0.11877	0.1307	ZONE8	0.1003	ZONE2
6	0.16972	0.2022	ZONE9	0.1479	ZONE2	0.12584	0.1436	ZONE9	0.1067	ZONE2
7	0.17859	0.2011	ZONE10	0.1593	ZONE7	0.13015	0.1505	ZONE10	0.1134	ZONE2
8	0.18155	0.2123	ZONE9	0.1491	ZONE7	0.1304	0.1508	ZONE10	0.1061	ZONE7
9	0.18218	0.2141	ZONE10	0.1473	ZONE7	0.13236	0.1617	ZONE10	0.1048	ZONE7
10	0.1916	0.2381	ZONE10	0.1654	ZONE7	0.14235	0.1847	ZONE10	0.1187	ZONE2
11	0.18933	0.2445	ZONE10	0.1588	ZONE9	0.14341	0.1946	ZONE10	0.1163	ZONE2
12	0.19443	0.2601	ZONE10	0.1406	ZONE9	0.14722	0.1988	ZONE10	0.1102	ZONE9
13	0.19674	0.2504	ZONE10	0.1444	ZONE9	0.14841	0.1938	ZONE10	0.1096	ZONE9
14	0.21686	0.2665	ZONE4	0.153	ZONE9	0.14948	0.1879	ZONE10	0.1153	ZONE9
15	0.21285	0.2553	ZONE10	0.1565	ZONE9	0.14904	0.1832	ZONE10	0.1121	ZONE9
16	0.18587	0.2209	ZONE10	0.1449	ZONE9	0.13975	0.1713	ZONE10	0.1106	ZONE9
17	0.19496	0.2347	ZONE10	0.1505	ZONE9	0.14238	0.1812	ZONE10	0.108	ZONE9
18	0.19384	0.2231	ZONE10	0.1505	ZONE9	0.14468	0.1746	ZONE10	0.1036	ZONE9
19	0.22365	0.3124	ZONE4	0.1632	ZONE7	0.15114	0.1823	ZONE4	0.1131	ZONE9
20	0.208	0.265	ZONE4	0.1595	ZONE9	0.14772	0.1784	ZONE10	0.112	ZONE9
21	0.19651	0.2355	ZONE10	0.1601	ZONE9	0.14866	0.1797	ZONE10	0.12	ZONE9
22	0.19929	0.2306	ZONE10	0.167	ZONE1	0.15109	0.1774	ZONE10	0.1226	ZONE1
23	0.19367	0.2163	ZONE10	0.1678	ZONE7	0.14543	0.1682	ZONE5	0.1219	ZONE7
24	0.19082	0.2175	ZONE6	0.1643	ZONE2	0.14409	0.165	ZONE6	0.1224	ZONE2

As in the natural cubic splines model's case, the grouping of the lags and of the weather variables in the B splines model did not yield any significant improvement over the sLV model.

4.6 Discussion

This chapter makes the in-depth discussion of the results presented in Section 4.5.

To establish a benchmark for comparison, two additional models were implemented: Persistence, which was discussed in Section 2.2.1, and Gradient Boosting Trees (XGB), which was introduced in Section 2.2.3.

4.6.1 LASSO-VAR Frameworks

This section discusses the results obtained with the two different LASSO-VAR frameworks implemented: Standard LASSO-VAR (sLV) and Lag-Group LASSO-VAR (lLV).

Overall, the use of lLV instead of sLV did not yield any improvement on the mean RMSE results. At this point, it is relevant to point out that these results are consistent with the idea that lLV is too restrictive for some applications (Section 3.3). By going through entire grouped sets of lags and weather forecasts, lLV ends up removing variables which would have a positive

impact on the forecasts and including variables that do not. The mean RMSE improvements in relation to the mean RMSE values obtained with Persistence were plotted for the different models implemented.

Figure 4.15: Mean RMSE improvement in relation to Persistence for all WPPs with the VAR model with sLV and the VAR model with lLV.

Whereas, in the VAR setting (Figure 4.15), the use of lLV resulted in similar results to sLV, in the VAR-X (Figure 4.16) and AVAR-X settings (Figures 4.17 and 4.18), the use of lLV significantly worsened the mean RMSE values obtained with the original framework.

In the VAR-X setting, the use of sLV resulted in a mean improvement of 25.0% in relation to the mean RMSE values obtained with Persistence, whereas the use of lLV results in a mean improvement of just 22.6%.

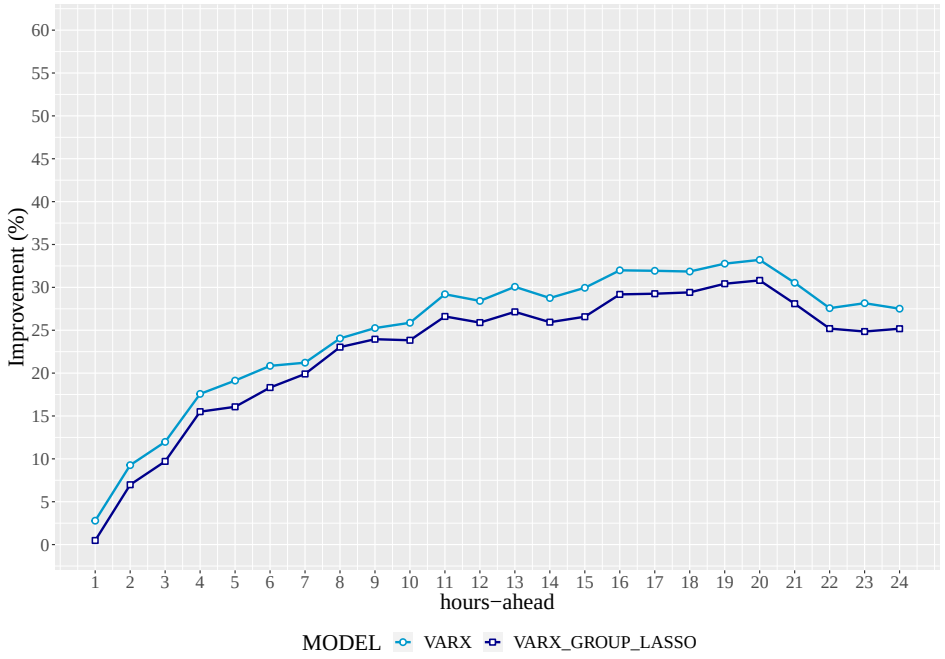

Figure 4.16: Mean RMSE improvement in relation to Persistence for all WPPs with the VAR model with sLV and the VAR model with lLV.

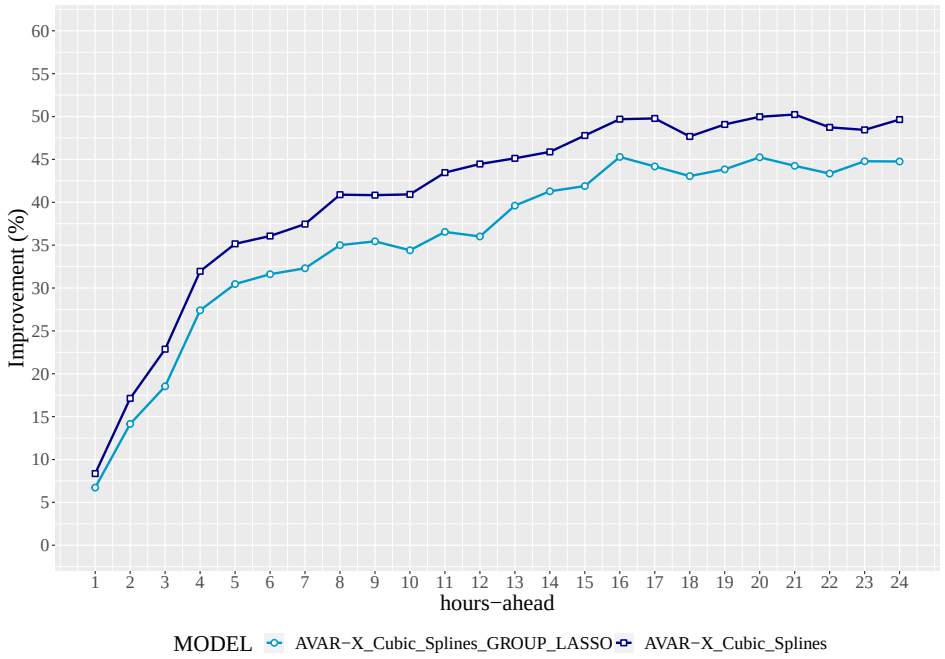

Figure 4.17: Mean RMSE improvement in relation to Persistence for all WPPs with the VAR model with sLV and the VAR model with lLV.

In the AVAR-X setting, the use of sLV resulted in mean improvements of 40.9% (natural cubic splines) and 42.6% (B splines). On the other hand, the use of sLV yielded mean improvements of 35.8% and 38%, respectively.

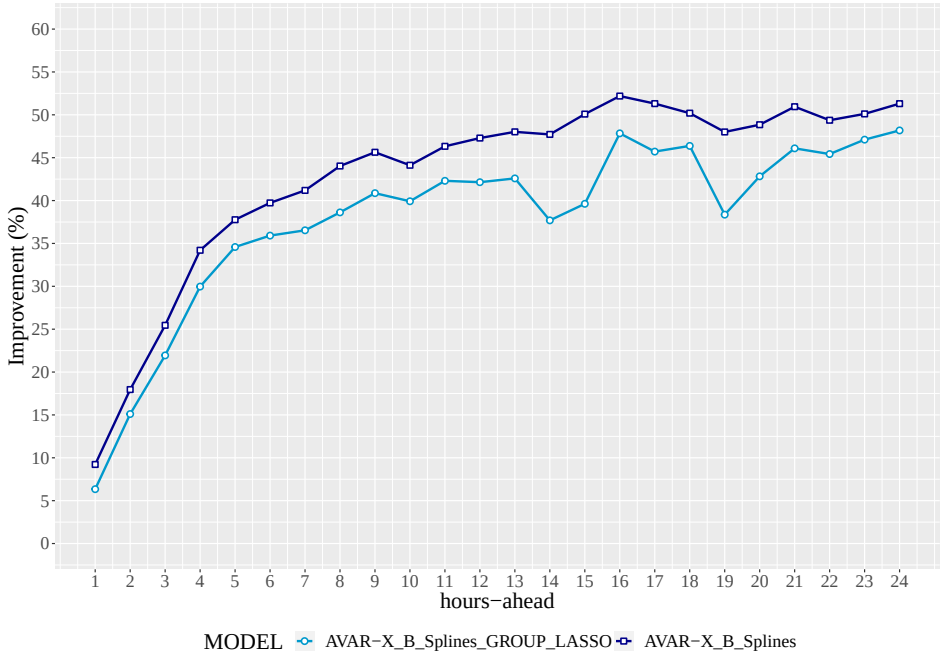

Figure 4.18: Mean RMSE improvement in relation to Persistence for all WPPs with the VAR model with sLV and the VAR model with lLV.

Given the aforementioned results, the results obtained with lLV will not be discussed in subsequent sections.

4.6.2 Exogenous Variables

This section addresses the subject of exogenous variables and whether their use in the models yields improvements in the forecasts. The models with exogenous variables discussed in this section use linear combinations of the weather variables, u and v. The subject of additive models is discussed in Section 4.6.3.

In the univariate setting, the use of exogenous variables yielded a positive result in the forecasting capability of the model, resulting in a mean improvement of 22.4% in relation to the mean RMSE values obtained with Persistence against a mean improvement of 16.3% yielded by the AR model, as displayed in Figure 4.19 and Table 5.15 (Appendix B.1). However, for the 1 hour-ahead forecast, this improvement is only marginal, representing an additional 1.2 % improvement in the accuracy of the forecast.

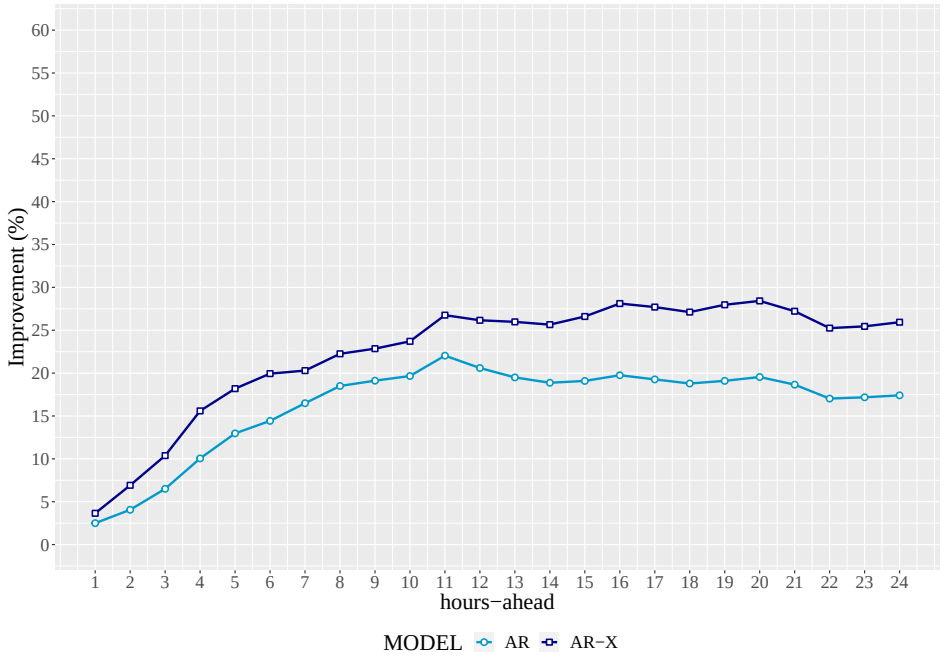

Figure 4.19: Mean RMSE improvement in relation to Persistence with the AR and AR-X models (%).

The Diebold-Mariano test was implemented on the RMSE results of the AR and AR-X models, as displayed in Table 4.16. The p-value results show that, for a level of significance of 5%, it is only possible to conclude that the results obtained with both models for the 1 hour-ahead horizon are significantly different for ZONE10. For ZONES 1 to 9, the null hypothesis stands and it is not possible to make such a statement. However, for the 24 hours-ahead horizon, for the same level of significance, the null hypothesis is rejected in 5 out of 10 ZONES.

Even though the results do not display the same level of statistical significance for all WPPs, it is fair to say that the AR-X model improves the accuracy of the forecasts made with the AR model, particularly in timescales of more than a few hours-ahead. As discussed in Section 4.5.2, this is likely due to the prevalence of the lags' coefficients over the weather variables' coefficients in the shorter forecasting horizons.

Table 4.16: P-Value results for the two-sided Diebold-Mariano Test (AR vs AR-X Model)

hours-ahead	ZONE1	ZONE2	ZONE3	ZONE4	ZONE5	ZONE6	ZONE7	ZONE8	ZONE9	ZONE10
h=1	0.8270	0.8727	0.2088	0.4525	0.2675	0.7364	0.4555	0.5019	0.2394	0.0404
h=24	0.0734	0.0202	0.2144	0.0301	0.0364	0.0112	0.0487	0.1523	0.2686	0.1277

In the multivariate setting, the VAR-X model yielded a mean improvement of up to 25.0 % in relation to the mean RMSE values obtained with Persistence against a mean improvement of 18.8% obtained with the VAR model, as displayed in Figure 4.20 and Table 5.15 (Appendix B.1). However, for the 1 hour-ahead forecast, the VAR-X model performed worse than the VAR

model, which seems to indicate a potential detrimental effect of the use of exogenous variables for this timescale.

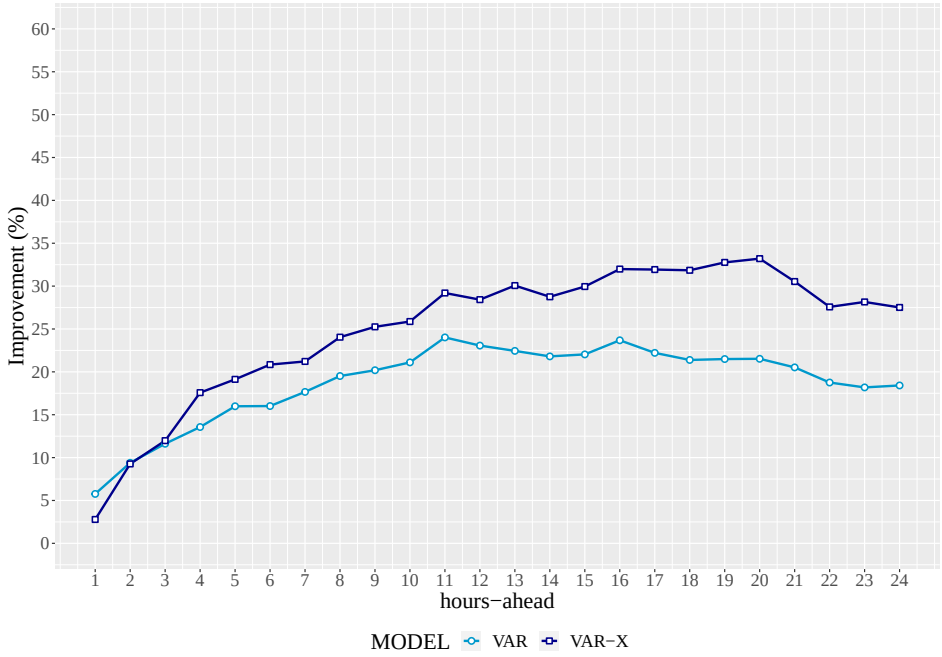

Figure 4.20: Mean RMSE improvement in relation to Persistence with the VAR and VAR-X models (%)

For the 1 hour-ahead time horizon, the Diebold-Mariano test results show that, for a level of significance of 5%, it is not possible to reject the null hypothesis in any of the 10 WPPs, which means that it is not possible to conclude that the models' performance is significantly different for this timescale. For the 24 hours-ahead time horizon, for the same level of significance, the null hypothesis is rejected in 4 of the 10 WPPs, meaning that, to a certain extent, it is possible to affirm that the models perform differently for this forecasting horizon.

Table 4.17: P-Value results for the two-sided Diebold-Mariano Test (VAR vs VAR-X Model)

hours-ahead	ZONE1	ZONE2	ZONE3	ZONE4	ZONE5	ZONE6	ZONE7	ZONE8	ZONE9	ZONE10
h=1	0.8592	0.7369	0.2887	0.8431	0.382	0.441	0.4761	0.3146	0.8333	0.7127
h=24	0.04899	0.04434	0.0981	0.07553	0.0476	0.04052	0.05541	0.5603	0.3004	0.1319

Overall, even though the results of the Diebold-Mariano test do not display the same level of statistical significance for all WPPs and forecasting horizons, it is fair to say that the use of exogenous variables increased the accuracy of the forecasts, yielding particularly good results in timescales of more than a few hours-ahead.

4.6.3 Spatiotemporal Models

This section discusses the subject of spatiotemporal models and whether the use of geographically distributed data yielded improvements in the forecasts.

In the models without exogenous variables, the use of data from all WPPs yielded marginal improvements in the forecast, as displayed in Figure 4.21 and Table 5.15 (Appendix B.1). The AR model yielded a mean improvement of 16.3% in relation to the mean RMSE values obtained with Persistence, while the VAR model resulted in a mean improvement of 18.8%. Therefore, it is possible to conclude that the VAR model was able to capture to some degree the cross-correlation displayed by the power generation time series, as discussed in Section 4.2.2.

The Diebold-Mariano test was implemented, as displayed in Table 4.18. For a level of significance of 5%, it is not possible to reject the null hypothesis in any circumstance, meaning that it is not possible to affirm that there is any significant difference in the forecasting accuracy of the AR and VAR models.

Table 4.18: P-Value results for the two-sided Diebold-Mariano Test (AR vs VAR Model)

hours-ahead	ZONE1	ZONE2	ZONE3	ZONE4	ZONE5	ZONE6	ZONE7	ZONE8	ZONE9	ZONE10
h=1	0.7067	0.9052	0.4831	0.8676	0.7215	0.7543	0.6658	0.9305	0.8861	0.5624
h=24	0.5852	0.3863	0.736	0.4066	0.2049	0.1696	0.5094	0.6311	0.1401	0.8005

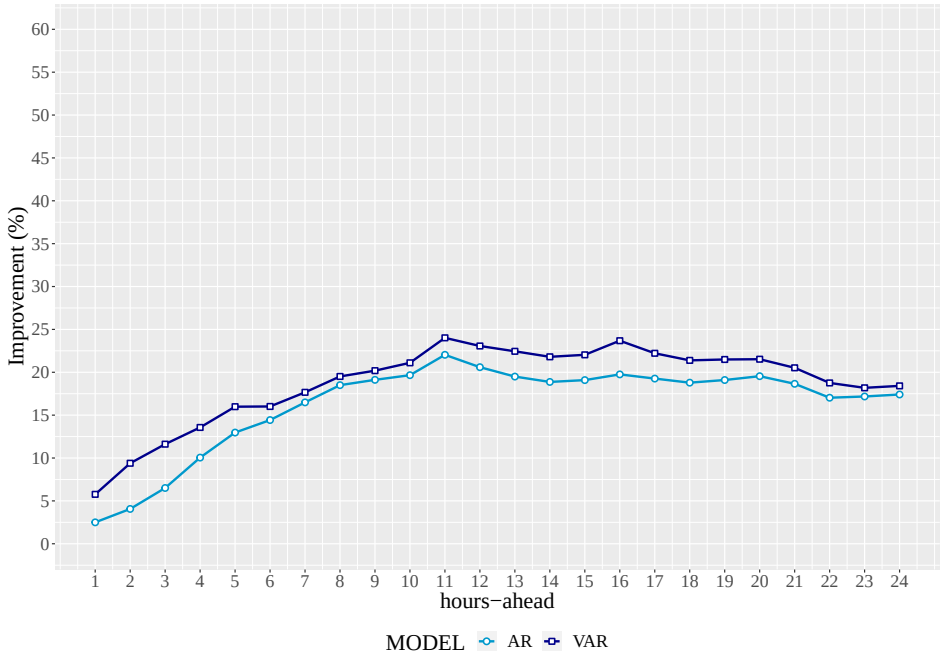

Figure 4.21: Mean RMSE improvement in relation to Persistence with the AR and VAR models (%).

The results obtained with the AR-X and VAR-X models are identical. The use of geographically distributed data represented a mean improvement of 25.0% in relation to the mean RMSE

values obtained with Persistence against a mean improvement of 22.4% obtained with the AR-X model, as displayed in Figure 4.22 and Table 5.15 (Appendix B.1).

For the 1 hour-ahead forecasting horizon, the mean improvement obtained with the VAR-X model (2.8%) is actually lower than that provided by the AR-X model (3.71%).

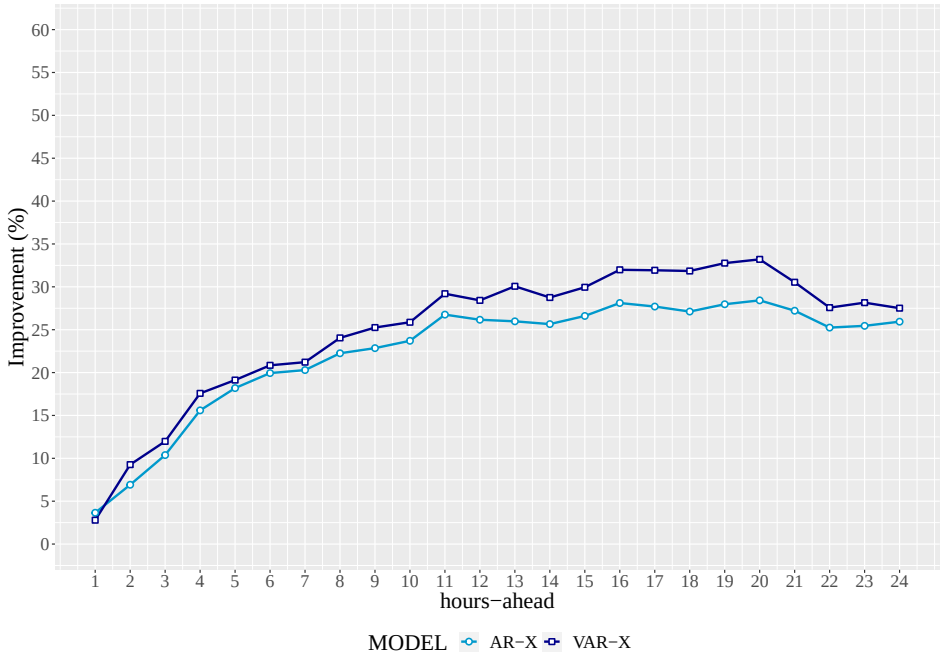

Figure 4.22: Mean RMSE improvement in relation to Persistence with the AR-X and VAR-X models (%).

Regarding the results of the Diebold-Mariano test, for a level of significance of 5%, it is not possible to affirm that the models have significantly different levels of performance in either the 1 hour-ahead or the 24 hours-ahead forecasting horizons.

Table 4.19: P-Value results for the two-sided Diebold-Mariano Test (AR-X vs VAR-X Model)

hours-ahead	ZONE1	ZONE2	ZONE3	ZONE4	ZONE5	ZONE6	ZONE7	ZONE8	ZONE9	ZONE10
h=1	0.9246	0.9741	0.454	0.7231	0.7081	0.669	0.6433	0.2722	0.9963	0.8301
h=24	0.6256	0.1756	0.2005	0.2917	0.05541	0.4117	0.71	0.5965	0.1703	0.4733

When it comes to the AAR-X and AVAR-X (natural cubic splines) models, in general, the use of geographically distributed data yielded similar results. The AAR-X model yielded a mean improvement of 39.4% in relation to the mean RMSE values obtained with Persistence, while the AVAR-X model yielded a mean improvement of 40.9%. The main disparities seem to occur after the 11^{th} hour. Given the predominance of the weather forecasts in this timescale, this probably results from the VAR-X model capturing the linear correlations between the weather forecasts from the different WPP locations.

The complete results are displayed in Figure 4.23 and Table 5.15 (Appendix B.1).

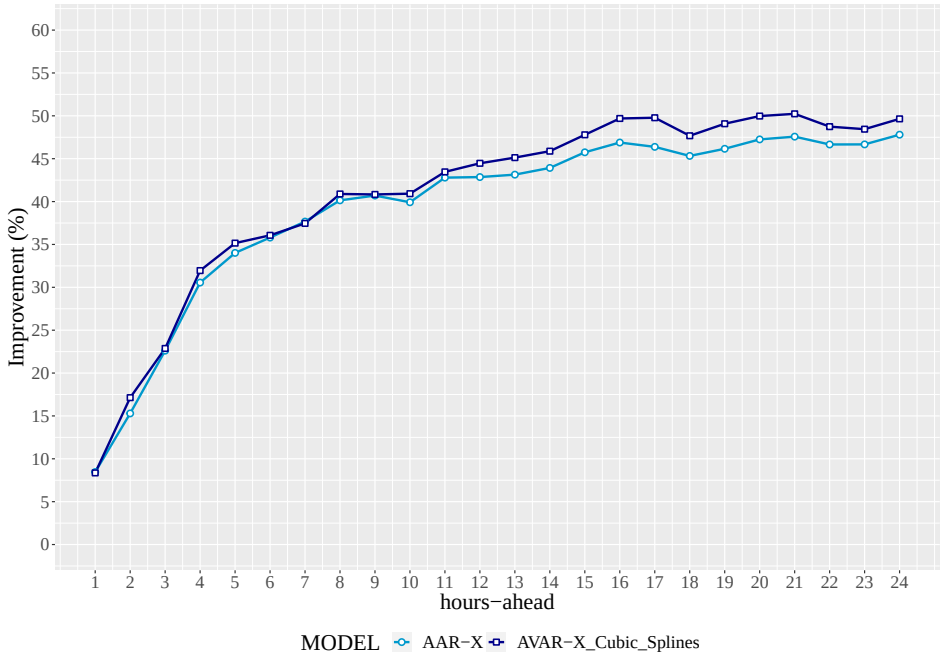

Figure 4.23: Mean RMSE improvement in relation to Persistence with the AAR-X (natural cubic splines) and AVAR-X models (natural cubic splines) (%).

The results of the Diebold-Mariano test show that, for a level of significance of 5%, the null hypothesis stands for all WWP in the 1 hour-ahead forecasting horizon. However, for the 24 hours-ahead forecasting horizon, the null hypothesis is rejected in ZONES 1 and 2, meaning that the models display a significantly different performance.

Table 4.20: P-Value results for the two-sided Diebold-Mariano Test [AAR-X (natural cubic splines) vs AVAR-X Model (natural cubic splines)]

hours-ahead	ZONE1	ZONE2	ZONE3	ZONE4	ZONE5	ZONE6	ZONE7	ZONE8	ZONE9	ZONE10
h=1	0.9819	0.996	0.8348	0.7572	0.6872	0.7086	0.8888	0.8265	0.9747	0.5239
h=24	1.21E-34	0.008907	0.6707	0.4278	0.3411	0.5808	0.118	0.3632	0.8096	0.3454

Overall, the improvements yielded by the use of geographically disperse data did not prove to be very statistically significant. However, the improvements seen in the RMSE seem to validate the concept behind spatiotemporal models.

4.6.4 Additive Models

This section discusses the subject of additive models and whether the use of piecewise smooth functions (splines) resulted in improvements in the forecasting capabilities of the models.

In the univariate setting, the use of natural cubic splines yielded very positive results, particularly in the longer term horizons. The use of the AAR-X model yielded a mean improvement of 39.4% in relation to the mean RMSE values obtained with Persistence against the 22.4% obtained with the AR-X model.

For the 24 hours-ahead horizon, the use of splines resulted in an additional improvement of more than 21% in relation to the linear model.

The results are displayed in Figure 4.24 and Table 5.15 (Appendix B.1).

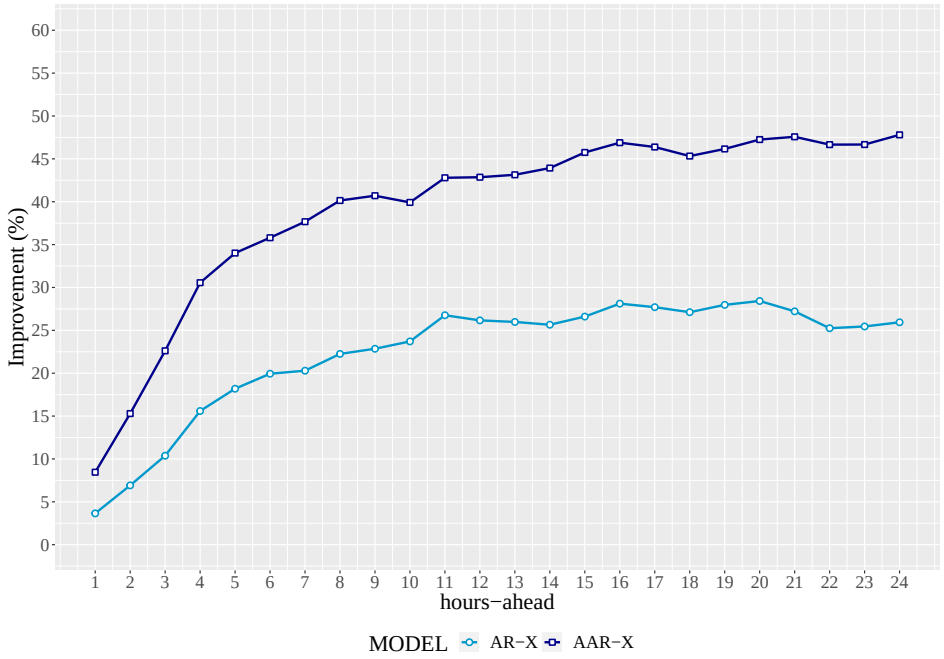

Figure 4.24: Mean RMSE improvement in relation to Persistence with the AR-X and AAR-X models (%).

The results from the Diebold-Mariano test show that, for the 1 hour-ahead forecast, for a level of significance of 5%, the null hypothesis is rejected in 5 WPPs. For the 24 hours-ahead forecast, the null hypothesis is rejected in all WPPs, meaning that it is possible to conclude that the AR-X and AAR-X models display significantly different levels of forecasting accuracy for this timescale.

Table 4.21: P-Value results for the two-sided Diebold-Mariano Test (AR-X vs AAR-X Model)

hours-ahead	ZONE1	ZONE2	ZONE3	ZONE4	ZONE5	ZONE6	ZONE7	ZONE8	ZONE9	ZONE10
h=1	0.6355	0.2884	0.168	0.02437	5.03E-05	0.02449	0.2823	0.9116	0.008304	0.000108
h=24	1.05E-12	2.25E-08	1.61E-23	4.12E-18	2.58E-21	1.74E-17	1.30E-93	5.73E-10	1.21E-09	6.58E-16

In the multivariate setting, the results yielded by the use of splines display similar results. For the 1 hour-ahead forecasting horizon, the use natural cubic splines resulted in an additional improvement of 5.6% in relation to the mean RMSE values obtained with Persistence. For the 24

hours-ahead forecasting horizon, the additional improvement is over 22%. The mean improvement obtained with the VAR-X model was 25.0% and the mean improvement yielded by the AVAR-X model was 40.9%.

The results are displayed in Figure 4.25 and Table 5.15 (Appendix B.1).

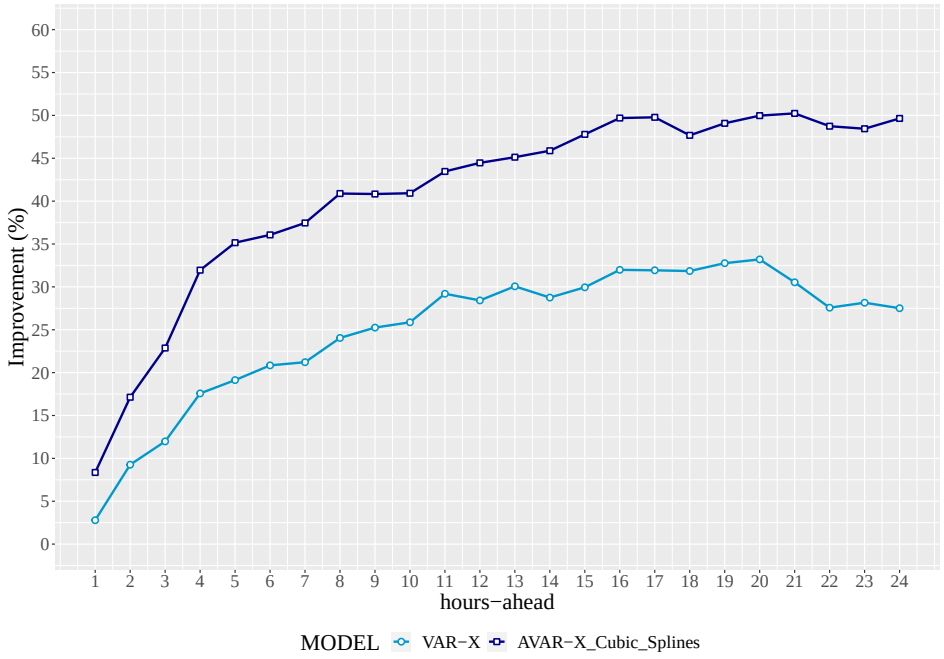

Figure 4.25: Mean RMSE Improvement from Persistence with the VAR-X and AVAR-X (natural cubic splines) models (%).

According to the Diebold-Mariano test results, for the 1 hour-ahead horizon, for a level of significance of 5%, it is not possible to affirm that the models are significantly different in 9 of the 10 WPPs, where ZONE5 is the exception. For the 24 hours-ahead forecast, the null hypothesis is rejected in all WPPs, meaning that the models are significantly different at forecasting this horizon.

Table 4.22: P-Value results for the two-sided Diebold-Mariano Test (VAR-X vs AVAR-X Model with Natural Cubic Splines)

hours-ahead	ZONE1	ZONE2	ZONE3	ZONE4	ZONE5	ZONE6	ZONE7	ZONE8	ZONE9	ZONE10
h=1	0.7991	0.815	0.4485	0.198	0.007648	0.5754	0.7076	0.159	0.7637	0.5698
h=24	4.96E-11	3.98E-06	5.94E-11	2.65E-13	8.77E-15	6.50E-09	3.46E-14	3.92E-08	1.45E-22	4.53E-08

Overall, the use of splines proved to have a statistically significant positive effect in the longer forecasting horizons. For the smaller term horizons, the results proved not to be as statistically significant. Nevertheless, the improvements seen in the RMSE seem to indicate that the use of additive models is beneficial for timescales of even a few hours-ahead.

AVAR-X model (Natural Cubic Splines) vs AVAR-X model (B Splines)

When it comes to the use of different types of smooth functions, the cubic B splines models seem to perform slightly better than the ones using natural cubic splines. The first yielded a mean improvement of 43.0% in relation to the mean RMSE values obtained with Persistence, while the latter resulted in a mean improvement of 40.9%. Apart from the 19 hours-ahead and 20 hours-ahead horizons, the B splines were the best performing model among the two splines models.

For the 1 hour-ahead horizon and a level of significance of 5%, the null hypothesis of the Diebold-Mariano test stands in all WPPs, meaning that the models are not significantly different at forecasting this horizon. For the 24 hours-ahead forecasting horizon and the same level of significance, the null hypothesis is rejected in two WPPs.

Table 4.23: P-Value results for the two-sided Diebold-Mariano Test (AVAR-X Model with Natural Cubic Splines vs AVAR-X Model with B Splines)

hours-ahead	ZONE1	ZONE2	ZONE3	ZONE4	ZONE5	ZONE6	ZONE7	ZONE8	ZONE9	ZONE10
h=1	0.261	0.1466	0.4629	0.1063	0.2554	0.1697	0.7064	0.2767	0.9303	0.512
h=24	0.7201	0.008111	0.001727	0.07711	0.05877	0.3347	0.7596	0.454	0.3203	0.227

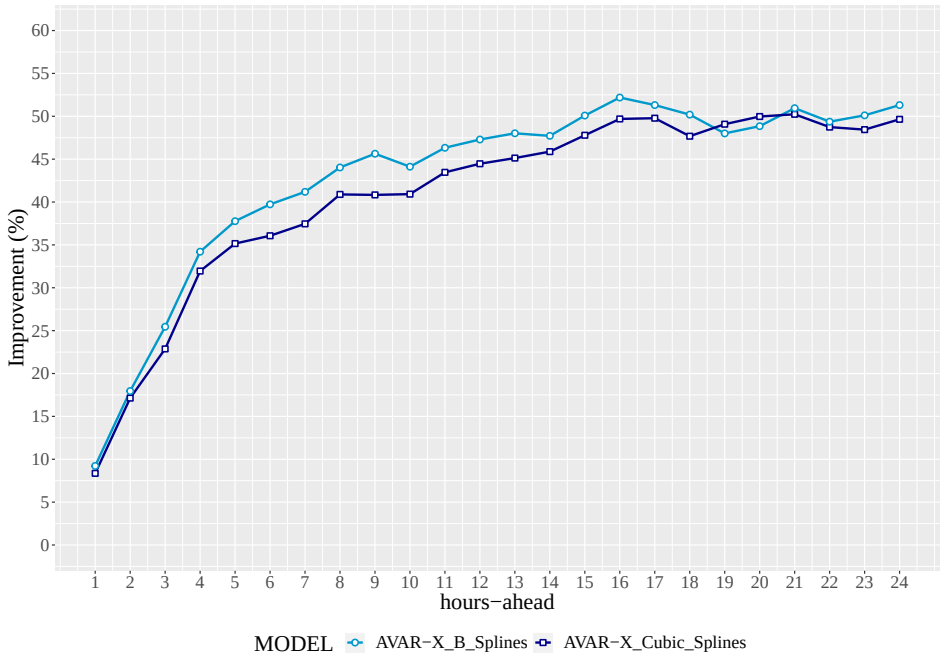

Figure 4.26: Mean RMSE Improvement from Persistence with the AVAR-X (natural cubic splines) and AVAR-X (B splines) models (%).

Overall, even though the results were not statistically significant for most WPPs, the improvements seen in RMSE seem to indicate a slight superiority of the B splines for forecasting wind power generation in most timescales.

4.7 Model Comparison

After an in-depth discussion of the individual models, the final section of this chapter compares the performance of all models used.

Results for each WPP location

The first part of this section discusses the results obtained for each WPP, identifying which models performed best in each WPP and for each timescale. Table 4.24 presents the results obtained for ZONE1, while the results for the remaining WPPs are disclosed in Appendix B.2.

Table 4.24: ZONE1 Mean RMSE Results per Timescale.

hours-ahead	AR	AR-X	AAR-X	VAR	VAR-X	AVAR-X (natual cubic splines)	AVAR-X (B splines)	XGB
[1,3]	0.1466	0.1427	0.1351	0.1396	0.1398	0.1221	0.1217	0.1325
]3, 12]	0.2263	0.2103	0.185	0.2156	0.2026	0.1519	0.1478	0.1549
]12, 24]	0.2863	0.2406	0.197	0.2679	0.23	0.1562	0.1703	0.1406

The ranking of the models for each WPP and for three different horizons were computed, as seen in Tables 4.25 to 4.27.

Among the models implemented, the one that performed better in the shorter forecasting horizon (1 to 3 hours-ahead) was the AVAR-X model with B splines, yielding the lowest mean RMSE in all WPPs. The second best performing models in the shorter forecasting horizon were the AVAR-X model with natural cubic splines (in 6 WPPs) and the AAR-X model (in 4 WPPs). The worst performing models in this horizon were the AR model (in 6 WPPs), the VAR-X model (in 3 WPPs) and the AR-X model (in 1 WPP).

Table 4.25: Model ranking for the shorter forecasting horizon (1 to 3 hours-ahead).

WPP	AR	AR-X	AAR-X	VAR	VAR-X	AVAR-X (natural cubic splines)	AVAR-X (B splines)	XGB
ZONE 1	8	7	4	5	6	2	1	3
ZONE 2	8	6	3	7	5	2	1	4
ZONE 3	8	7	3	6	5	2	1	4
ZONE 4	8	7	3	5	6	2	1	4
ZONE 5	8	7	3	5	6	2	1	4
ZONE 6	7	6	2	5	8	4	1	3
ZONE 7	7	6	2	5	8	3	1	4
ZONE 8	6	5	2	7	8	3	1	4
ZONE 9	7	8	3	4	6	2	1	5
ZONE 10	8	7	2	6	5	3	1	4

In the medium term forecasting horizon (3 to 12 hours-ahead), the best performing model was, once again , the AVAR-X model with B splines, followed by the XGB (in 4 WPPs) and the AVAR-X with natural cubic splines (in 3 WPPs).

The worst performing models were the AR model (in 8 WPPs) and the VAR model (in 2 WPPs).

Table 4.26: Model ranking for the medium term horizon (3 to 12 hours-ahead).

WPP	AR	AR-X	AAR-X	VAR	VAR-X	AVAR-X (natural cubic splines)	AVAR-X (B splines)	XGB
ZONE 1	8	6	4	7	5	2	1	3
ZONE 2	8	6	4	7	5	2	1	3
ZONE 3	8	7	3	6	5	2	1	4
ZONE 4	7	6	4	8	5	3	1	2
ZONE 5	8	6	3	7	5	4	1	3
ZONE 6	7	6	3	8	5	4	1	2
ZONE 7	8	5	2	7	6	3	1	4
ZONE 8	8	5	2	7	6	4	1	3
ZONE 9	8	7	4	6	5	3	1	2
ZONE 10	8	6	3	7	5	4	1	2

Finally, in the long term forecasting horizon (12 to 24 hours-ahead), the best performing models were the XGB model (in 7 WPPs) and the AVAR-X model with B splines (in 3 WPPs). Once again, the worst performing models were the AR model (in 8 WPPs) and the VAR model (in 2 WPPs).

Table 4.27: Model ranking for the longer forecasting horizon (12 to 24 hours-ahead).

WPP	AR	AR-X	AAR-X	VAR	VAR-X	AVAR-X (natural cubic splines)	AVAR-X (B splines)	XGB
ZONE 1	8	6	4	7	5	2	3	1
ZONE 2	7	6	4	8	5	3	1	2
ZONE 3	8	6	2	7	5	3	1	4
ZONE 4	8	6	4	7	5	3	2	1
ZONE 5	8	6	4	7	5	2	1	3
ZONE 6	8	6	4	7	5	3	2	1
ZONE 7	8	6	4	7	5	3	2	1
ZONE 8	8	6	4	7	5	3	2	1
ZONE 9	8	6	4	7	5	3	2	1
ZONE 10	7	6	4	8	5	3	2	1

Overall, the rankings of the models by WPP do not display significant differences. As expected, the approaches capable of modelling the non-linear relation between the power measurements and the weather forecasts prove to be the most adequate for all forecasting horizons. However, as seen in Sections 4.6.2 and 4.6.4 , this difference is not statistically significant for the 1 hour-ahead horizon, meaning that, as the forecasting horizon decreases, so does the positive effect of the use of the weather forecasts.

General Results

A brief overview of the results obtained with all models is presented in this section. Figure 4.27 and Table 5.15 (Appendix B.1) display the mean improvements yielded by all models in relation to the mean RMSE values obtained with Persistence for all forecasting horizons.

To statistically compare all the models, the Friedman test was performed and the critical difference diagrams computed for all WPPs (1 hour-ahead and 24 hours-ahead forecasting horizons), as displayed in Figures 4.28 and 4.29 and Figures 5.19 to 5.36 (Appendix B.3).

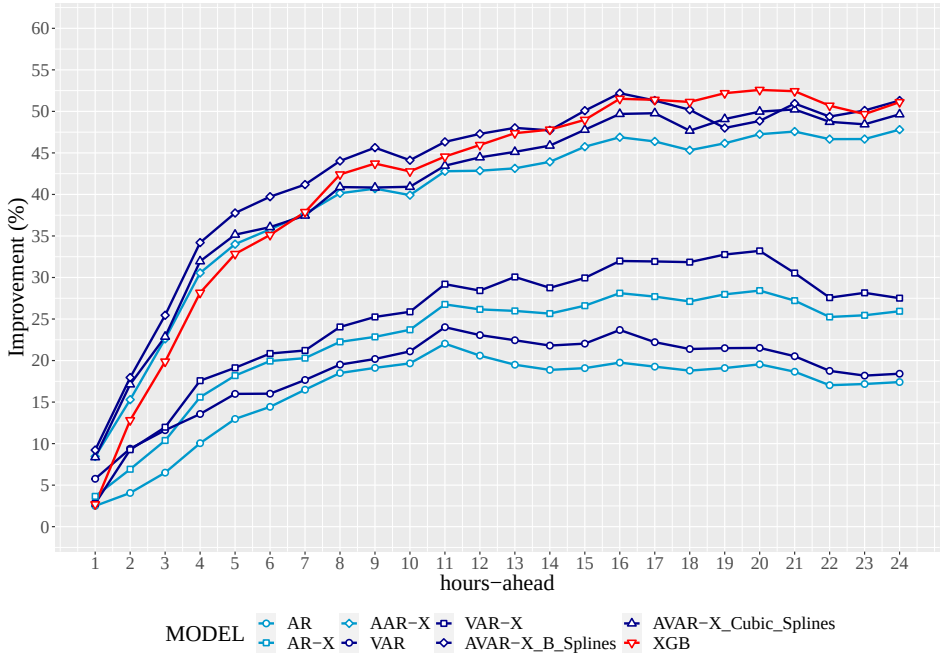

Figure 4.27: Mean RMSE improvement in relation to Persistence with all models (%).

For the 1 hour-ahead forecasting horizon, one of the key insights from the results is that none of the models implemented was able to improve the mean RMSE values obtained with Persistence more than 10%, which validates the use of this method as a reference tool in very-short term wind power generation forecasting. In fact, as highlighted throughout Section 4.2, the mean RMSE results obtained for this horizon were, in most cases, not significantly different.

However, the results of the Friedman test for the 1 hour-ahead forecast show that, for a level of significance of 5%, it is possible to conclude that the models display significantly different levels of accuracy for all WPPs, with the horizontal lines of the critical difference diagrams linking models where no statistical significant differences were found between the results.

Nevertheless, given that these results are statistically less significant than the results obtained for the 24 hours-ahead forecasting horizon, and taking into account the changes in the rankings' positions between WPPs, it is difficult to conclude which model, or models, are the definitive best for this forecasting horizon.

In this regard, and even though the results for all models resulted in marginal to small improvements in respect to the mean RMSE values obtained with Persistence, the AVAR-X models and the AAR-X model, methods which have yielded the highest improvements for this timescale, seem to prevail slightly over the others.

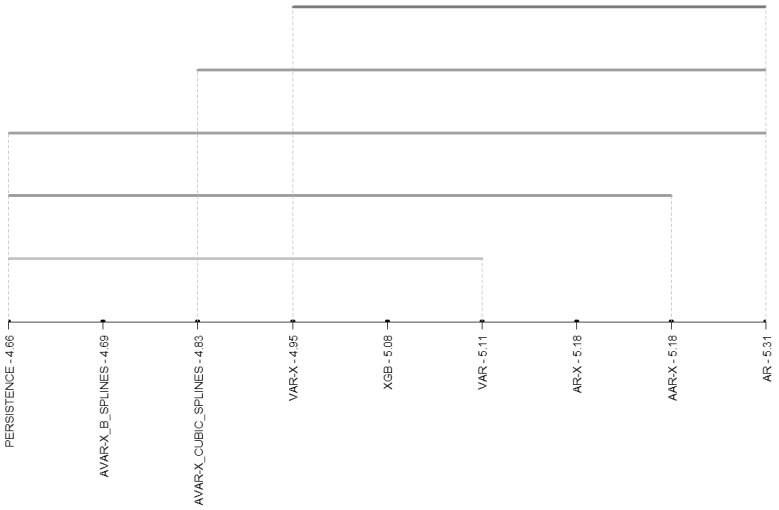

Figure 4.28: Critical Difference diagram for ZONE1 and 1 hour-ahead (Result: Different; p-value = 4.6e-06; Critical Distance = 0.457).

For the 24 hours-ahead forecast, the results show a statistically significant difference between the XGB, the AVAR-X and the AAR-X and the remaining models in all WPPs, result which validates the thesis which states that the use of weather forecasts and, in particular, the use of these variables in such a way that non-linear correlations between them and the power measurements are captured, improves the forecasting capabilities of the models in horizons of more than a few hours-ahead. Furthermore, although not with the same level of statistical significance, the VAR-X and AR-X models seem to prevail over Persistence and the AR and VAR models.

By the same token, in Figure 4.27, it is possible to distinguish the three aforementioned clusters of predictor models being created as the forecasting horizon increases.

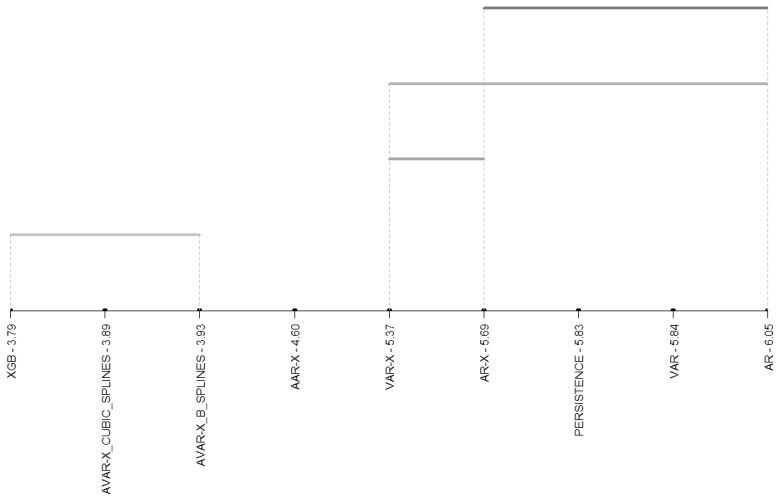

Figure 4.29: Critical Difference diagram for ZONE1 and 24 hours-ahead (Result: Different; p-value = 1.5e-135; Critical Distance = 0.458).

As discussed in Sections 4.6.3 and 4.6.4, the AVAR-X model with B splines seems to improve slightly the results obtained with the AVAR-X with natural cubic splines. The final part of this section is dedicated to the comparison of the AVAR-X model with B splines and the XGB model, which proved to be, on average, the two best methods for intraday and day-ahead renewable power forecasting, particularly in forecasting horizons of more than 6 to 8 hours-ahead.

The main difference between the models resides in the fact that, although both approaches are able to capture the correlations between the power generated in the different WPP locations, unlike the XGB, the AVAR-X with B splines model is only able to capture the linear interdependencies between these variables. Both models are, however, able to capture the non-linear relation between the weather forecasts and the power generated, even if in different ways.

For the 1 hour-ahead forecast, the AVAR-X model with B splines yielded a mean improvement of 9.2% in relation to the mean RMSE values obtained with Persistence, while the XGB model resulted merely in a 2.7% improvement. The Diebold-Mariano test results show that, for a level of significance of 5%, for the 1 hour-ahead time horizon, it is possible to conclude that the models have a significantly different performance in 6 of the 10 WPPs locations. Even though the results are not statistically significant for all WPPs, it is fair to say, given the improvements in the RMSE, that the AVAR-X model with B splines is the best model of the two for this forecasting horizon.

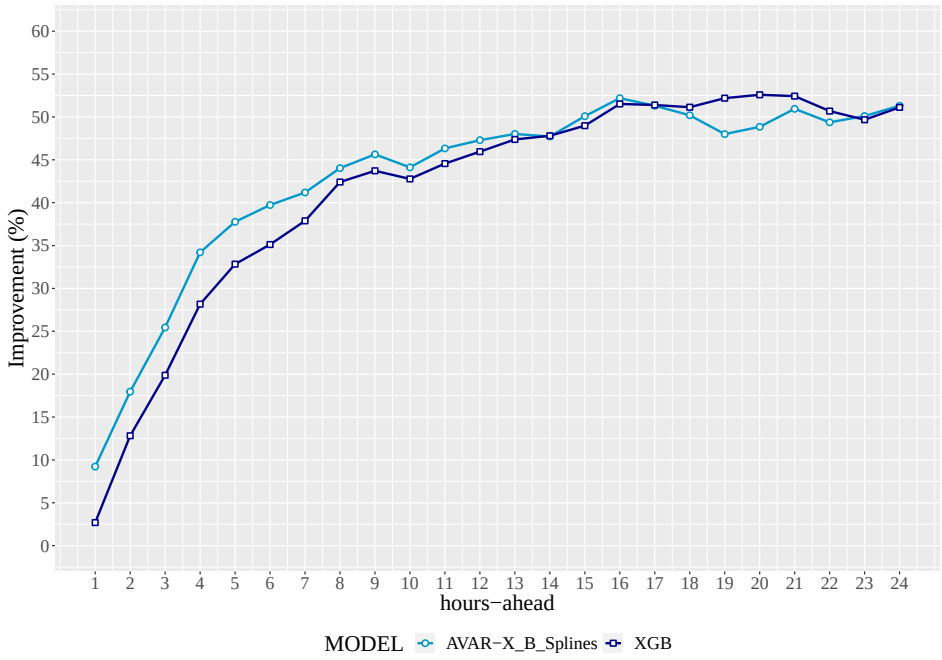

Figure 4.30: Mean RMSE improvement in relation to Persistence with the AVAR-X (B splines) and XGB models (%).

For the 24 hours-ahead horizon, the AVAR-X model with B splines yielded a mean improvement of 51.3% in relation to the mean RMSE values obtained with Persistence, while the XGB model resulted in a 51.1% improvement. For this horizon and a significance level of 5%, the

null hypothesis is rejected in 3 WPPs, meaning that, in 7 WPP locations, it is not possible to distinguish the performance of both models.

Table 4.28: P-Value results for the two-sided Diebold-Mariano Test (AVAR-X Model with B Splines vs XGB)

hours-ahead	ZONE1	ZONE2	ZONE3	ZONE4	ZONE5	ZONE6	ZONE7	ZONE8	ZONE9	ZONE10
h=1	0.0495	0.03934	0.002881	0.0355	0.003847	0.1297	0.1334	0.05098	0.08851	0.01088
h=24	0.0118	0.7589	0.00359	0.3303	0.06765	0.6876	0.05327	0.01194	0.8601	0.5204

Overall, the use of AVAR-X model with B splines resulted in a mean improvement of 43.0% in relation to the mean RMSE values obtained with Persistence against a mean improvement of 41.5% yielded by the XGB model. Furthermore, the mean results obtained with the AVAR-X model were better in 17 of the 24 forecasting horizons.

Given the RMSE results yielded by both models, the results by WPP presented earlier in this section and the results of the Diebold-Mariano test, it is possible to conclude that the AVAR-X with B splines proved to be the best model for horizons of up to 12 hours-ahead.

For horizons of more than 12 hours-ahead, where the use of AVAR-X model with B splines resulted in a mean improvement of 49.8% in relation to the mean RMSE values obtained with Persistence and the XGB model a mean improvement of 50.6%, it is possible to affirm that the AVAR-X proved to be able to compete against the XGB model.

Chapter 5

Conclusion and Future Work

The present work implemented a total of 11 autoregression-based models to wind power forecasting. Among these were models that used different LASSO-VAR frameworks, models that used linear combinations of weather forecasts to make predictions, models that used geographically distributed power measurements to capture the linear interdependencies between neighbouring WPPs, and models that used weather variables in additive frameworks.

The use of lag-group LASSO-VAR (lLV) proved not to yield any positive impact on the forecasts over the standard LASSO-VAR (sLV) framework. The reason for this is most likely related with a lack of flexibility of the first model, which drops or includes entire groups of lags and weather forecasts from the process even if only a small number of coefficients is significant.

The use of linear combinations of exogenous variables can be said to have had a positive impact on the forecasting results. Even though the results were not statistically significant for the 1 hour-ahead horizon, it is clear that, as the predominance of the lags' coefficients shrinks over time, the use of weather forecasts can prove to have a positive impact on the results.

The use of geographically distributed data proved not to yield statistically significant improvements over the results obtained with univariate models. However, the marginal improvements observed validate the concept behind spatiotemporal models.

The use of additive models led to statistically significant improvements for the 24 hours-ahead forecasting horizon. For the shorter horizons, even though the results proved to be not as statistically significant, the marginal improvements seem to indicate that these models are a good solution even timescales of a few hours-ahead.

The AVAR-X model with B splines proved to be the autoregressive model yielding the best overall results. For forecasting horizons of up to 12 hours-ahead, this model proved to be able to improve on the results obtained with Persistence and the XGB model. For forecasting horizons of more than 12 hours-ahead, even though the results proved not to be statistically significant, it is possible to conclude that the AVAR-X model proved to be capable of competing against machine learning models such as the XGB.

To conclude, some of the possible future works on this subject may encompass:

- The increase of the solution space used in the Bayesian Optimization process which, for computational reasons, was very limited;

- The use of different LASSO-VAR frameworks, namely lag-sparse-group LASSO-VAR (lsLV), which adds within-group sparsity to lLV;
- The use of different types of smooth functions, namely splines of varying polynomial degrees.

Bibliography

Abbe, C. (1901). The physical basis of long-range weather forecasts. *Monthly Weather Review*, *29*(12), 555–561. doi: 10.1175/1520-0493(1901)29[551c:tpbolw]2.0.co;2

Bauer, P., Thorpe, A., & Brunet, G. (2015). The quiet revolution of numerical weather prediction. *Nature*, *525*, 47–55. doi: 10.1038/nature14956

Bessa, R. J. (2008). *Treino de Redes Neuronais Aplicado à Previsão Eólica* (Unpublished doctoral dissertation). Universidade do Porto.

Bessa, R. J., Trindade, A., & Miranda, V. (2015). Spatial-temporal solar power forecasting for smart grids. *IEEE Transactions on Industrial Informatics*, *11*(1), 232–241. doi: 10.1109/TII.2014.2365703

Bjerknes, V., Volken, E., & Brönnimann, S. (1904). The problem of weather prediction, considered from the viewpoints of mechanics and physics. *Meteorologische Zeitschrift*, *21*, 1 – 7. doi: 10.1127/0941-2948/2009/416

Boyd, S., Parikh, N., Chu, E., Peleato, B., & Eckstein, J. (2010). *Distributed optimization and statistical learning via the alternating direction method of multipliers.* doi: 10.1561/2200000016

Cavalcante, L., Bessa, R. J., Reis, M., & Browell, J. (2017). LASSO vector autoregression structures for very short-term wind power forecasting. *Wind Energy*, *20*, 657–675. doi: 10.1002/we.2029

Diebold, F. X., & Mariano, R. S. (1995). Comparing predictive accuracy. *Journal of Business and Economic Statistics*. doi: 10.1080/07350015.1995.10524599

Frazier, P. I. (2018). *A Tutorial on Bayesian Optimization.* eprint arXiv:1807.02811.

Gama, J., Carvalho, A., Faceli, K., Lorena, A., & Oliveira, M. E. (2012). *Extração de conhecimento de dados: data mining* (Third ed.). Lisbon: Edições Sílabo.

Geurts, M., Box, G. E. P., & Jenkins, G. M. (1977). Time Series Analysis: Forecasting and Control. *Journal of Marketing Research*. doi: 10.2307/3150485

Ghofrani, M., & Alolayan, M. (2018). Time Series and Renewable Energy Forecasting. In *Time series analysis and applications* (chap. 6). doi: 10.5772/intechopen.70845

GWEC. (2021). *Global Wind Report 2021* (Tech. Rep.). Global Wind Energy Council.

Hsu, N. J., Hung, H. L., & Chang, Y. M. (2008). Subset selection for vector autoregressive processes using Lasso. *Computational Statistics and Data Analysis*, *52*(7), 3645–3657. doi: 10.1016/j.csda.2007.12.004

James, G., Witten, D., Hastie, T., & Tibshirani, R. (2000). *An introduction to Statistical Learning.* doi: 10.1007/978-1-4614-7138-7

Lai, J. P., Chang, Y. M., Chen, C. H., & Pai, P. F. (2020). A survey of machine learning models in

renewable energy predictions. *Applied Sciences*, *10*(17). doi: 10.3390/app10175975

Leisch, J., & Cochran, J. (2016). *Forecasting wind and solar generation: improving system operations.* USAID Office of Global Climate Change. National Renewable Energy Laboratory. Retrieved from https://www.nrel.gov/docs/fy16osti/66376.pdf

Lütkepohl, H. (2005). *New introduction to multiple time series analysis* (First ed.). Heidelberg. doi: 10.1007/978-3-540-27752-1

Messner, J. W., & Pinson, P. (2019, oct). Online adaptive lasso estimation in vector autoregressive models for high dimensional wind power forecasting. *International Journal of Forecasting*, *35*(4), 1485–1498. doi: 10.1016/j.ijforecast.2018.02.001

Mockus, J., Tiesis, V., & Zilinskas, A. (1978). The application of Bayesian methods for seeking the extremum. *Towards Global Optimisation*.

Monteiro, C., Bessa, R., Miranda, V., Botterud, A., Wang, J., & Conzelmann, G. (2009). *Wind power forecasting : state-of-the-art 2009*. (Tech. Rep.). Argonne National Laboratory. doi: 10.2172/968212

Mujtaba, H. (2020). *What is Gradient Boosting and how is it different from AdaBoost?* https://www.mygreatlearning.com/blog/gradient-boosting/ (visited on 03/07/2021 at 23:38).

Nemenyi, P. (1963). *Distribution-free Multiple Comparisons* (Unpublished doctoral dissertation). Princeton University.

Sims, C. A. (1980). Macroeconomics and Reality. *Econometrica*, *48*(1), 1 – 48. doi: 10.2307/1912017

Snoek, J., Larochelle, H., & Adams, R. P. (2012). Practical Bayesian optimization of machine learning algorithms. In *Advances in neural information processing systems*.

Sweeney, C., Bessa, R. J., Browell, J., & Pinson, P. (2019). The future of forecasting for renewable energy. *Wiley Interdisciplinary Reviews: Energy and Environment*, *9*(2), 1–18. doi: 10.1002/wene.365

Tastu, J., Pinson, P., Trombe, P. J., & Madsen, H. (2014). Probabilistic forecasts of wind power generation accounting for geographically dispersed information. *IEEE Transactions on Smart Grid*, *5*(1), 480–489. doi: 10.1109/TSG.2013.2277585

Tibshirani, R. (1996). Regression Shrinkage and Selection Via the Lasso. *Journal of the Royal Statistical Society: Series B (Methodological)*, *58*(1), 267–288. doi: 10.1111/j.2517-6161.1996.tb02080.x

Wand, M. P. (2000). A comparison of regression spline smoothing procedures. *Computational Statistics*, *15*, 443–462. doi: 10.1007/s001800000047

Wang, X., Guo, P., & Huang, X. (2011). A review of wind power forecasting models. *Energy Procedia*, *12*, 770–778. doi: 10.1016/j.egypro.2011.10.103

Appendix

A Exploratory Data Analysis

A.1 Autocorrelation

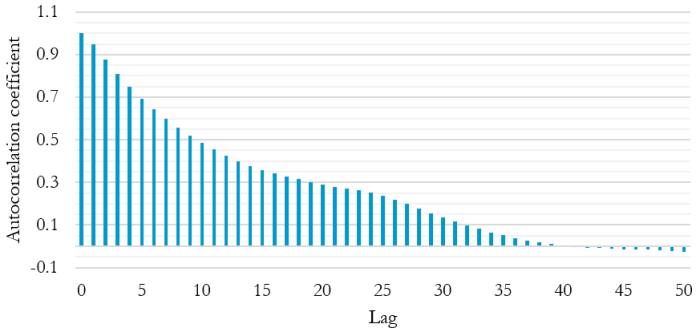

Figure 5.1: Lag autocorrelation for WPP_2.

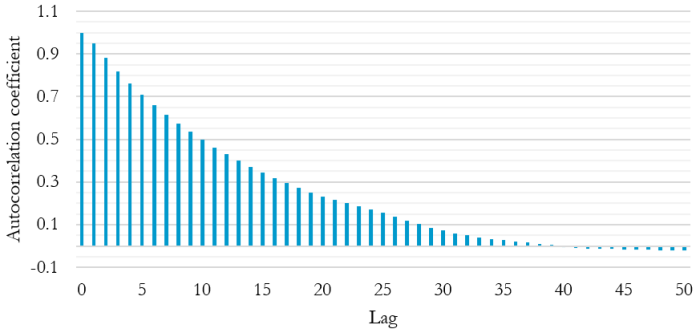

Figure 5.2: Lag autocorrelation for WPP_3.

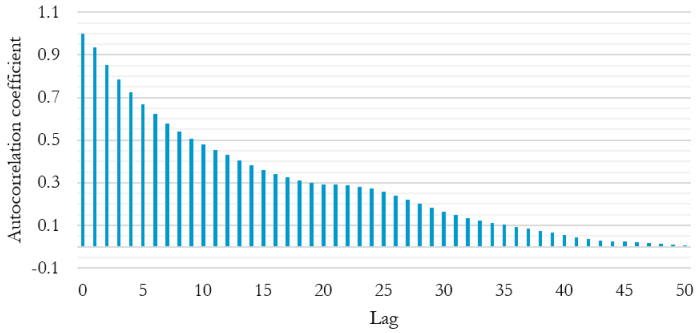

Figure 5.3: Lag autocorrelation for WPP_4.

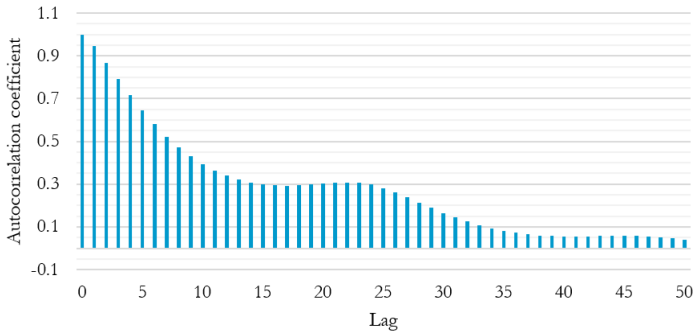

Figure 5.4: Lag autocorrelation for WPP_5.

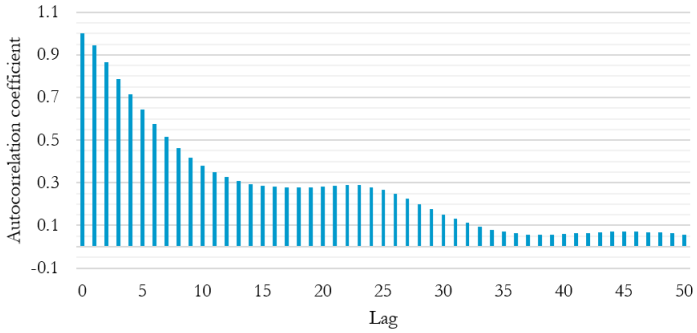

Figure 5.5: Lag autocorrelation for WPP_6.

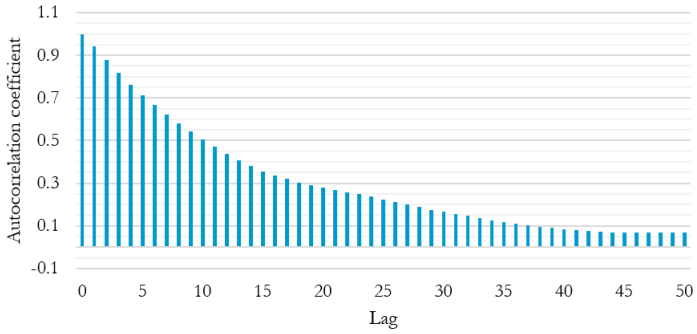

Figure 5.6: Lag autocorrelation for WPP_7.

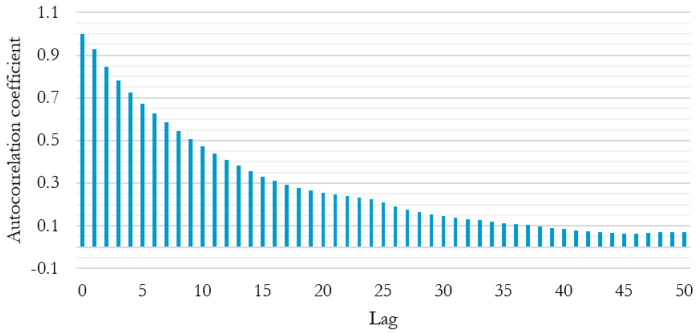

Figure 5.7: Lag autocorrelation for WPP_8.

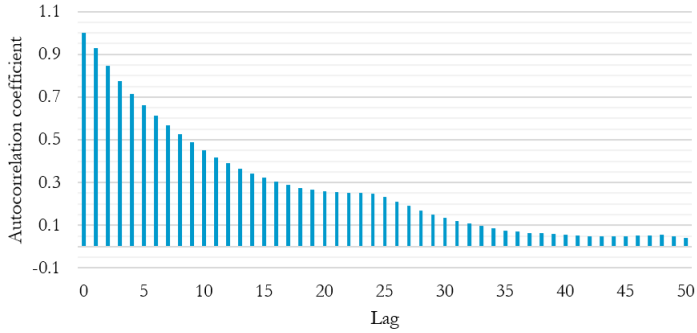

Figure 5.8: Lag autocorrelation for WPP_9.

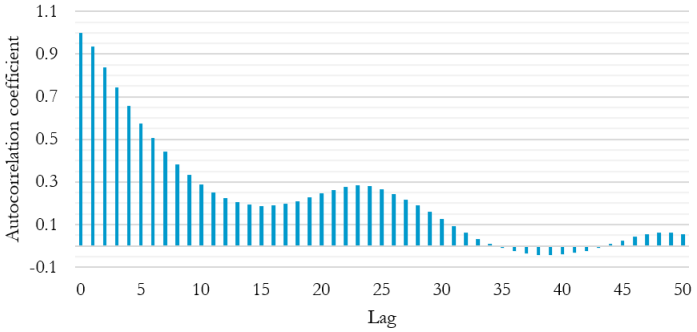

Figure 5.9: Lag autocorrelation for WPP_10.

A.2 Crosscorrelation

Table 5.1: Crosscorrelation Coefficients for ZONE2

Lag	ZONE1	ZONE3	ZONE4	ZONE5	ZONE6	ZONE7	ZONE8	ZONE9	ZONE10
0	0.4097	0.3441	0.5637	0.5256	0.5273	0.3601	0.3208	0.3811	0.6322
1	0.3932	0.3155	0.5419	0.5018	0.5033	0.3444	0.3072	0.3635	0.6031
2	0.3705	0.2844	0.5160	0.4737	0.4732	0.3244	0.2907	0.3420	0.5658
3	0.3454	0.2533	0.4866	0.4423	0.4396	0.3021	0.2714	0.3193	0.5227
4	0.3194	0.2241	0.4556	0.4072	0.4029	0.2797	0.2510	0.2940	0.4793
5	0.2958	0.1954	0.4241	0.3710	0.3659	0.2588	0.2320	0.2676	0.4372
6	0.2703	0.1677	0.3941	0.3356	0.3291	0.2356	0.2119	0.2402	0.3983
7	0.2441	0.1427	0.3644	0.3022	0.2946	0.2111	0.1891	0.2108	0.3587
8	0.2183	0.1180	0.3353	0.2709	0.2626	0.1863	0.1661	0.1835	0.3208
9	0.1938	0.0946	0.3069	0.2415	0.2342	0.1624	0.1441	0.1579	0.2867
10	0.1693	0.0725	0.2802	0.2149	0.2092	0.1397	0.1236	0.1340	0.2544

Table 5.2: Crosscorrelation Coefficients for ZONE3

Lag	ZONE1	ZONE2	ZONE4	ZONE5	ZONE6	ZONE7	ZONE8	ZONE9	ZONE10
0	0.4909	0.3441	0.4142	0.4033	0.4169	0.4805	0.4456	0.6421	0.3950
1	0.5144	0.3690	0.4292	0.4139	0.4266	0.4991	0.4629	0.6626	0.4025
2	0.5325	0.3901	0.4390	0.4205	0.4328	0.5133	0.4759	0.6670	0.4049
3	0.5460	0.4093	0.4462	0.4240	0.4346	0.5233	0.4852	0.6570	0.4012
4	0.5558	0.4263	0.4497	0.4241	0.4338	0.5297	0.4913	0.6413	0.3932
5	0.5608	0.4398	0.4493	0.4216	0.4302	0.5318	0.4916	0.6199	0.3852
6	0.5597	0.4484	0.4489	0.4165	0.4234	0.5288	0.4879	0.5968	0.3751
7	0.5556	0.4528	0.4462	0.4108	0.4163	0.5235	0.4819	0.5719	0.3623
8	0.5483	0.4562	0.4413	0.4031	0.4076	0.5143	0.4731	0.5459	0.3491
9	0.5370	0.4587	0.4335	0.3944	0.3974	0.5022	0.4609	0.5186	0.3354
10	0.5258	0.4589	0.4241	0.3846	0.3860	0.4898	0.4492	0.4931	0.3258

Table 5.3: Crosscorrelation Coefficients for ZONE4

Lag	ZONE1	ZONE2	ZONE3	ZONE5	ZONE6	ZONE7	ZONE8	ZONE9	ZONE10
0	0.5010	0.5637	0.4142	0.8780	0.8626	0.4534	0.4253	0.4941	0.6110
1	0.4929	0.5787	0.3950	0.8394	0.8254	0.4419	0.4139	0.4873	0.6075
2	0.4792	0.5849	0.3721	0.7802	0.7685	0.4266	0.3988	0.4732	0.5859
3	0.4625	0.5817	0.3472	0.7227	0.7091	0.4095	0.3821	0.4547	0.5519
4	0.4433	0.5732	0.3210	0.6648	0.6505	0.3903	0.3637	0.4292	0.5126
5	0.4197	0.5595	0.2938	0.6071	0.5945	0.3678	0.3424	0.4001	0.4696
6	0.3925	0.5424	0.2660	0.5553	0.5444	0.3435	0.3204	0.3706	0.4291
7	0.3659	0.5264	0.2396	0.5081	0.5002	0.3174	0.2966	0.3426	0.3930
8	0.3388	0.5090	0.2147	0.4669	0.4612	0.2908	0.2721	0.3148	0.3638
9	0.3134	0.4920	0.1913	0.4322	0.4266	0.2668	0.2484	0.2893	0.3413
10	0.2879	0.4765	0.1697	0.4037	0.3976	0.2437	0.2259	0.2668	0.3215

Table 5.4: Crosscorrelation Coefficients for ZONE5

Lag	ZONE1	ZONE2	ZONE3	ZONE4	ZONE6	ZONE7	ZONE8	ZONE9	ZONE10
0	0.4632	0.5256	0.4033	0.8780	0.9243	0.4394	0.4178	0.4501	0.6497
1	0.4573	0.5409	0.3885	0.8477	0.8912	0.4303	0.4104	0.4449	0.6543
2	0.4460	0.5448	0.3694	0.7977	0.8320	0.4164	0.3978	0.4345	0.6353
3	0.4313	0.5405	0.3472	0.7454	0.7643	0.4007	0.3835	0.4213	0.5995
4	0.4139	0.5330	0.3239	0.6925	0.6943	0.3833	0.3672	0.4045	0.5547
5	0.3936	0.5200	0.3001	0.6392	0.6249	0.3628	0.3469	0.3860	0.5060
6	0.3731	0.5031	0.2764	0.5914	0.5627	0.3417	0.3267	0.3641	0.4576
7	0.3519	0.4859	0.2526	0.5505	0.5078	0.3193	0.3067	0.3402	0.4133
8	0.3301	0.4678	0.2289	0.5146	0.4591	0.2966	0.2842	0.3161	0.3754
9	0.3093	0.4506	0.2067	0.4827	0.4166	0.2749	0.2606	0.2944	0.3422
10	0.2885	0.4340	0.1865	0.4552	0.3811	0.2537	0.2383	0.2757	0.3129

Table 5.5: Crosscorrelation Coefficients for ZONE6

Lag	ZONE1	ZONE2	ZONE3	ZONE4	ZONE5	ZONE7	ZONE8	ZONE9	ZONE10
0	0.4682	0.5273	0.4169	0.8626	0.9243	0.4453	0.4252	0.4523	0.6601
1	0.4632	0.5446	0.4029	0.8400	0.8928	0.4373	0.4180	0.4515	0.6697
2	0.4524	0.5520	0.3845	0.7921	0.8309	0.4230	0.4042	0.4456	0.6550
3	0.4378	0.5509	0.3619	0.7424	0.7640	0.4058	0.3882	0.4367	0.6222
4	0.4218	0.5469	0.3390	0.6905	0.6947	0.3891	0.3728	0.4209	0.5785
5	0.4024	0.5369	0.3163	0.6387	0.6250	0.3687	0.3533	0.4014	0.5296
6	0.3809	0.5198	0.2921	0.5917	0.5603	0.3474	0.3346	0.3801	0.4804
7	0.3589	0.5022	0.2683	0.5513	0.5041	0.3254	0.3142	0.3577	0.4338
8	0.3364	0.4844	0.2451	0.5162	0.4562	0.3025	0.2915	0.3352	0.3910
9	0.3159	0.4680	0.2222	0.4844	0.4140	0.2818	0.2686	0.3133	0.3546
10	0.2969	0.4530	0.1998	0.4551	0.3787	0.2625	0.2467	0.2928	0.3241

Table 5.6: Crosscorrelation Coefficients for ZONE7

Lag	ZONE1	ZONE2	ZONE3	ZONE4	ZONE5	ZONE6	ZONE8	ZONE9	ZONE10
0	0.9298	0.3601	0.4805	0.4534	0.4394	0.4453	0.9145	0.6563	0.3100
1	0.8927	0.3732	0.4567	0.4568	0.4399	0.4463	0.8688	0.6360	0.3093
2	0.8424	0.3829	0.4307	0.4555	0.4363	0.4425	0.8101	0.6108	0.3021
3	0.7933	0.3894	0.4040	0.4500	0.4290	0.4342	0.7557	0.5851	0.2935
4	0.7469	0.3937	0.3752	0.4443	0.4201	0.4244	0.7053	0.5583	0.2837
5	0.7007	0.3939	0.3481	0.4369	0.4113	0.4149	0.6595	0.5306	0.2745
6	0.6544	0.3925	0.3227	0.4284	0.4031	0.4048	0.6161	0.5009	0.2656
7	0.6121	0.3901	0.2988	0.4160	0.3924	0.3937	0.5769	0.4704	0.2582
8	0.5719	0.3875	0.2764	0.4035	0.3816	0.3824	0.5397	0.4398	0.2521
9	0.5356	0.3826	0.2557	0.3913	0.3696	0.3714	0.5040	0.4097	0.2470
10	0.4992	0.3761	0.2372	0.3800	0.3567	0.3585	0.4701	0.3835	0.2426

Table 5.7: Crosscorrelation Coefficients for ZONE8

Lag	ZONE1	ZONE2	ZONE3	ZONE4	ZONE5	ZONE6	ZONE7	ZONE9	ZONE10
0	0.8394	0.3208	0.4456	0.4253	0.4178	0.4252	0.9145	0.6103	0.2818
1	0.8130	0.3326	0.4241	0.4287	0.4176	0.4256	0.8714	0.5930	0.2789
2	0.7726	0.3425	0.4026	0.4267	0.4137	0.4205	0.8160	0.5709	0.2702
3	0.7326	0.3495	0.3795	0.4219	0.4062	0.4121	0.7629	0.5503	0.2609
4	0.6921	0.3551	0.3549	0.4174	0.3982	0.4022	0.7143	0.5296	0.2505
5	0.6516	0.3565	0.3319	0.4104	0.3902	0.3936	0.6701	0.5063	0.2427
6	0.6104	0.3568	0.3113	0.4038	0.3821	0.3849	0.6266	0.4798	0.2350
7	0.5712	0.3558	0.2905	0.3930	0.3712	0.3764	0.5851	0.4516	0.2291
8	0.5353	0.3534	0.2708	0.3835	0.3615	0.3671	0.5481	0.4246	0.2259
9	0.5026	0.3489	0.2530	0.3735	0.3514	0.3574	0.5135	0.3982	0.2227
10	0.4697	0.3453	0.2374	0.3623	0.3401	0.3462	0.4803	0.3753	0.2203

Table 5.8: Crosscorrelation Coefficients for ZONE9

Lag	ZONE1	ZONE2	ZONE3	ZONE4	ZONE5	ZONE6	ZONE7	ZONE8	ZONE10
0	0.6639	0.3811	0.6421	0.4941	0.4501	0.4523	0.6563	0.6103	0.3384
1	0.6814	0.3945	0.6096	0.4938	0.4499	0.4496	0.6690	0.6211	0.3296
2	0.6877	0.4051	0.5711	0.4932	0.4483	0.4455	0.6684	0.6194	0.3208
3	0.6856	0.4142	0.5301	0.4917	0.4454	0.4412	0.6602	0.6117	0.3140
4	0.6751	0.4216	0.4894	0.4860	0.4401	0.4360	0.6454	0.5989	0.3055
5	0.6563	0.4264	0.4504	0.4777	0.4331	0.4297	0.6250	0.5807	0.2951
6	0.6338	0.4288	0.4132	0.4667	0.4228	0.4214	0.6017	0.5608	0.2879
7	0.6056	0.4279	0.3783	0.4539	0.4126	0.4115	0.5737	0.5362	0.2821
8	0.5740	0.4274	0.3474	0.4388	0.4026	0.3997	0.5430	0.5074	0.2758
9	0.5429	0.4259	0.3197	0.4203	0.3897	0.3862	0.5125	0.4779	0.2716
10	0.5133	0.4208	0.2950	0.4012	0.3761	0.3724	0.4824	0.4485	0.2705

Table 5.9: Crosscorrelation Coefficients for ZONE10

Lag	ZONE1	ZONE2	ZONE3	ZONE4	ZONE5	ZONE6	ZONE7	ZONE8	ZONE9
0	0.3343	0.6322	0.3950	0.6110	0.6497	0.6601	0.3100	0.2818	0.3384
1	0.3270	0.6490	0.3807	0.5963	0.6222	0.6268	0.3021	0.2734	0.3440
2	0.3171	0.6503	0.3597	0.5666	0.5771	0.5782	0.2897	0.2603	0.3433
3	0.3044	0.6386	0.3336	0.5297	0.5213	0.5230	0.2751	0.2454	0.3346
4	0.2907	0.6179	0.3057	0.4911	0.4639	0.4660	0.2603	0.2309	0.3220
5	0.2738	0.5926	0.2778	0.4530	0.4070	0.4115	0.2439	0.2163	0.3060
6	0.2559	0.5625	0.2490	0.4159	0.3554	0.3599	0.2280	0.2009	0.2860
7	0.2351	0.5300	0.2226	0.3785	0.3078	0.3104	0.2094	0.1833	0.2626
8	0.2136	0.4975	0.1974	0.3431	0.2647	0.2664	0.1878	0.1635	0.2369
9	0.1927	0.4639	0.1731	0.3096	0.2281	0.2287	0.1657	0.1436	0.2121
10	0.1727	0.4325	0.1503	0.2781	0.1975	0.1965	0.1449	0.1245	0.1891

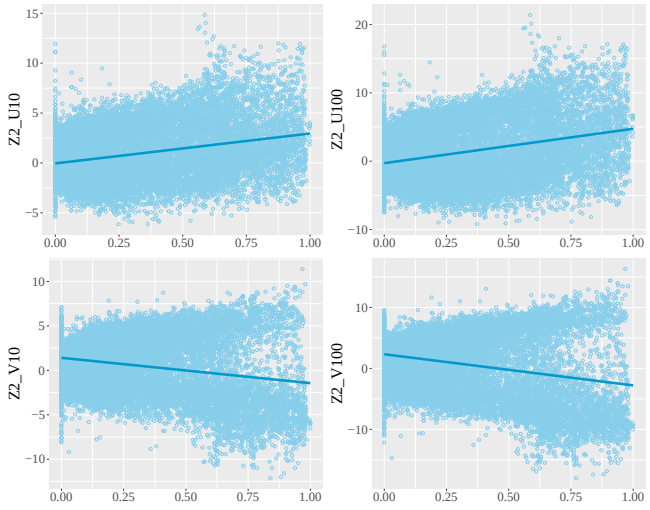

Figure 5.10: Correlation between power production and the weather forecasts, z and u, for ZONE2.

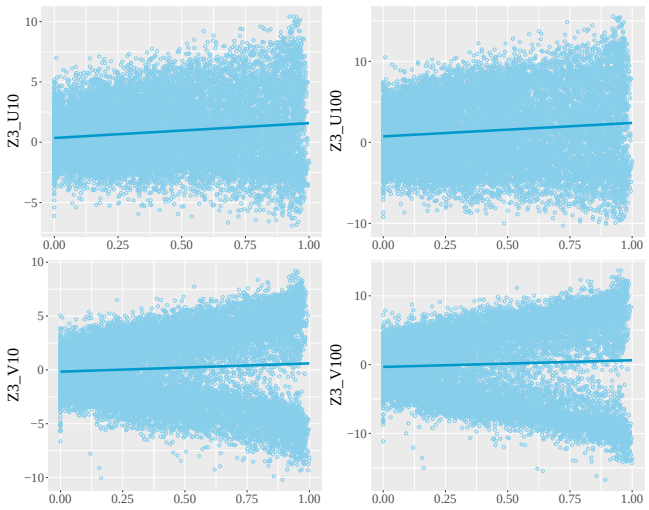

Figure 5.11: Correlation between power production and the weather forecasts, z and u, for ZONE3.

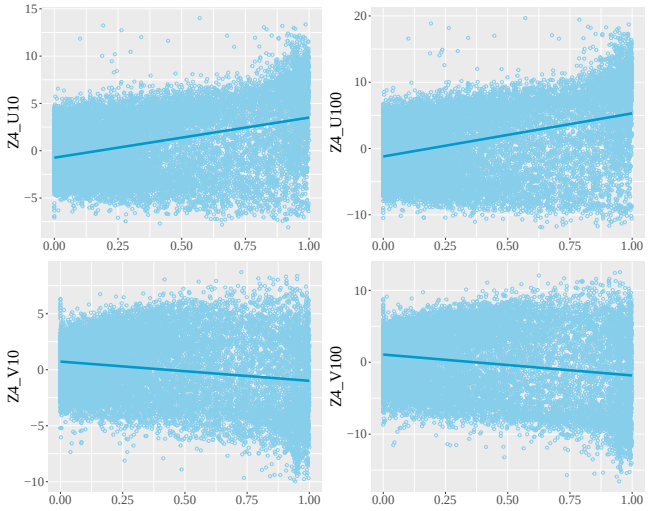

Figure 5.12: Correlation between power production and the weather forecasts, z and u, for ZONE4.

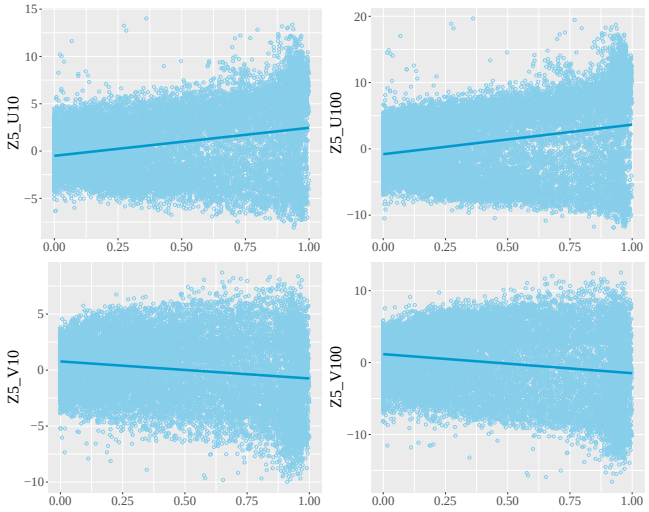

Figure 5.13: Correlation between power production and the weather forecasts, z and u, for ZONE5.

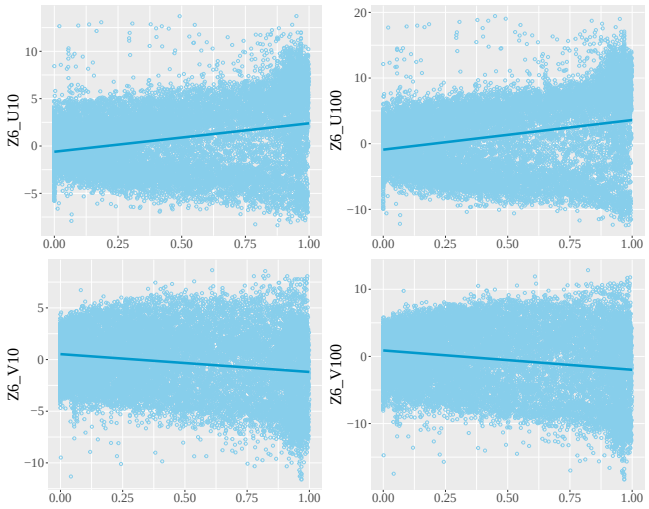

Figure 5.14: Correlation between power production and the weather forecasts, z and u, for ZONE6.

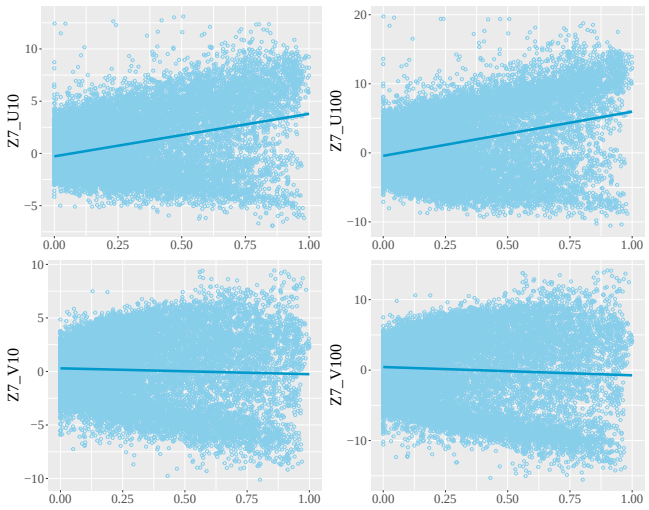

Figure 5.15: Correlation between power production and the weather forecasts, z and u, for ZONE7.

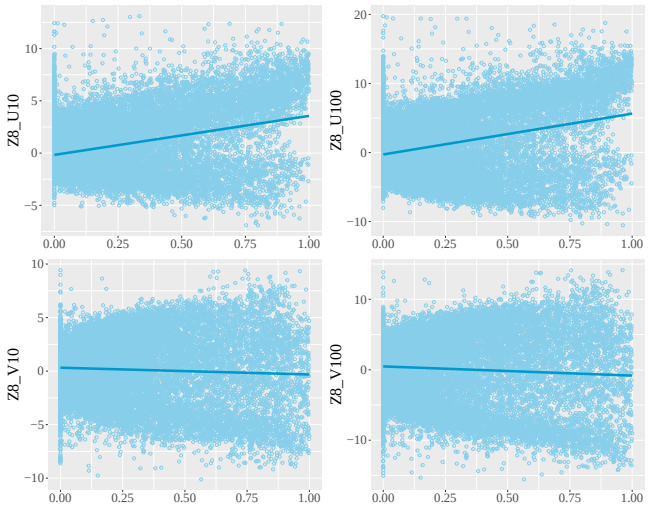

Figure 5.16: Correlation between power production and the weather forecasts, z and u, for ZONE8.

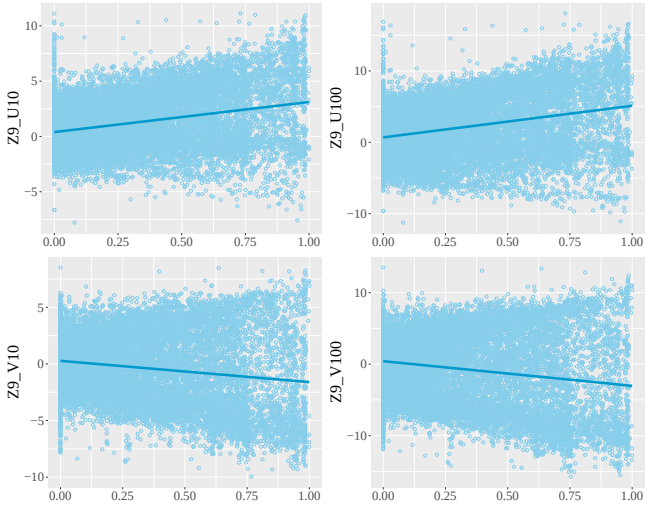

Figure 5.17: Correlation between power production and the weather forecasts, z and u, for ZONE9.

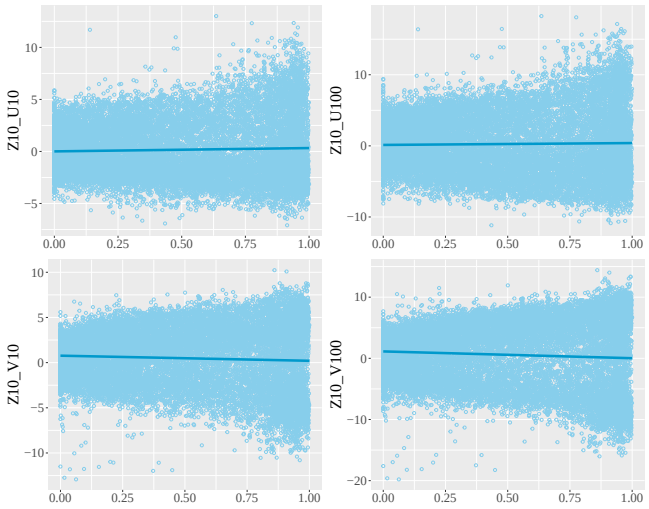

Figure 5.18: Correlation between power production and the weather forecasts, z and u, for ZONE10.

A.3 Model Optimization

Table 5.10: Bayesian Optimization Parameters (AR models).

Model	Optimization Parameters				
	Iterations	No. Lags	Lambda	Rho	Degrees of Freedom (Splines)
AR	150	1 - 24	0 - 1	0 - 1	-
AR-X	150	1 - 24	0 - 1	0 - 1	-
AAR-X	150	1 - 24	0 - 1	0 - 1	1 - 10
VAR	150	1 - 24	0 - 1	0 - 1	-
VAR-X	150	1 - 24	0 - 1	0 - 1	-
AVAR-X (natural cubic splines)	50	1 - 24	0 - 1	0 - 1	1 - 10
AVAR-X (B splines)	50	1 - 24	0 - 1	0 - 1	1 - 10
VAR with Lag Group LASSO	150	1 - 24	0 - 1	0 - 1	-
VAR-X with Lag Group LASSO	50	1 - 24	0 - 1	0 - 1	-
AVAR-X (natural cubic splines) with Lag Group LASSO	50	1 - 7	0 - 1	0 - 1	2 - 6
AVAR-X (B splines) with Lag Group LASSO	50	1 - 7	0 - 1	0 - 1	2 - 6

Table 5.11: Bayesian Optimization Results (AR models).

Model	Optimization Results			
	No. Lags	Lambda	Rho	Degrees of Freedom (Splines)
AR	21	0.69714	0.85129	-
AR-X	15	0.74901	0.65448	-
AAR-X	7	0.51266	0.00497	5
VAR	14	0.60890	0.03652	-
VAR-X	1	0.44674	0.67143	-
AVAR-X (natural cubic splines)	3	0.32470	0.38730	3
AVAR-X (B splines)	2	0.32750	0.03650	4
VAR with Lag Group LASSO	1	1.00000	0.04674	-
VAR-X with Lag Group LASSO	1	0.38680	0.05400	-
AVAR-X (natural cubic splines) with Lag Group LASSO	2	0.56150	0.09890	4
AVAR-X (B splines) with Lag Group LASSO	1	0.70140	0.18030	4

Table 5.12: Bayesian Optimization Parameters (XGB model).

Model	Optimization Parameters				
	Iterations	No. Lags	Maximum Depth	Minimum Child Weight	Subsample
XGB	100	3 - 24	1 - 20	1 - 20	0 - 1

Table 5.13: Bayesian Optimization Results (XGB model).

Model	Optimization Results			
	No. Lags	Maximum Depth	Minimum Child Weight	Subsample
XGB	3	2	18	0.06524

B Discussion

B.1 Complete Results

Table 5.14: Mean RMSE Results

hours-ahead	Persistence	AR	AR-X	AAR-X	VAR	VAR-X	AVAR-X (natural cubic splines)	AVAR-X (B splines)	XGB
h=1	0.1041	0.1015	0.1003	0.0953	0.0981	0.1012	0.0954	0.0945	0.1013
h=2	0.1576	0.1512	0.1467	0.1335	0.1428	0.143	0.1306	0.1293	0.1374
h=3	0.1937	0.1811	0.1736	0.1499	0.1712	0.1705	0.1494	0.1444	0.1552
h=4	0.2219	0.1996	0.1873	0.1541	0.1918	0.1829	0.151	0.146	0.1594
h=5	0.2452	0.2134	0.2006	0.1618	0.206	0.1983	0.159	0.1526	0.1647
h=6	0.2648	0.2266	0.212	0.17	0.2224	0.2096	0.1693	0.1596	0.1718
h=7	0.2814	0.235	0.2243	0.1754	0.2317	0.2217	0.176	0.1655	0.1748
h=8	0.2957	0.241	0.2299	0.177	0.238	0.2246	0.1748	0.1655	0.1703
h=9	0.3081	0.2492	0.2377	0.1827	0.2459	0.2303	0.1823	0.1675	0.1734
h=10	0.3189	0.2562	0.2433	0.1916	0.2516	0.2364	0.1884	0.1782	0.1825
h=11	0.3281	0.2558	0.2403	0.1877	0.2493	0.2323	0.1855	0.1761	0.1819
h=12	0.336	0.2668	0.2481	0.192	0.2585	0.2405	0.1866	0.1771	0.1816
h=13	0.3426	0.2758	0.2536	0.1948	0.2657	0.2396	0.188	0.1781	0.1803
h=14	0.3481	0.2824	0.2588	0.1952	0.2722	0.248	0.1884	0.182	0.1817
h=15	0.3526	0.2853	0.2588	0.1913	0.2749	0.247	0.1841	0.176	0.1799
h=16	0.3564	0.286	0.2562	0.1893	0.272	0.2424	0.1793	0.1704	0.1728
h=17	0.3592	0.29	0.2597	0.1926	0.2794	0.2445	0.1804	0.1749	0.1746
h=18	0.3614	0.2935	0.2634	0.1976	0.2841	0.2463	0.1891	0.18	0.1766
h=19	0.3629	0.2936	0.2614	0.1954	0.2849	0.244	0.1848	0.1887	0.1735
h=20	0.3638	0.2927	0.2604	0.1919	0.2855	0.243	0.182	0.1861	0.1725
h=21	0.3645	0.2965	0.2653	0.1911	0.2897	0.2532	0.1814	0.1788	0.1734
h=22	0.3652	0.303	0.273	0.1948	0.2967	0.2645	0.1872	0.1849	0.1801
h=23	0.3662	0.3033	0.273	0.1953	0.2996	0.2631	0.1888	0.1827	0.1843
h=24	0.3682	0.3041	0.2727	0.1922	0.3004	0.2669	0.1854	0.1793	0.18

Table 5.15: Mean RMSE Improvement from Persistence Results (%)

hours-ahead	AR	AR-X	AAR-X	VAR	VAR-X	AVAR-X (natural cubic splines)	AVAR-X (B splines)	XGB
h=1	2.5	3.7	8.5	5.8	2.8	8.4	9.2	2.7
h=2	4.1	6.9	15.3	9.4	9.3	17.1	18.0	12.8
h=3	6.5	10.4	22.6	11.6	12.0	22.9	25.5	19.9
h=4	10.0	15.6	30.6	13.6	17.6	32.0	34.2	28.2
h=5	13.0	18.2	34.0	16.0	19.1	35.2	37.8	32.8
h=6	14.4	19.9	35.8	16.0	20.8	36.1	39.7	35.1
h=7	16.5	20.3	37.7	17.7	21.2	37.5	41.2	37.9
h=8	18.5	22.3	40.1	19.5	24.0	40.9	44.0	42.4
h=9	19.1	22.8	40.7	20.2	25.3	40.8	45.6	43.7
h=10	19.7	23.7	39.9	21.1	25.9	40.9	44.1	42.8
h=11	22.0	26.8	42.8	24.0	29.2	43.5	46.3	44.6
h=12	20.6	26.2	42.9	23.1	28.4	44.5	47.3	46.0
h=13	19.5	26.0	43.1	22.4	30.1	45.1	48.0	47.4
h=14	18.9	25.7	43.9	21.8	28.8	45.9	47.7	47.8
h=15	19.1	26.6	45.7	22.0	29.9	47.8	50.1	49.0
h=16	19.8	28.1	46.9	23.7	32.0	49.7	52.2	51.5
h=17	19.3	27.7	46.4	22.2	31.9	49.8	51.3	51.4
h=18	18.8	27.1	45.3	21.4	31.8	47.7	50.2	51.1
h=19	19.1	28.0	46.2	21.5	32.8	49.1	48.0	52.2
h=20	19.5	28.4	47.3	21.5	33.2	50.0	48.8	52.6
h=21	18.7	27.2	47.6	20.5	30.5	50.2	50.9	52.4
h=22	17.0	25.2	46.7	18.8	27.6	48.7	49.4	50.7
h=23	17.2	25.5	46.7	18.2	28.2	48.4	50.1	49.7
h=24	17.4	25.9	47.8	18.4	27.5	49.6	51.3	51.1

Table 5.16: Mean MAE Results

hours-ahead	Persistence	AR	AR-X	AAR-X	VAR	VAR-X	AVAR-X (natural cubic splines)	AVAR-X (B splines)	XGB
h=1	0.0672	0.071	0.07	0.0673	0.0691	0.0713	0.0668	0.0663	0.0701
h=2	0.1052	0.111	0.1068	0.0959	0.1057	0.1052	0.0951	0.0933	0.0991
h=3	0.1328	0.1364	0.1289	0.1092	0.1294	0.1266	0.108	0.1044	0.1135
h=4	0.1553	0.1547	0.1418	0.1151	0.1475	0.1377	0.1121	0.1085	0.1184
h=5	0.1746	0.1676	0.1543	0.1215	0.1597	0.151	0.1183	0.1138	0.1224
h=6	0.1912	0.1796	0.1645	0.1281	0.1732	0.1608	0.1268	0.1196	0.1288
h=7	0.2056	0.1866	0.1755	0.1309	0.181	0.1737	0.1317	0.1234	0.1323
h=8	0.2181	0.1932	0.1812	0.1325	0.187	0.1751	0.1303	0.1225	0.1282
h=9	0.2292	0.2013	0.1895	0.1378	0.1948	0.1807	0.1355	0.1251	0.1316
h=10	0.2389	0.2086	0.1959	0.1484	0.2	0.1882	0.1453	0.1352	0.1415
h=11	0.247	0.2087	0.1957	0.1474	0.2	0.1871	0.1449	0.1351	0.1414
h=12	0.254	0.2187	0.2029	0.1511	0.2079	0.1932	0.1463	0.1369	0.1422
h=13	0.26	0.2268	0.2075	0.1532	0.2153	0.194	0.1483	0.1388	0.1412
h=14	0.2649	0.2332	0.2126	0.1526	0.2218	0.1995	0.1468	0.1403	0.141
h=15	0.2687	0.2354	0.2112	0.1497	0.2224	0.1989	0.1431	0.136	0.1386
h=16	0.2718	0.2353	0.2084	0.1477	0.2195	0.1929	0.139	0.1312	0.1337
h=17	0.274	0.2409	0.2106	0.1484	0.2279	0.1934	0.1387	0.1331	0.1344
h=18	0.2758	0.2455	0.2154	0.152	0.2345	0.1956	0.1428	0.1368	0.1353
h=19	0.2769	0.2463	0.2161	0.1517	0.2354	0.1964	0.1432	0.139	0.133
h=20	0.2772	0.2464	0.2153	0.1504	0.236	0.1957	0.1416	0.1381	0.1331
h=21	0.2773	0.2521	0.2197	0.149	0.2411	0.2057	0.1416	0.1369	0.1351
h=22	0.2774	0.2574	0.2276	0.1521	0.2473	0.217	0.1464	0.1416	0.1407
h=23	0.2779	0.2562	0.2267	0.1504	0.2482	0.2145	0.1463	0.1402	0.1416
h=24	0.2794	0.2565	0.2261	0.1476	0.249	0.2164	0.1427	0.1363	0.1366

Table 5.17: Mean MAE Improvement from Persistence Results (%)

hours-ahead	AR	AR-X	AAR-X	VAR	VAR-X	AVAR-X (natural cubic splines)	AVAR-X (B splines)	XGB
h=1	0.0	0.0	0.0	0.0	0.0	0.6	1.3	0.0
h=2	0.0	0.0	8.8	0.0	0.0	9.6	11.3	5.8
h=3	0.0	2.9	17.8	2.6	4.7	18.7	21.4	14.5
h=4	0.4	8.7	25.9	5.0	11.3	27.8	30.1	23.8
h=5	4.0	11.6	30.4	8.5	13.5	32.2	34.8	29.9
h=6	6.1	14.0	33.0	9.4	15.9	33.7	37.4	32.6
h=7	9.2	14.6	36.3	12.0	15.5	35.9	40.0	35.7
h=8	11.4	16.9	39.2	14.3	19.7	40.3	43.8	41.2
h=9	12.2	17.3	39.9	15.0	21.2	40.9	45.4	42.6
h=10	12.7	18.0	37.9	16.3	21.2	39.2	43.4	40.8
h=11	15.5	20.8	40.3	19.0	24.3	41.3	45.3	42.8
h=12	13.9	20.1	40.5	18.1	23.9	42.4	46.1	44.0
h=13	12.8	20.2	41.1	17.2	25.4	43.0	46.6	45.7
h=14	12.0	19.7	42.4	16.3	24.7	44.6	47.0	46.8
h=15	12.4	21.4	44.3	17.2	26.0	46.7	49.4	48.4
h=16	13.4	23.3	45.7	19.2	29.0	48.9	51.7	50.8
h=17	12.1	23.1	45.8	16.8	29.4	49.4	51.4	50.9
h=18	11.0	21.9	44.9	15.0	29.1	48.2	50.4	50.9
h=19	11.1	22.0	45.2	15.0	29.1	48.3	49.8	52.0
h=20	11.1	22.3	45.7	14.9	29.4	48.9	50.2	52.0
h=21	9.1	20.8	46.3	13.1	25.8	48.9	50.6	51.3
h=22	7.2	18.0	45.2	10.9	21.8	47.2	49.0	49.3
h=23	7.8	18.4	45.9	10.7	22.8	47.4	49.6	49.0
h=24	8.2	19.1	47.2	10.9	22.5	48.9	51.2	51.1

B.2 Results for each WPP

Table 5.18: ZONE2 Mean RMSE Results per Timescale

hours-ahead	AR	AR-X	AAR-X	VAR	VAR-X	AVAR-X (natural cubic splines)	AVAR-X (B splines)	XGB
[1,3]	0.1263	0.1196	0.1115	0.125	0.1193	0.1111	0.1093	0.1164
]3, 12]	0.2167	0.2023	0.1603	0.2137	0.2003	0.1564	0.1486	0.1568
]12, 24]	0.2722	0.2372	0.1823	0.2749	0.2358	0.1814	0.1742	0.1794

Table 5.19: ZONE3 Mean RMSE Results per Timescale

hours-ahead	AR	AR-X	AAR-X	VAR	VAR-X	AVAR-X (natural cubic splines)	AVAR-X (B splines)	XGB
[1,3]	0.1396	0.1306	0.1086	0.1281	0.1223	0.1064	0.104	0.1177
]3, 12]	0.2443	0.234	0.1572	0.2279	0.2128	0.1554	0.1465	0.1714
]12, 24]	0.2835	0.274	0.1667	0.2778	0.2595	0.1681	0.1618	0.1771

Table 5.20: ZONE4 Mean RMSE Results per Timescale

hours-ahead	AR	AR-X	AAR-X	VAR	VAR-X	AVAR-X (natural cubic splines)	AVAR-X (B splines)	XGB
[1,3]	0.1511	0.1466	0.1285	0.1379	0.1417	0.1265	0.1217	0.1313
]3, 12]	0.2499	0.2329	0.1862	0.2504	0.2283	0.1857	0.1741	0.1815
]12, 24]	0.3372	0.2915	0.2142	0.3264	0.268	0.2044	0.201	0.1964

Table 5.21: ZONE5 Mean RMSE Results per Timescale

hours-ahead	AR	AR-X	AAR-X	VAR	VAR-X	AVAR-X (natural cubic splines)	AVAR-X (B splines)	XGB
[1,3]	0.1422	0.1343	0.1171	0.1299	0.1337	0.1155	0.1137	0.1226
]3, 12]	0.2564	0.2361	0.1824	0.2554	0.2349	0.1854	0.1718	0.1824
]12, 24]	0.326	0.2988	0.207	0.3206	0.272	0.203	0.1912	0.2038

Table 5.22: ZONE6 Mean RMSE Results per Timescale

hours-ahead	AR	AR-X	AAR-X	VAR	VAR-X	AVAR-X (natural cubic splines)	AVAR-X (B splines)	XGB
[1,3]	0.1464	0.1448	0.1314	0.1392	0.1468	0.1344	0.131	0.1339
]3, 12]	0.2511	0.2394	0.1837	0.2515	0.239	0.1909	0.1795	0.1812
]12, 24]	0.3214	0.29	0.2153	0.3158	0.2775	0.211	0.2036	0.2023

Table 5.23: ZONE7 Mean RMSE Results per Timescale

hours-ahead	AR	AR-X	AAR-X	VAR	VAR-X	AVAR-X (natural cubic splines)	AVAR-X (B splines)	XGB
[1,3]	0.1353	0.1342	0.1231	0.1335	0.1362	0.1256	0.1223	0.1288
]3, 12]	0.2093	0.1975	0.1525	0.2065	0.2002	0.153	0.1439	0.154
]12, 24]	0.2617	0.2351	0.1714	0.2523	0.2218	0.1605	0.1556	0.1433

Table 5.24: ZONE8 Mean RMSE Results per Timescale

hours-ahead	AR	AR-X	AAR-X	VAR	VAR-X	AVAR-X (natural cubic splines)	AVAR-X (B splines)	XGB
[1,3]	0.143	0.1416	0.1353	0.1436	0.1467	0.1359	0.1342	0.1404
]3, 12]	0.2247	0.2133	0.1721	0.222	0.2166	0.1752	0.1689	0.174
]12, 24]	0.2755	0.2508	0.1959	0.2631	0.2447	0.1911	0.184	0.1782

Table 5.25: ZONE9 Mean RMSE Results per Timescale

hours-ahead	AR	AR-X	AAR-X	VAR	VAR-X	AVAR-X (natural cubic splines)	AVAR-X (B splines)	XGB
[1,3]	0.1508	0.1514	0.1414	0.1441	0.1472	0.141	0.1404	0.1446
]3, 12]	0.2304	0.2213	0.1825	0.214	0.2093	0.1813	0.175	0.1773
]12, 24]	0.2409	0.2163	0.1599	0.2212	0.2015	0.1528	0.1495	0.1459

Table 5.26: ZONE10 Mean RMSE Results per Timescale

hours-ahead	AR	AR-X	AAR-X	VAR	VAR-X	AVAR-X (natural cubic splines)	AVAR-X (B splines)	XGB
[1,3]	0.1646	0.1563	0.1305	0.1531	0.1485	0.1328	0.1291	0.1448
]3, 12]	0.2728	0.2611	0.2073	0.271	0.2523	0.2126	0.1974	0.2002
]12, 24]	0.3172	0.296	0.2247	0.3175	0.2913	0.2204	0.2102	0.2077

B.3 Friedman Test Results

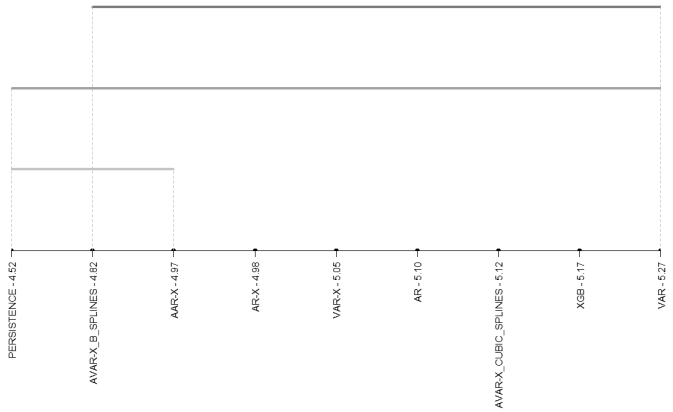

Figure 5.19: Critical Difference diagram for ZONE2 and 1 hour-ahead (Result: Different; p-value = 1.5e-05; Critical Distance = 0.457).

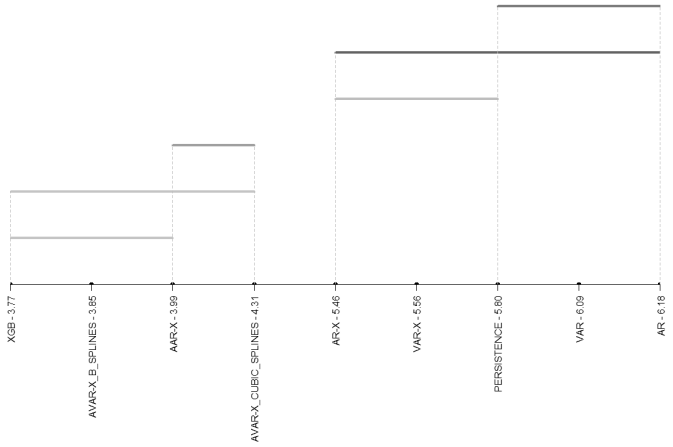

Figure 5.20: Critical Difference diagram for ZONE2 and 24 hours-ahead (Result: Different; p-value = 2.0e-155; Critical Distance = 0.458).

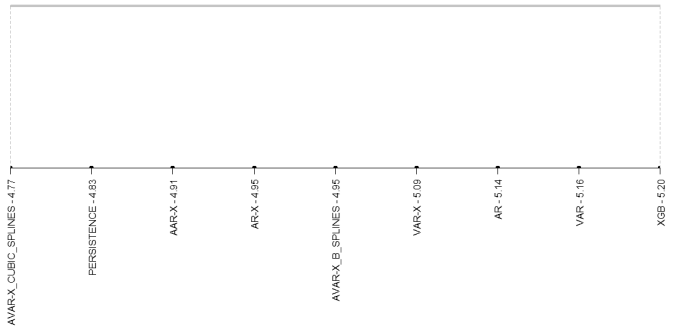

Figure 5.21: Critical Difference diagram for ZONE3 and 1 hour-ahead (Result: Different; p-value = 0.026; Critical Distance = 0.457).

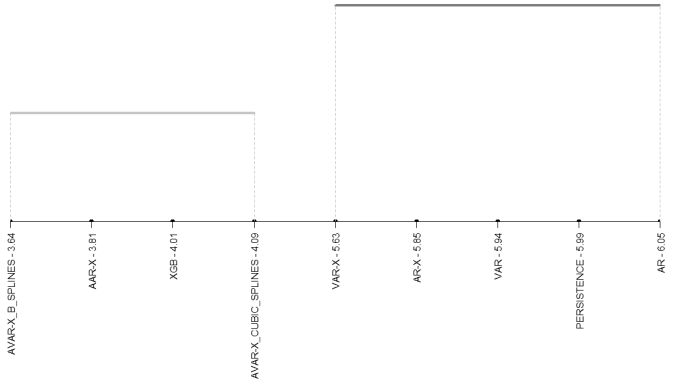

Figure 5.22: Critical Difference diagram for ZONE3 and 24 hours-ahead (Result: Different; p-value = 3.7e-176; Critical Distance = 0.458).

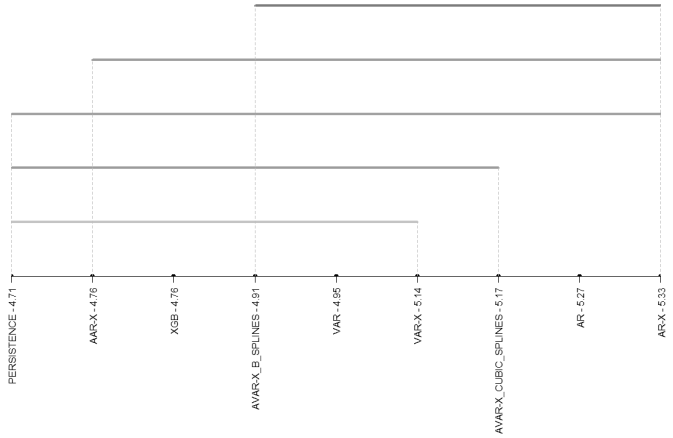

Figure 5.23: Critical Difference diagram for ZONE4 and 1 hour-ahead (Result: Different; p-value = 2.3e-06; Critical Distance = 0.457).

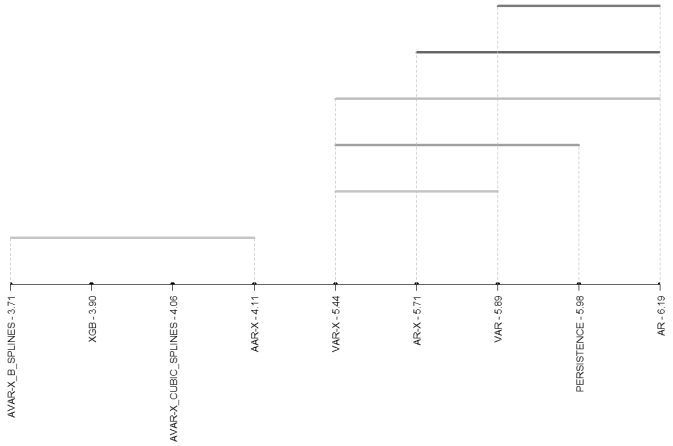

Figure 5.24: Critical Difference diagram for ZONE4 and 24 hours-ahead (Result: Different; p-value = 3.9e-161; Critical Distance = 0.458).

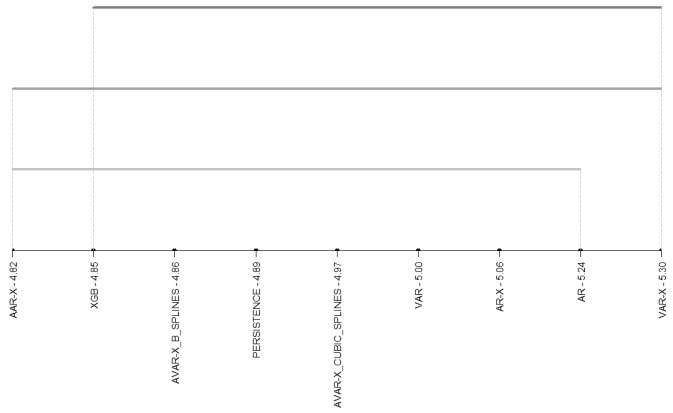

Figure 5.25: Critical Difference diagram for ZONE5 and 1 hour-ahead (Result: Different; p-value = 0.0048; Critical Distance = 0.457).

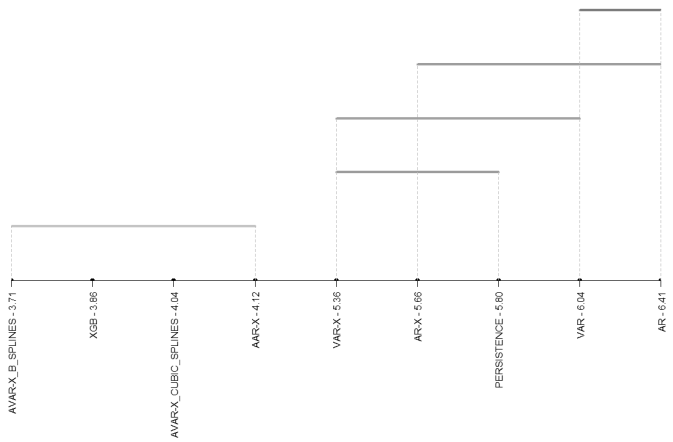

Figure 5.26: Critical Difference diagram for ZONE5 and 24 hours-ahead (Result: Different; p-value = 1.7e-171; Critical Distance = 0.458).

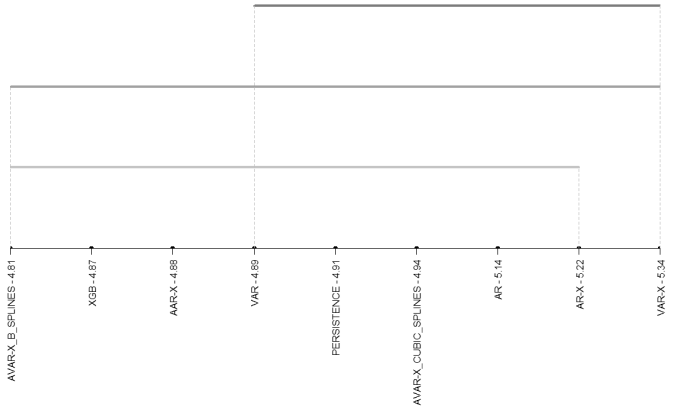

Figure 5.27: Critical Difference diagram for ZONE6 and 1 hour-ahead (Result: Different; p-value = 0.0012; Critical Distance = 0.457).

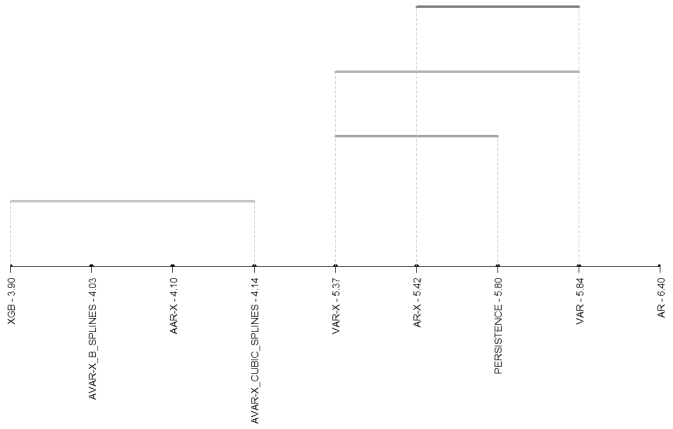

Figure 5.28: Critical Difference diagram for ZONE6 and 24 hours-ahead (Result: Different; p-value = 3.5e-140; Critical Distance = 0.458).

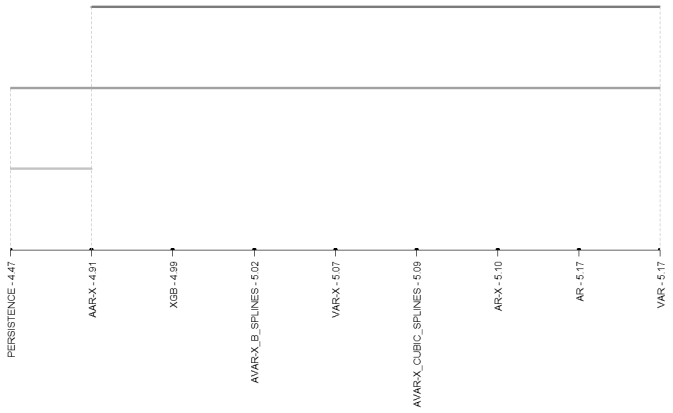

Figure 5.29: Critical Difference diagram for ZONE7 and 1 hour-ahead (Result: Different; p-value = 3.9e-05; Critical Distance = 0.457).

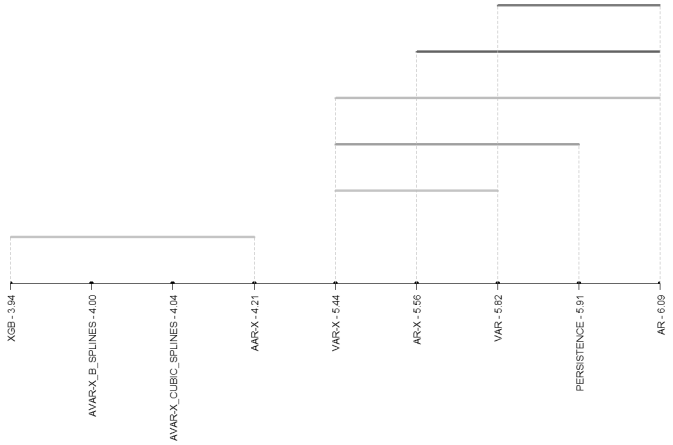

Figure 5.30: Critical Difference diagram for ZONE7 and 24 hours-ahead (Result: Different; p-value = 5.4e-131; Critical Distance = 0.458).

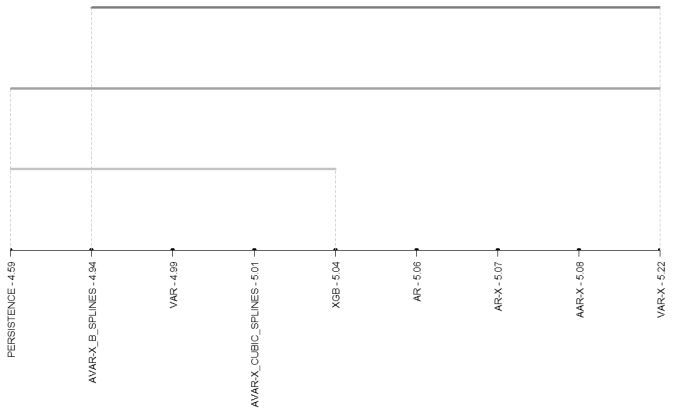

Figure 5.31: Critical Difference diagram for ZONE8 and 1 hour-ahead (Result: Different; p-value = 0.0061; Critical Distance = 0.457).

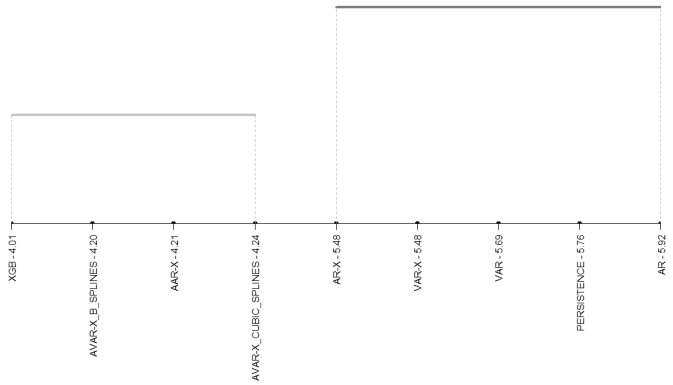

Figure 5.32: Critical Difference diagram for ZONE8 and 24 hours-ahead (Result: Different; p-value = 8.1e-98; Critical Distance = 0.458).

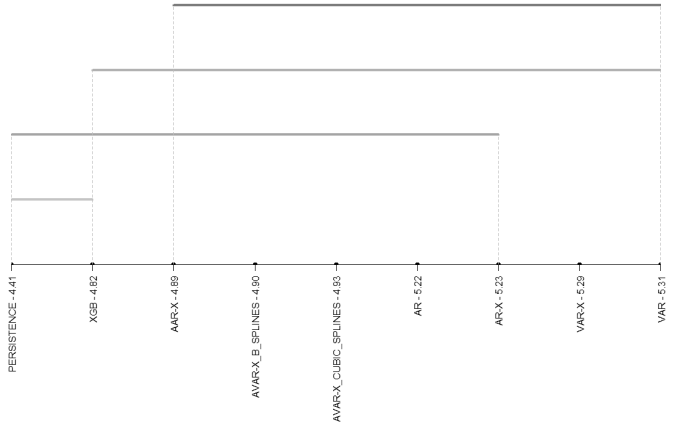

Figure 5.33: Critical Difference diagram for ZONE9 and 1 hour-ahead (Result: Different; p-value = 9.2e-11; Critical Distance = 0.457).

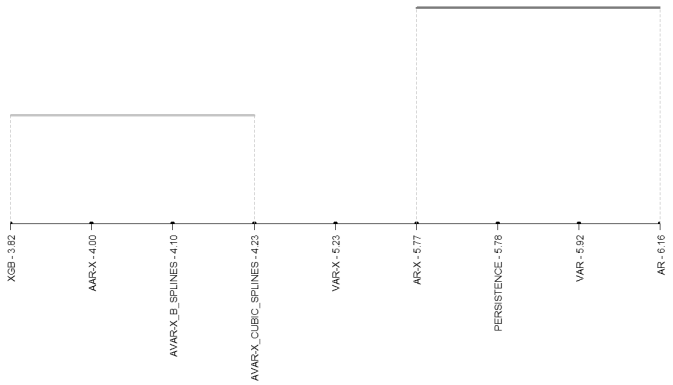

Figure 5.34: Critical Difference diagram for ZONE9 and 24 hours-ahead (Result: Different; p-value = 9.4e-138; Critical Distance = 0.458).

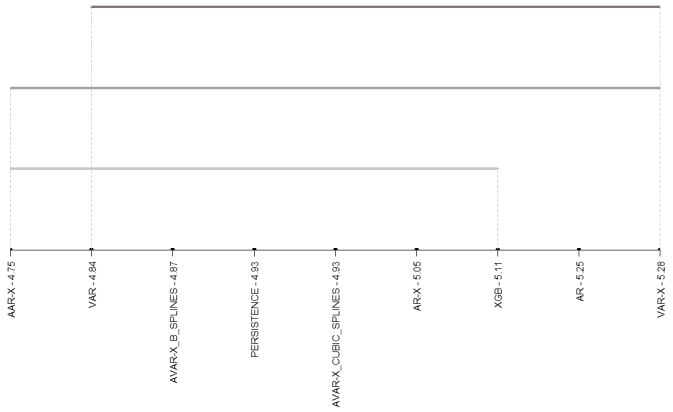

Figure 5.35: Critical Difference diagram for ZONE10 and 1 hour-ahead (Result: Different; p-value = 0.0016; Critical Distance = 0.457).

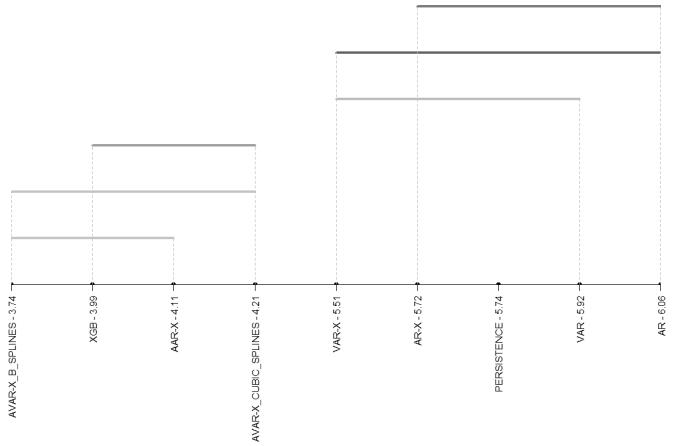

Figure 5.36: Critical Difference diagram for ZONE10 and 24 hours-ahead (Result: Different; p-value = 4.4e-140; Critical Distance = 0.458).